

Exploring the potential reuse of glass bottles in structural columns

Investigating the Structural Behaviour of Glass Columns Containing Glass Bottles through FE-modelling and Physical testing



Younes Maachi - 4714687

MSc Building Engineering – Structural Design
Faculty of Civil Engineering and Geosciences

 **TU Delft**

Contact information

Author:

Name: Y. (Younes) Maachi

Occupation: Master Student Building Engineering, Structural Design – TU Delft

Graduation committee:

Name: prof. dr. ir. P.C. (Christian) Louter [\[Chairman\]](#)

Occupation: Professor of Structural Design & Building Engineering – TU Delft

Name: MSc. H. (Hoessein) Alkisaie [\[Daily Supervisor\]](#)

Occupation: Lecturer Structural and Building Engineering – TU Delft

Name: Ir. C. (Chris) Noteboom

Occupation: Lecturer Structural Glass – Researcher – TU Delft

Name: dr. C. (Clarissa) Justino de Lima

Occupation: Senior Scientist – American Glass Research

Publication Date:

December 2022

Faculty of Civil Engineering and Geosciences

Delft University of Technology



Foreword

I have always been interested in innovative materials and the sustainability aspect of designing structures. It was a challenge to create ideas to build with glass bottles, but my endeavour to contribute to glass research and knowledge on building with glass waste helped me in this. This thesis project was the first time I experienced and set up a large research project. I learnt a lot of things about glass that I did not yet know and I also learnt a lot about how to manage a large research project, how to plan experiments and how to solve tough problems. This thesis project has also helped me improve my communication skills with my colleagues and increased my network of contacts in the structural glass community. When I looked at a glass bottle before my thesis, I thought it was an ordinary object that could only hold drinks and food. At the end of my thesis, I look at an used glass bottle as something with great potential in the structural glass industry. My ambition to lay down the foundation for a new research possibilities helped me creating this master thesis. That ambition was strengthened by the following people, who I want to thank individually.

I want to thank prof. dr. ir. P.C. Louter for his expertise on structural glass and his guidance during my thesis as chairman. I want to thank H. Alkisaiei for his guidance during the thesis as a daily supervisor. His help with initiating the project, involving multiple contacts with committee members and AGR, created the foundation for the thesis. Moreover, his advice on how to tackle a MSc Thesis greatly helped me during my 10 month project. I want to thank ir. C. Noteboom for his expertise in structural glass, his help in problem solving and also his guidance during the thesis. Finally, I want to thank dr. C. Justino de Lima for her guidance and help during the testing at AGR, the information she taught me during visits at AGR, her expertise on glass bottles and her overall support during my thesis.

Outside my thesis committee, I want to thank G. Stamoulis for his guidance of the testing in Stevinlab as a lab assistant. His guidance and problem solving skills helped me to create satisfactory test results and conclusions. I want to thank P.A. de Vries for his introduction to the Stevinlab and the suggestions he gave me for the testing. I want to thank Mrs. Ir. T. Bristogianni for her allowing me to use the glass sanding machine for the cut samples.

Younes Maachi
2-12-2022 Delft

Abstract

This thesis is made to investigate the potential of using glass bottles in structural elements, more specifically in structural columns. Glass bottles are re-used as elements in a structural column. The goal of this is to increase the reusability of the bottles, reduce the glass waste and to provide an innovative and sustainable alternative for conventional building materials. Very little research has been done on the potential use of glass bottles in a structural system. In collaboration with AGR, American Glass Research, and Technische Universiteit Delft, this thesis investigates how columns can be made out of glass bottles. The main question of this thesis is formulated as follows:

“How can structural columns be constructed out of glass bottles?”

The thesis is subdivided into eight parts (i.e. A till G), which are created to research four distinct areas: mechanical behaviour of individual bottles, connections between bottles, configurations of bottles, and limitations of using glass bottles in a column.

Projects of using glass bottles can be observed all around the world, with the temple ‘*Wat Pa Maha Chedi Kaew*’ in Thailand being one of the most magnificent of them all. Knowledge gathered from past projects showed that individuals or communities usually tend to create structures with glass bottles with a cementitious material in their walls. This cementitious material is usually concrete or mortar. The buildings with these elements are often single storey buildings.

A literature study and finite element modelling have shown that under vertical compressive loading, rings of tension stresses form in the shoulder and heel of the bottle. Under vertical compressive loading, the corresponding failure mechanisms should predominantly be fractures in either the heel or the shoulder of the bottle. Research is done on the characteristic tensile strength of line-simulated and abraded container glass to retrieve a value to eventually calculate with, rather than taking the characteristic tensile strength of float glass of 45 MPa . Using two different finite element models and Weibull Analysis, it was concluded that the characteristic tensile strength of line-simulated bottles is equal to 27 MPa and more importantly, the characteristic tensile strength of abraded bottles is equal to 20 MPa . When structures are created out of glass waste, in this case glass bottles, designs should be made with the abraded state of the bottles in mind.

Connections between glass bottles can be made in three different manners. In this thesis, these are called the ‘*Masonry*’, ‘*Stacked*’ and ‘*Bundled*’ options respectively. The ‘*Masonry*’ option is using glass bottles as brickwork in walls, which is the conventional way of using glass bottles in structures. The ‘*Stacked*’ option is stacking the bottles with plates. The last option, the ‘*Bundled*’ option, was made with inspiration from the bundled columns that were created at the TUDelft. Eventually, a choice was made for the stacked option on the basis of argumentation provided in this thesis.

Eight different configurations of the ‘*Stacked*’ option are created, of which four are eventually tested at Stevinlab in a hydraulic compression machine: ‘*Whole-Up*’, ‘*Whole-FF*’, ‘*Whole-BB*’

and 'Cut-Double-BB'. The acronym 'FF' stands for finish-finish and the acronym 'BB' stands for bottom-bottom, which denotes the sections of the bottle that are connected with each other. The finish of the bottle is the upper most part of the bottle. The suffix 'Up' denotes the orientation of the bottle, where the hole of the bottle is facing upwards. The Whole-Up configuration consists of stacking bottles in the most simple manner between plates. The Whole-FF configuration contains an intermediate steel plate on which the bottles are plugged. The Whole-BB configurations consists of an adhesive connection between the bottoms of bottles. The adhesive that is used in this thesis is tile adhesive. Lastly, the Cut-Double-BB consists of cut bottles with an adhesive connection. Cut bottles were also observed to investigate whether they are worth the money, time and effort to complete in comparison with whole bottles.

Results of the compression tests of different configurations showed that the Whole-Up had the highest failure load, followed by the Whole-FF and Whole-BB concept, and the Cut-Double-BB being much weaker than the other three configurations. The Cut-Double-BB showed failure loads that were almost four times as small compared to the Whole-Up concept, and it was thus concluded that cut bottles were not a viable option for these columns.

Results from experiments at American Glass Research with individual glass bottles and experiments with configurations of glass bottles led to creating a proposed design formula for the vertical compression resistance of a bottle column, based upon the characteristic strength of abraded container glass, the load-duration factor, a system factor taking into account the different tolerances, the material factor of glass and the influence of bottle thickness on the vertical load strength.

From these results, design options of columns are made, containing either the Whole-FF concepts or a combination of Whole-FF and Whole-BB. Because a demountable option was the preference, Option B was chosen. A prototype of Option B was eventually made with bottles that were left over after the testing and bottles that were recycled from a restaurant. By comparing the bottle column with more conventional materials, it was discovered that the bottle column is still far off from more conventional materials, such as steel, concrete or timber. It was calculated for instance that an Option B column consisting of layers with 6 bottles had a vertical compressive design load of about 5.38 kN , whilst most glass bottles had a maximum failure load of around 20 kN . This limiting factor of the column is part of an array of limitations, which also included the freedom of design of glass bottles per layer, the height tolerances of the bottles themselves and the current costs of the connection materials to name a few.

However, the potential for using glass bottles is definitely there for small or temporary projects and if the costs of the connection materials can be lowered even more, the glass bottle column can compete with more conventional materials.

Table of Contents

Contact information.....	i
Foreword.....	ii
Abstract.....	iii
1 Introduction.....	1
1.1. Problem statement of this thesis.....	2
1.2. Main research question and sub-questions.....	2
1.3. Research methodology.....	3
1.4. Research objectives and audience.....	3
1.5. Report Outline.....	4
A Literature Study.....	6
2 Glass Bottles as a Structural Material.....	7
2.1. Glass Bottle Temple: Wat Pa Maha Chedi Kaew.....	7
2.2. Glass Bottle House: The Bottle Houses.....	8
2.3. Glass Bottle Column: Art-Piece.....	9
2.4. Glass Bottle Beach Shed: Interlocking bottles.....	10
2.5. Other construction projects involving glass bottles.....	11
2.6. Conclusion from past projects.....	12
3 Physical characteristics of glass bottles.....	13
3.1. Geometrical characteristics of glass bottles.....	13
3.1.1. Bottom.....	13
3.1.2. Heel.....	14
3.1.3. Body.....	15
3.1.4. Shoulder.....	16
3.1.5. Neck and finish.....	17
3.2. Coatings and surfaces of glass bottles.....	17
3.2.1. Glass Bottle Coatings in general.....	17
3.2.2. Hot End Coatings.....	18
3.2.3. Cold End Coatings.....	18
3.2.4. Hot-End and Cold-End Coatings: Mechanical behavior.....	19
3.2.5. Glass bottle coatings and adhesives.....	20
4 Mechanical behaviour of individual glass bottles.....	22
4.1. Surfaces and defects of glass bottles.....	22
4.2. Finite-element modelling of glass bottles.....	23
B AGR Experiments.....	26
5 Fracture testing and FEM of individual bottles.....	27
5.1. Methodology of AGR Testing.....	28
5.2. Damage evaluation of glass bottles.....	30
5.3. Weibull Analysis.....	30
5.4. Results of the AGR Tests.....	32
5.5. Verification with second model in DIANA.....	36
5.6. Verification of Weibull parameters.....	37

5.7. Discussion of AGR Tests.....	38
5.8. Conclusion on AGR Tests	39
C Connections and Configurations	40
6 Connection concepts between glass bottles.....	41
6.1. Masonry Concept	41
6.2. Stacked Concept.....	42
6.3. Bundled Concept	43
6.4. Conclusion on connection concepts	44
7 Stacked Bottle Concepts.....	45
7.1. Weighing criteria for judgement bottle configurations	45
7.2. Configurations with whole bottles	46
7.2.1. Single bottles	46
7.2.2. Multiple bottles	46
7.3. Configurations with cut bottles	48
7.3.1. Single bottles	49
7.3.2. Multiple bottles	49
7.4. Comparison of bottle configurations	51
7.5. Investigation on stress distributions of different configurations.....	51
7.6. Conclusions on bottle configurations and choices for testing.....	52
D Stevinlab Experiments.....	54
8 Compression Tests of Bottle Configurations	55
8.1. Previous experiments with glass columns in Stevinlab.....	55
8.2. Methodology of compression tests of bottle configurations.....	56
8.2.1. Approach	56
8.2.2. Materials	58
8.2.3. Equipment and tools	58
8.2.4. Preparation phase and safety measures	59
8.2.5. Failed test trial and solution	61
8.3. Results of the compression tests of configurations	62
8.3.1. Collected data from compression tests of configurations	62
8.3.2. Hand-calculation Whole-Up axial stiffness	65
8.4. Discussion of the compression tests of configurations.....	65
8.5. Conclusion on the compression tests of configurations and answering third sub-question	66
9 Relation between individual bottle tests and configuration tests	67
9.1. Characteristic tensile strengths of manually abraded and line-simulated bottles	67
9.2. Load duration factor for glass strength.....	69
9.3. Calculating the tensile design strength of container glass	70
9.4. Calculating the vertical load resistance of an individual bottle	70
9.5. Influence of intermediate connections on the vertical failure loads.....	72
9.6. Design formula for vertical load resistance of a bottle column	73
E Column Design.....	74
10 Column Designs and Limitations	75
10.1. Bottle Patterns	75

10.2. Design options glass bottle columns	77
10.3. Case study calculation for a bottle column	81
10.4. Prototype of a bottle column	83
10.5. Comparison bottle column with conventional materials	85
10.5.1. Concrete option	86
10.5.2. Steel Option	87
10.5.3. Timber Option	88
10.5.4. Glass Bottle Option	89
10.6. Limitations of the stacked glass bottle column	90
10.6.1. Height tolerances	90
10.6.2. Bottle designs	90
10.6.3. Bottle patterns	90
10.6.4. Connection costs	90
10.6.5. Vertical load resistance compared to conventional materials	90
10.6.6. Post breakage behavior and safety	91
11 Design explorations	92
11.1. Combining Whole-FF with bundled option	92
11.2. External tension element around bottle column	94
11.3. Overview of other design explorations	94
F Discussion, Conclusion and Recommendations	95
12 Thesis Discussion and Conclusion	96
12.1. Thesis Discussion	96
12.1.1. Mechanical behavior of glass bottles under vertical load	96
12.1.2. Connection between glass bottles	97
12.1.3. Configurations of glass bottles	97
12.1.4. Limitations of glass bottles	98
12.2. Thesis Conclusion	98
13 Research Recommendations	100
Bibliography	102
References	102
Figures	106
Tables	107
A1 Fracture Mirror Pictures	110
A2 Configuration models	113
A3 Hand-calculation Axial Stiffness Whole-Up	126
A4 AGR Experiments Tables	133
A5 Technical Drawing Brouwland Bottle	136
A6 MDF Plate Drawings Stevinlab	138
A7 Fractured Samples Stevinlab	141
A.7.1. Whole Samples	141
A.7.1.1. Fractured Whole-Up Samples	141
A.7.1.2. Fractured Whole-FF Samples	147

A.7.1.3. Fractured Whole-BB Samples.....	152
A.7.2. Cut Samples (Cut-Double-BB)	156
A8 Finite Element Model Bottle	159
A.8.1. DIANA Model.....	159
A.8.2. ANSYS Model.....	162

1 Introduction

In 2012, the total glass production in the EU-27 was equal to 33.5 million tonnes (Glass Alliance Group, 2013). The portion of glass containers was equal to 65% percent of the total glass production in the EU-27 in 2012 (Glass Alliance Group, 2013) . In comparison, in 2018, the glass container production in the EU-27 was equal to 21.76 million tons (Glass Alliance Group, 2019). This was equal to 59% of the glass container production (Glass Alliance Group, 2019). The percentage of glass container production of the total glass production seems to be decreasing slightly, however the glass container production is still growing. Likewise, in 2016, a total of 305 billion units of glass packaging was sold globally (FEVE, 2018). Up to 96% of the 305 billion units worldwide came from alcoholic drinks, soft drinks and food packaging (FEVE, 2018).

It was also reported that the recycling of glass containers was equal to 73% in the EU-28 in 2012 (FEVE, 2015). Values were also given for separate countries. For instance, 546,000 tons of glass containers were consumed in the Netherlands in 2013, of which 430,000 tons (i.e. 79%) were collected for recycling (FEVE, 2015). According to Afvalfonds Verpakkingen (2018), a total of 500 kilotons of glass packaging was put into the market in the Netherlands in 2017. A total of 431 kilotons of glass packaging was recycled in the Netherlands in 2017, which corresponds to 86.2%. The goal for the European Union in 2017 was only set to 60% of all glass packaging. (Afvalfonds Verpakkingen, 2018). The recycling process of glass bottles mainly consist of remelting the cullet back into new bottles.

Europe is however the leader in the glass recycling sector. Harder (2018) states that the worldwide recycling rate is about 32% for container glass. In 2013, only 33.6% of recycled glass was used again in the United States container glass industry (Harder, 2018). Volte Sempre, a program for glass recycling in Belo Horizonte in Brazil in collaboration with Owens-Illinois and Heineken, state that currently only 40% of the produced glass packaging is being recycled in Brazil (Heineken, n.d.).

According to a study from Liebenberg (2007), there exist a few barriers to recycling waste in developing countries. Firstly, in developing countries, the recycling industry is very informal (Liebenberg, 2017). Secondly, the market for recycling is very limited in for instance Africa. The high transport costs deter reclaimers from collecting waste over a larger distance (Liebenberg, 2017). As a result, Liebenberg (2007) mentions that '*informal salvaging*' can be seen across a lot of Africa's landfills, often to find materials to build a shelter out of.

Besides recycling of glass bottles, reuse of glass bottles is also an option. However, returning used bottles back to the fillers is rather difficult due to the widespread production and distribution of these glass bottles (Dyer, 2014). Citizens of relatively more remote areas or developing countries, who produce glass waste, have even less access to this option. Moreover, melting cullet back into new products costs energy. Finding a second life for their glass waste, such as being a building material, is therefore very beneficial.

As far as it is known, scientific research on the potential of using glass bottles as a structural material is non-existent. This thesis is written to fill this knowledge gap and to further understand how glass bottles can be used as a structural material.

1.1. Problem statement of this thesis

Individuals and communities in developing countries have been building shelters and homes that are made out of beer or wine bottles. These are usually mixed with cement mixtures in order to create solid-like structural elements. Moreover, there is still room for improvement left for the re-usability of glass packaging around the world. It is understood that the potential of using glass bottles in structural elements has not yet been assessed scientifically.

This thesis focuses on obtaining the characteristics of a structural column that consists of beer bottles. The following knowledge gaps will be analysed:

- how columns made out of beer bottles can be constructed
- how glass bottles behave mechanically under a vertical load
- how glass bottles can be connected to each other
- how different bottle configurations affect the characteristics of the column
- what limitations the columns have

1.2. Main research question and sub-questions

After formulating the problem statement, the main research question for this thesis is as follows:

‘How can structural columns be constructed out of glass bottles?’

The main question will be answered with the help of four sub-questions. The four sub-questions are made to divide the main-question into four distinct areas. These are as follows:

Investigating individual glass bottles:

1. *‘What is the mechanical behaviour of an individual glass bottle subjected to vertical compressive load?’*

This sub-question investigates individual bottles separately on their mechanical behaviour during vertical loading. The strengths and weaknesses of glass bottles are investigated.

Investigating connection types for glass bottles:

2. *‘How can glass bottles be connected to each other to resist applied vertical loads?’*

This sub-question is dedicated to connection types between glass bottles that are either already being used or could be used. The ways of connecting two glass bottles together are investigated. One connection type will be chosen to further elaborate upon.

Investigating configurations of glass bottles:

3. *'Which configurations of glass bottles in a structural column are most sufficient in terms of resisting tensile stresses?'*

This sub-question is dedicated to the different configurations that are created from the connection type chosen after sub-question 2. These configurations are designed and tested. One or a combination of configurations will be used to design a column out of glass bottles.

Investigating the limitations of columns out of glass bottles

4. *'What are the limitations of columns made from glass bottles?'*

The final sub-question investigates the limitations of using glass bottles in a structural manner, more specifically in a column. The practical problems that might arise when building such as column are named. Furthermore, the resistance of a compression load is formulated and the comparison with more conventional materials is made. Solutions to make the glass bottle column more competitive are also given. Design explorations to improve the current glass bottle column design are provided.

1.3. Research methodology

The first sub-question will be answered on the basis of an extensive literature study, testing of individual bottles under vertical load at American Glass Research and FEM-modelling of individual glass bottles.

The second sub-question will be answered on the basis of a literature study on the existing methods of connecting glass bottles together, as well as new ideas for connecting glass bottles together.

The third sub-question will be answered on the basis of failure tests at Stevinlab with a hydraulic compression machine. Several configurations will be tested on their failure loads. This results in force-displacement graphs of the different configurations.

The final sub-question is answered on the basis of formulating the design strength of the glass bottles and the comparison with more conventional materials. Furthermore, a prototype of a design of a bottle column will be made. Experiences from building such a model will be formulated as well. Based on these findings, the limitations of a bottle column can be formulated. Recommendations and design explorations are also given to elaborate on possible improvements for a bottle column.

1.4. Research objectives and audience

This thesis addresses the following main objectives:

- Exploring the potential of using glass bottles as a building material.
- Increase the knowledge on the mechanical behaviour of glass bottles.
- Design a column made from glass bottles.

- Create other design explorations of glass bottles in columns.
- Mention the limitations of a bottle column and the improvements that should be made before wide-scale implementation.

The information and conclusions that are gathered are intended for the following audience:

- Individuals or communities with limited access to conventional building materials who are in need for an alternative.
- Individuals or communities who desire to create more sustainable and environmentally friendly glass structures by using waste products, in this case glass bottles, as a building material.

1.5. Report Outline

The thesis report is subdivided into several sections.

- *Section A: Literature study*
- *Section B: AGR Experiments*
- *Section C: Connections and Configurations*
- *Section D: Stevinlab Experiments*
- *Section E: Column Design*
- *Section F: Discussion, Conclusion and Recommendations*

These sections are then subdivided into chapters. Figure 1 shows a diagram of the report outline. The diagram also shows which chapters are used to answer the relevant sub-questions. The methodology is split into five categories: Literature Research, Experimental Research, FEM, Design. The acronym 'SQ' stands for sub-question.

Section	Chapter	Methods	Content	SQ
A Literature Study	2. Glass Bottles as a Structural Material	Literature Research	Overview of projects with glass bottles as structural elements	
	3. Physical characteristics of glass bottles	Literature Research	Information on nomenclature of bottles, different sections of bottles and coatings of glass bottles	
	4. Mechanical behaviour of individual glass bottles	Literature Research FEM	Information on surfaces of bottles, strengths and defects Information on tensile principle stress under vertical load	SQ 1
B AGR Experiments	5. Fracture testing and FEM of individual bottles	Experimental Research	Vertical Load testing of individual bottles at AGR	
		FEM	Fracture Stress retrieval Weibull Analysis Characteristic tensile strength of container glass	
C Connections & Configurations	6. Connection concepts between glass bottles	Literature Research Design	Overview of connection concepts between glass bottles Design options for connecting glass bottles together	SQ 2
	7. Stacked Bottle Concepts	Design	Design of eight different configurations for stacking glass bottles	SQ 3
D Stevinlab Experiments	8. Compression Tests of Bottle Configurations	Experimental Research	Compression tests of bottle configurations at Stevinlab	SQ 3
	9. Relation between individual bottle tests and configuration tests	Experimental Research	Reduction factors for the strengths of abraded glass bottles	
FEM		Proposal design formula for compression capacity		
E Column Design	10. Column Designs and Limitations	Design	Design patterns Design options of glass bottle column Case study of a bottle column Limitations of the bottle column	SQ 4
	11. Design explorations	Design	Design explorations of final design concept	
F Discussion Conclusions Recommendations	12. Thesis Discussion and Conclusion			
	13. Research Recommendations			
Appendices	A1. Fracture Mirror Pictures	Experimental Research		
	A2. Configuration Models	FEM		
	A3. Hand-calculation Axial Stiffness Whole-Up			
	A4. AGR Experiments Tables	Experimental Research		
	A5. Technical Drawing Brouwland Bottle			
	A6. MDF Plate Drawings Stevinlab			
	A7. Fractured Samples Stevinlab	Experimental Research		
	A8. Finite Element Model Bottle	FEM		

Figure 1 – Report outline of thesis report

A

A Literature Study

2 Glass Bottles as a Structural Material

Building structures out of glass bottles is not a novel idea. Present-day examples of creations and structures out of glass bottles are however limited. These projects are often thought through and executed by an individual or a small local collective. Designs are created from past experiences of other projects, but mechanical understanding of these structures is generally lacking. Rules or guidelines for creating elements out of glass bottles simply do not exist and different techniques are observed between designs.

For the creation of a design in this thesis, examples from around the world have to be studied beforehand. This chapter gives an extensive overview of those examples of glass bottles used in structures. The projects range from art works to buildings, all showing diverse techniques of combining bottles for a structural element or non-structural element. Some projects merely serve as a gimmick, other projects fulfill an important functional purpose. This thesis cannot focus on every project, but a few are taken out to describe into further detail.

2.1. Glass Bottle Temple: Wat Pa Maha Chedi Kaew

One of the most famous examples that one can find is Wat Pa Maha Chedi Kaew in Thailand. The nickname for this temple is *'the Temple of a Million Bottles'*. The construction of this temple began in 1984 and the temple was completed in two years (Sunkara, 2018). The temple has been standing for 36 years. The temple was built with the help of donations from the community. After the temple was completed, the project expanded to an array of 20 buildings surrounding the temple (Sunkara, 2018).

The bottles were used as construction materials in combination with concrete. The structure of the temple contains a few designs for columns. Two of these designs will be explored further.

On the outside of the temple, rectangular columns were made to support the overhang of the roof. The rectangular column has a distinct pattern, which is shown in figure 2.

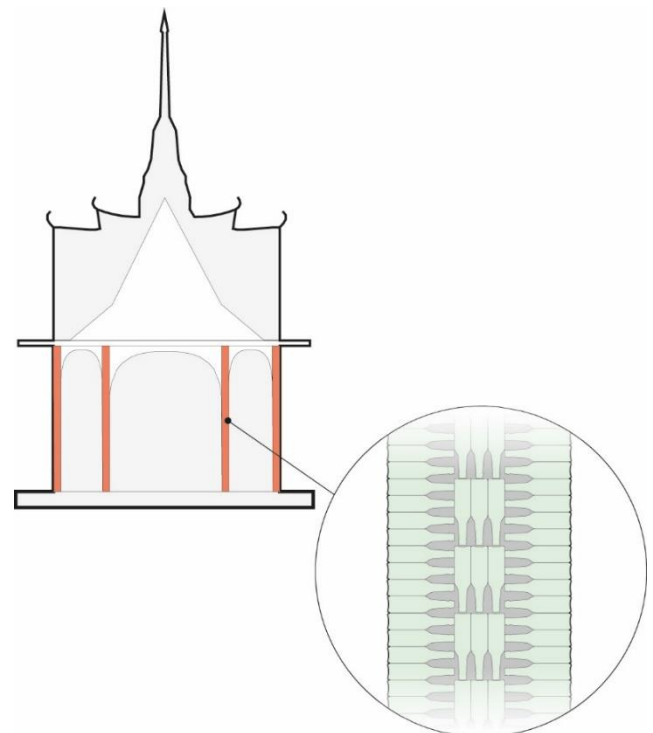


Figure 2 – Schematic drawing of the outer column of the temple with close-up

The bottles are placed both horizontally and vertically. The inside of the temple also contains circular columns made out of glass bottles. This design contains bottles that are placed upside down in a round pattern. This is shown in figure 3. Figure 4 shows a picture taken of the *Million Bottle Temple*.

The project of Wat Pa Maha Chedi Kaew has shown that glass bottles can be used as a substrate in combination with concrete for massive structures. There is however an uncertainty about how much the bottles contribute to the load carrying capacity. Furthermore, the structure is very much a permanent structure, which means that the bottles cannot be used again for their primary use. It does appear that the bottles reduce the amount of concrete used for the element by taking up a part of the vertical compressive load.

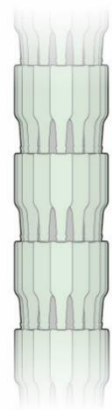


Figure 3 – Column design in the temple

Figure 4 – Million Bottle Temple (Fischer, 2011)

2.2. Glass Bottle House: The Bottle Houses

This project is located in Wellington, Canada. In total, 25000 bottles were used for the construction of this project (Lecacheur, 2020). Cement was used to bind the bottles together (Rom, 2015). The bottles that were used for this building were collected across the community (The Bottle Houses, n.d.). Construction began in 1980 and the whole project, consisting of three houses, was finished in 1984 (The Bottle Houses, n.d.). The houses are still in use to this day, which indicates a lifespan of 38 years. These houses mainly serve as a tourist attraction (Lecacheur, 2020).



Figure 5 – Column design in The Bottle Houses (Rom, 2015)



Figure 6 – Circular column Design in The Bottle Houses (Byers, 2018)

The first house contains about 12000 bottles and 85 bags of cement were used to bind them together (Rom, 2015). A picture of this building is shown in figure 5, which showcases the walls and arches made out of glass bottles. The second house contains about 8000 bottles and was built in a hexagonal shape (Rom, 2015). A large circular column made out of cement and bottles stands in the centre of the building. The idea is similar to that of ‘Glass Bottle Temple’, but the bottles are placed in different orientations. A picture of that column is shown in figure 5.

2.3. Glass Bottle Column: Art-Piece

Eli Hansen and Oscar Tuazon created a column out of glass bottles in 2014, which was used in several art galleries. The intriguing part of this project is configuration of the bottles to create a column, which is different to the projects mentioned before. In comparison to the other projects, this column does not contain concrete or cement, but it has to be analysed whether this configuration can be used for load-bearing purposes. The column has a length of about 1.4 meters and takes up an area of 19.1 by 19.1 centimetres (Hansen & Tuazon, 2014). A schematic of the column is shown in figure 7, followed by a picture of the column in figure 8.

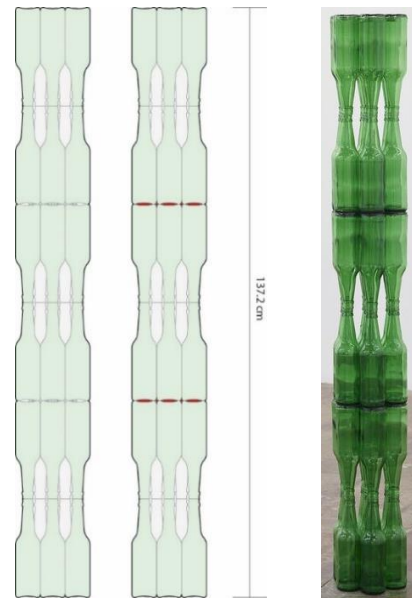


Figure 7 & 8 – Schematic side view of the bottle column art work (Maachi, 2022) and a picture of the artwork (Hansen & Tuazon, 2014)

2.4. Glass Bottle Beach Shed: Interlocking bottles

In the 1960s, the owner of Heineken initiated the idea to create a bottle that could also be used as a building block: the WOBO-Bottle. In collaboration with the architect John Habraken, a bottle was designed and developed (Heineken Collection Foundation, n.d.). However, concerns on the marketing side eventually led to abandoning of the project (Heineken Collection Foundation, n.d.). In the following years, several attempts were made to revive the introduction of the WOBO-bottle, which included building a structure out of WOBO-bottles at the TU Eindhoven (Heineken Collection Foundation, n.d.).

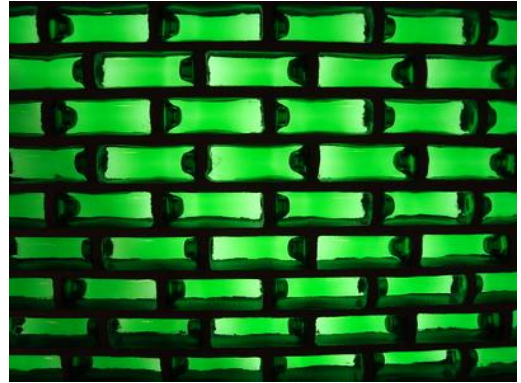


Figure 9 – Heineken Wobo Wall (Stark, 2009)

Figure 9 shows a wall made out of WOBO-bottles. The bottles were made to lay horizontally and interlocking features were made to connect the bottles together. Yoneda (2012) mentions that a small shed in Noordwijk and a wall in the Heineken Museum in Amsterdam are the only examples of structures with these bottles that are left.



The WOBO-bottle is designed with re-use already mind, which is different to the projects discussed earlier. A picture of the aforementioned shed is shown in figure 10.

Figure 10 - WOBO House in Noordwijk (Heineken International, n.d.)

Another less famous example of adapting the design of a glass bottle for sustainability purposes is the Heineken Cube. The Heineken Cube was developed to reduce shipping cost by saving space with efficient stacking (Boyer, 2014). The intention was not to use it as a building block, but the shape of the Heineken cube could be of great use for stackable elements in for instance a wall. A picture of the Heineken Cube is shown in figure 11.



Figure 11 – Heineken Cube (Petit, 2008)

2.5. Other construction projects involving glass bottles

Other than the projects mentioned before, a vast array of projects involving the structural use of glass bottles exist around the world. Table 1 gives a concise catalogue of these projects with locations. Most of the projects in the catalogue are houses. The catalogue shows that building with glass bottles is something that is done all over the world. Moreover, most of the projects are also single story buildings.












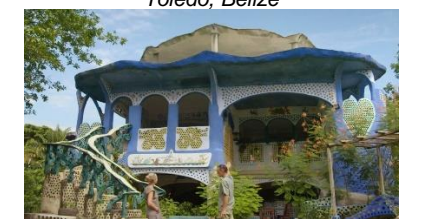
<p><i>George's Glass Castle</i> Sanca, British Columbia, Canada</p>  <p>(Alisson, n.d.)</p>	<p><i>Glass Bottle House</i> Bohatyryivka, Ukraine</p>  <p>(Maboulette, n.d.)</p>	<p><i>Tom Kelly's Glass Bottle House</i> Rhyolite, Nevada, United States of America</p>  <p>(Schaller, 2011)</p>
<p><i>Glass Bottle House</i> Foz de Iguacu, Brazil</p>  <p>(Dias, 2022)</p>	<p><i>Glass Bottle House</i> Quilmes, Argentina</p>  <p>(Vaca, 2022)</p>	<p><i>Glass Bottle House</i> Chelyabinsk, Russia</p>  <p>(Zvonarev, n.d.)</p>
<p><i>Glass Bottle House</i> Florianopolis, Brazil</p>  <p>(Gaudi, 2017)</p>	<p><i>Blotto Grotto (Glass Bottle Dome)</i> Pembroke, United Kingdom</p>  <p>(Daily Mail, 2014)</p>	<p><i>Glass Bottle Construction</i> Watamu, Kenya</p>  <p>(Building from glass bottles, n.d.)</p>
<p><i>Glass Bottle House</i> Pyramiden, Svalbard, Norway</p>  <p>(Bott, 2017)</p>	<p><i>Glass Bottle School</i> Shikharapur, Nepal</p>  <p>(Shikharapur CLC, n.d.)</p>	<p><i>Glass Bottle House</i> Toledo, Belize</p>  <p>(NPO, 2022)</p>

Table 1 – Catalogue of projects with glass bottles in buildings around the world

Likewise with the Bottle Houses and the Thai bottle temple, the bottles are used as bricks in masonry in combination with mortar on concrete. Finally, the glass bottles are often used in walls, where sometimes an additional structure is used in combination with the glass bottle walls.

2.6. Conclusion from past projects

From the information gathered in this chapter, various points can be concluded from these projects. Firstly, the environments in which these techniques are used in are truly diverse: from the cold regions of Svalbrad and central Russia to more arid regions of Nevada and Kenya. Secondly, these projects are often carried out by a single individual or a small collective. The only projects named in this thesis that were carried out by a community were the *Million Bottle Temple* by Buddhist monks, the Glass Bottle School in Nepal and the Glass Bottle Building in Watamu, Kenya.

The construction technique for these projects is even more noticeable. Across all these cultures, people tend to use glass bottles somewhat in the same manner for construction purposes. This technique is using glass bottles as a substrate in combination with cement, concrete or sometimes more environmentally friendly materials such as cob. From the pictures provided in the catalogue, the buildings tend to be only single storey buildings most of the time. Moreover, the bottles are often integrated in the walls. The idea of using bottles in columns has not been explored yet, other than the project of Wat Pa Maha Chedi Kaew and the Bottles Houses in Canada. Those projects definitely show the huge potential of glass bottles in massive structures and columns.

The orientation of the bottles in the elements differ from project to project. The bottles are predominately placed horizontally in these walls due to the ease of stacking them. On top of that, the bottom of the bottle is usually faced towards the outside of the building. A more advanced project, such as Wat Pa Maha Chedi Kaew, experimented with placing the bottles in different directions in their columns. It is unclear whether this was done for aesthetic purposes or to create a stronger column.

Finally, the only project without the use of a cementitious material in between the bottles is the artwork by Hansen & Tuazon. The intriguing part about this artwork is the configuration of the bottles that form a column. Furthermore, the marketing projects from Heineken with the WOBO Bottle and Heineken Cube are interesting options to consider, but these options will not be investigated further in the thesis. However, these marketing projects do show that companies have already been thinking about linking their products with reusability. It has to be explored whether there are other ways to connect these bottles together.

3 Physical characteristics of glass bottles

This chapter gives an overview of the distinctive features of the glass bottle. Terminology and nomenclature developed by CETIE, Centre Technique International de l'Embouteillage (*International Technical Center For Bottling*), are used in this thesis together with terms from the industry and other institutions. It is important to first understand the different features on a glass bottle before any simulation is made or ideas are created. The different sections of the bottle contain both opportunities and weaknesses. The information in this chapter has been retrieved with the help of a literature study.

3.1. Geometrical characteristics of glass bottles

A glass bottle or glass container is generally divided into the following sections: Bottom, Heel, Body, Shoulder, Neck and finish.

3.1.1. Bottom

The bottom of the bottle is divided into two main parts: the bearing surface and the push-up

According to Smith & Gifford (2007), the bearing surface is the area on the bottom of the bottle on which it rests. In other words, this is the general contact area of the bottom between the bottle and a surface, such as a table. Moreover, Smith & Gifford (2007) mention that the bearing surface contains so-called 'stacked features', which exist to provide interlocking between jars or bottles when stacking. In datasheet CETIE DT 23.01 (2004), this area of the bottle is also called the 'standing base'

Glass bottles usually have protuberances or ridges on these bearing surfaces. These are called knurls or knurling. They are also sometimes used under the term 'stippling'. There are several reasons to have these on the bottom of the bottle. Robertson (2012) explained the following on these protuberances: *"Good design will incorporate specific contact areas (e.g., knurls or small protrusions) that concentrate abrasions where they will have minimal effect on glass strength (Robertson, 2012)"*.

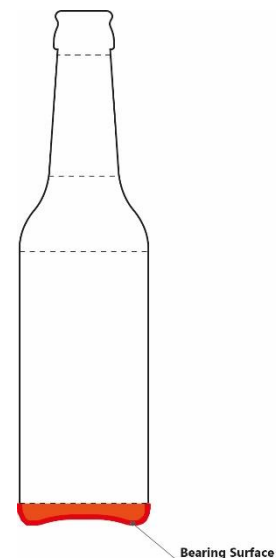


Figure 12 – The bottom of the bottle with the location of the bearing surface

In essence, the knurls on the bearing surface behave as an additional layer between the bottom of the bottle and a flat surface and mask potential damage that can be inflicted on the bottom. In the same way, Davis (2009) formulates the function of these knurls as follows: *"Also, including knurling on the bearing surface in the design concentrates any handling damage to the knurl tips. The knurls act as stress relievers, exhibit lower stresses, and protect the base glass from becoming damaged (see Figure 14) (Davis, 2009)."*

Lockhart & Hoenig (2016) explain that the phenomenon of 'stippling' came into existence to protect the base of the glass bottle from a sudden decrease of temperature, which could

lead to cracking. They further explain that somewhere around the 1970s a form of stippling was introduced that is more familiar in today's glass bottles. These are the familiar rows of crescents that can be found on the bearing surface of the bottle. Similarly, Syrett (2006) formulated improvements that were introduced to these glass bottles and one of which was a remark on the stippling or knurling on the base: *"Stippling on the bearing surface; this prevented sudden cooling of the base and thermal shock defects. (Syrett, 2006),"* The dimensions of these knurls can vary between manufacturers.

Moreover, the knurls on the bearing surface increase the overall surface area of this bearing surface. Surface treatments such as edging and sandblasting on glass surfaces are often used to create more adhesion between adhesive and glass, but it can decrease the surface strength (Machalická & Eliášová, 2012). However, the knurls are designed to mask the damage during handling and manufacturing, which means that etching these knurls is possible for better adhesion. On top of that, roughness on a surface can create better adhesion in itself, but the adhesive needs to have a relatively low viscosity to flow into the dents (Machalická & Eliášová, 2012). This means that the increased surface area due to the knurls can create a relatively larger bonded area than on a flat surface, which creates better adhesion. This area of the bottle can therefore be of great potential for adhesive connections.

The push-up is the area on the bottom of the bottle that has been pushed up to create a concave surface (White, 1978). Kick or kick-up are also terms to denote this area. There are various reasons as to why these push-ups appear on glass bottles. Jones (1971) explains that historically the reason was that it would lead a bottle with higher strength. During glass-making, glass would flow towards the bottom. The annealing process would not be as effective with areas with a relatively larger thickness. Pushing up the glass on the bottom would redistribute the glass again (Jones, 1971). The push-up on the base can also contribute to the overall stability of the bottle, because the area around it, the bearing surface, would be uniform enough for the bottle to rest on (Berlin Packaging, 2019). The overall stability of a bottle with a push-up would be a better than a bottle without a push-up (Grayhurst, 2012). A larger diameter of the base of the bottle will allow for greater overall stability. (Grayhurst, 2012). This coincides with the notion of having the center of gravity of the bottle as low as possible, so that it is harder to topple over. This is why the base of the bottle is usually thicker than the walls of the body.

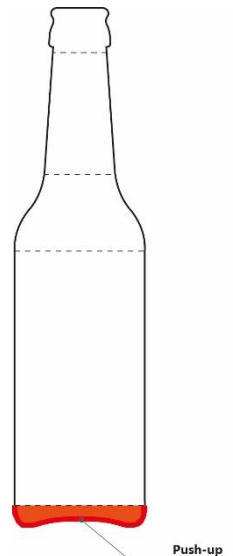


Figure 13 – The bottom of the bottle with the location of the bearing surface

3.1.2. Heel

The heel of a glass bottle is described in the following manner by Jones & Sullivan (1989):

"The area at the bottom of a container, usually a curve or a corner, which joins the body to the resting point (Jones & Sullivan, 1989)".

In other words, this is the part of the glass bottle that joins the body with the bearing surface of the bottle. The heel contains some interesting features, such as 'punt mark' to showcase the company who created the bottle, the capacity of the bottle and which machine was used. Sometimes, the term 'insweep' is also used as stated in ISO 7348:1992(en) (1992). The stiffness of this area is relatively higher than for instance the body of the bottle, because of the curved nature of the area (Davis, 2009). Feldmann *et al* (2010) concluded in a study that a curved glass element may contain a larger stiffness compared to a flat glass element. However, this also depends on the overall shape of the curved element and the load direction of the applied force

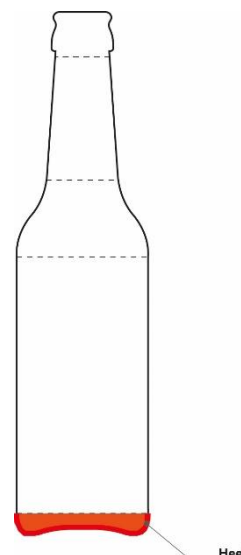


Figure 14 – The bottom of the bottle with the location of the bearing surface

The heel surface of the glass bottle can be denoted as a synclastic surface. A synclastic surface is defined by having a positive Gaussian curvature, which means that the two principal curvatures need to have the same sign i.e. equal directions. Another way to describe this surface is a 'concave' surface.

On the contrary, the heel of the glass bottle is one of the areas that is most prone to damage due to handling. (Davis, 2009).

In a report developed by UNIDO, *United Nations Industrial Development Organization*, (1982), it was noted that a curved heel can greatly reduce the bending stresses in that region. Moreover, the condition of the heel is significant for the overall thermal shock resistance of the bottle (UNIDO, 1982). Thermal shock is a phenomenon that will not be discussed in this thesis, but it is important to denote the importance of it for glass container design.

3.1.3. Body

The body of the glass bottle is the region between the heel and the shoulder of a glass bottle. This is the cylindrical part of the bottle that usually contains the label from the brand.

The term 'sidewall' was used by ASTM International (2015) to denote this area of the container. The term 'barrel' is rarely used for this area. Contemporary glass bottles sometimes use recessed label panels, where the body of the glass bottle is pushed inwards, where the diameter of the body becomes smaller than the heel diameter.

Labels themselves can protect the surface of the body on these panels, which can lower the probability of damage during handling (Slusser *et al*, 2018). It is important to note that these label panels can cause asymmetry in the cross-section of the bottle if only one part is recessed.

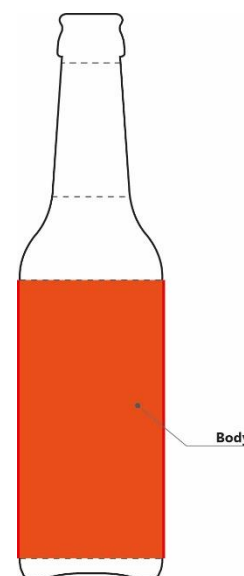
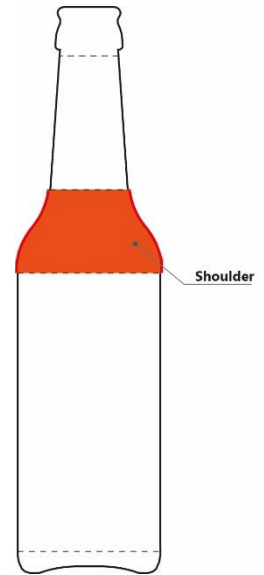


Figure 15 – Body of the bottle

The 330 ml Heineken Star bottle for instance contains a small recession on the back of the bottle. Asymmetry can cause bending stresses to develop in this region (Slusser *et al*, 2018), when a vertical load is applied. Furthermore, the thickness of walls is small enough so that the theory of thin tubes from structural mechanics can be applied. (Preston, 1933).

3.1.4. Shoulder

The shoulder is the region between the base of the neck and the upper part of the body. For some bottle designs, it can be difficult to distinguish when this region exactly starts and ends due to a curved design. For the upper boundary, the base of the neck of a glass bottle is located at the inflection point of the curvature of the bottle. The lower boundary is situated at the point where the Gaussian curvature becomes zero i.e. where the walls become straight and the cylindrical shape starts.



The shoulder region has a significant effect on the strength of the bottle during filling or capping. The ratio between the diameter of the body and the diameter of the neck has an influence on the developing tensile stresses under vertical loading. The reason for this is the relatively higher curvature in the geometry of the shoulder region. This effect is mentioned by Natarajan *et al* (2014): *“The shoulder radius of curvature gives better effect for load bearing during stacking (Natarajan et al, 2014)”*. Batchelor (2012) notes that radius of curvature in this region is an important parameter when dealing with vertical compressive forces on top of the bottle.

Figure 16– Shoulder of the bottle

The largest stresses due to compressive vertical loading on top of the bottle can be found in the shoulder area (UNIDO, 1982). The radius of curvature of the shoulder is therefore an important parameter and directly linked to the load-bearing capacity of vertical compressive loads. It becomes clear that bottles are designed to take up vertical compressive loads and that this could be useful for elements under axial compressive loading, such as a column.

3.1.5. Neck and finish

The neck is the region between the shoulder and the parting line at the top of the neck. The parting line is the mark left from the division of the separate moulds used for the finish and the body. The finish of the bottle is often the part that contains the most detailing. As with many parts of the bottle, the design can differ from manufacturer to manufacturer. However, the types of finishes that are you used the most are the 'threaded finish', 'lug finish' and 'crown finish' (Prakash, 2013). This is part of the bottle on which the closure is fastened. The famous Heineken Bottle for instance contains a crown finish, which is often found on other beer bottles.

According to CETIE (2004), the hole at the top of the bottle is simply called the 'through bore'. Girling (2003) explains that there are four basic dimensions that govern the finish of the bottle, one of which is the dimension l . The dimension l is the smallest dimension on the inside of the finish, which refers to the through bore mentioned before. A crown finish usually consists of two rings, which protrude from the outer diameter of the neck. CETIE (2020) denotes the upper ring as the 'crimp' and the lower as the 'bead'.

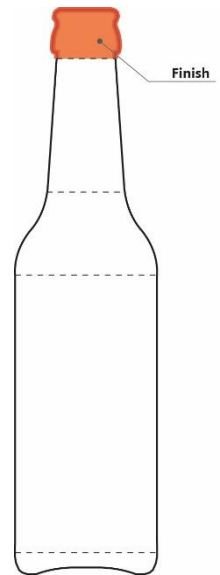


Figure 17 – The finish of the bottle

The top of the bottle is called the 'sealing surface' (CETIE, 2020) and makes contact with the seal. For the modelling of glass bottles, the vertical force which is introduced during manufacturing or stacking is introduced on the sealing surface (Davis, 2009). On inspection, whilst the finish contains protuberances in the form of the crimp and bead, the inside of the finish is rather smooth, which means that the crimp and the bead are one of the thickest parts in a glass bottle.

3.2. Coatings and surfaces of glass bottles

It is important to understand the behaviour on the surface of the glass bottle for strength evaluations, modelling and possible connections with adhesives or cementitious materials later on. This chapter contains a literature study on the outer surface of glass bottles, coatings and their effect on the mechanical behaviour of an individual glass bottle.

The large difference between the usable strength of glass and the intrinsic strength is due to the surface flaws that are created on the glass surface during its lifecycle (Guin & Gueguen, 2019). Similarly, a quote from Southwick *et al* (1981) formulates the following:

"The one major factor governing the strength of glass is the condition of the surface (Southwick et al, 1981)."

3.2.1. Glass Bottle Coatings in general

For the current design of glass bottles, two separate coatings can be distinguished on the surface of glass bottles: hot-end coatings and cold-end coatings. These coatings are applied for strength preservation during the life cycle of the bottle (CETIE, 2020). Both coatings have different attributes that help with this strength preservation of the surface of the bottle.

3.2.2. Hot End Coatings

Hot end coatings are applied on the bottle after moulding and before the annealing process (CETIE, 2020). The molecule mono-butyl tin tri-chloride (MBTC) is used as a precursor for the application of tin oxide (SnO_2) on the surface of the glass bottle (Smay, 2017). The process of applying this tin oxide on the surface is also known as chemical vapour deposition (CVD) (Nakawaga *et al*, 1997). The temperature of the glass surface of the bottle is usually between 400 and 500 degrees Celsius (Nakawaga *et al*, 1997). The material MBTC tends to break down on the glass surface at high temperatures, which means that the layer of tin oxide might not fully cover the glass surface (Roos *et al*, 2014).

The thickness of the hot-end coating can vary a lot. Nakawaga *et al* (1997) mentions a typical hot-end coating thickness of 40 nm. In comparison, Penlington (2000) mentions a typical hot-end coating thickness between 2 and 10 nm, whilst Smay (2017) mentions a conventional thickness of about 40 CTU. For optimum bursting pressure, scratch resistance and coefficient of friction, Bhargava *et al* (2000) indicate a hot-end coating thickness of about 50 CTU. The unit CTU means 'Coating Thickness Unit' and 1 CTU equals about 0.25 nm (Hoekman, 2019) in the case of SnO_2 coating. Likewise, Roos *et al* (2014) also indicate that 1 CTU equals about 0.25 nm.

Hot-end coatings help with the application and adhesion of the cold-end coatings. Penlington (2000) mentions the function of the hot-end coating as being a 'bond coat', and the adhesion of the cold-end coating is improved with the introduction of the hot-end coating (Robertson, 2012). The reason for this is that tin-oxide is more hydrophobic than a general glass surface and has therefore a better attraction towards the cold-end coating (organic compounds) than glass (Patano, 2016). Bhargava *et al* (2000) explain that the hot-end coating can actually be seen as a 'primer' for the cold-end coating. Moreover, hot-end coating lowers possible surface damage between moulding and annealing (Robertson, 2012). A quote from Nakawaga *et al* (1997) formulates the following:

*'The surface treatment of one-way bottles with a SnO_2 or TiO_2 coating is an established practice of providing an abrasion resistant surface, and this effect has been well documented during about 20 years (Nakawaga *et al*, 1997).'*

3.2.3. Cold End Coatings

Cold-end coatings come in a wide variety of options, such as polyethylene emulsions, waxes and glycols (CETIE, 2020). The most common combination with the before-mentioned tin oxide is however polyethylene (Gauthier, 1995). Cold-end coating usually takes place at a temperature of less than 100 degrees Celsius (Robertson, 2012) or as mentioned by Jackson & Ford (1981) between 90 and 150 degrees Celsius. Whilst the hot-end coating mainly acts a primer, cold-end coating meanwhile is the reason for an increase in lubricity and decrease of coefficient of friction (Bhargava *et al*, 2000). Glass in itself is a non-lubricious material and this surface treatment helps with preserving the strength (Robertson, 2012). The thickness of the cold-end coating is smaller in comparison with the hot-end coating, ranging from 1 to 2 nm (Bhargava *et al*, 2020). However, Davis (2009) mentions that the effectiveness of these coatings is lost after three or five lifecycle for returnable bottles, which means that the lubricity and therefore resistance to abrasion will decrease.

3.2.4. Hot-End and Cold-End Coatings: Mechanical behavior

Southwick *et al* (1981) found coefficients of friction of the surface depending on the presence and type of the coating. A glass bottle surface with only a hot-end coating has a coefficient of friction of 0.38, which was constant over 50 tests, whereas a glass bottle surface with both hot-end coating and cold-end coating had a coefficient of friction of 0.03 (Southwick *et al*, 1981).

In the same paper, the effect of glass bottle coatings on the mechanical performance was investigated. In table 2, the relative measured strengths are shown with their corresponding coating condition. The reference value is the bottle that is both uncoated and damaged.

<i>Coating Condition</i>	<i>Impact</i>	<i>Pressure</i>	<i>Vertical load</i>
Uncoated and damaged	1.0	1.0	1.0
Uncoated	2.65	3.16	2.68
Heavy Hot-End Coating	3.86	2.47	2.71
Heavy Hot-End Coating and damaged	2.67	2.44	2.66
Medium Hot-End Coating, Cold-End Coating, Cold-End Coating and damaged	3.67	3.00	2.66
Heavy Hot-End Coating, Cold-End coating and damaged	3.71	2.53	2.74

Table 2 – Relative measured strengths compared by coating condition (Southwick et al, 1981)

Comparing the *uncoated damaged, heavy hot-end damaged, heavy hot-end cold-end damaged*, it can be seen that the strength increases for impact strength and internal pressure. However, the relative measured strength is lower for heavy coating of ‘hot-end, cold-end and damaged’ than for medium coating in case of internal pressure. This means that there is a certain optimum coating thickness for the internal pressure. This phenomenon was captured by Bhargava *et al* (2000), where the maximum internal bursting pressure would increase with an increasing coating thickness to about 50 CTU, after which it would decrease. The amount of coating does not seem to have an effect on the measured strengths for vertical load. However, it can be seen that the measured strength rather stays the same when comparing the coated damaged and coated not-damaged bottles. The same cannot be said for uncoated damaged and uncoated not-damaged bottles.

3.2.5. Glass bottle coatings and adhesives

It has been shown that the combination of hot-end coating and cold-end coating can have an effect on the mechanical behaviour of a glass bottle, and more importantly on the preservation of the surface strength of these bottles. However, it should be checked whether this increase in lubricity has an effect on the adhesion of possible adhesives for structural purposes.

There are many examples out there where waste glass cullet from bottles is used as aggregate in concrete mixtures. However, Dawson (2012) explains that using glass cullet from glass bottles in mixtures is rather difficult because of the smooth surface. This could be down to the low coefficient of friction and high degree of lubricity of the surface. Nevertheless, whole glass bottles have been used in combination with Portland cement into structural walls (Dawson, 2012).

For the primary use of the bottles, it was investigated whether these coatings have an effect on the adhesion of labels on the bottles. The labels themselves are not of high importance, but the adhesion properties of the surface of the bottle are. To discover which types of adhesives are suited for glass bottles for a structural purpose, or which problems might occur with these bottles, it is important to study the effect of these coatings on the adhesion of adhesives. Kothe & Weller (2014) refer to the quality of the surface as being major factor for the adhesion properties. The coverage of cold-end coating or 'wettability' of the surface can be found by making contact angle measurements, as mentioned by Kothe & Weller (2014), Smay (2017) and Levene (1989).

During a contact angle measurement, a polar liquid, for instance water, is dropped on a surface and the angle between the droplet and surface is called the contact angle. The angle between the droplet and the surface is also explained by Smay (2017) as: *'The angle that the periphery of the droplet made with the glass surface (Smay, 2017)'*. It has to be understood why this contact angle measurement is of such importance and what kind of information it can acquire. A quote from Kothe & Weller (2014) summarizes this relationship:

"Thereby, the contact angle depends on the energetic interaction between surface and the chemical compositions and the topography of the solid (Kothe & Weller, 2014)."

In other words, contact angle measurements can show how much cold end coating is present on the bottles. The relationship between contact angle and coverage has already been found by Smay (2017) and is shown in figure 18.

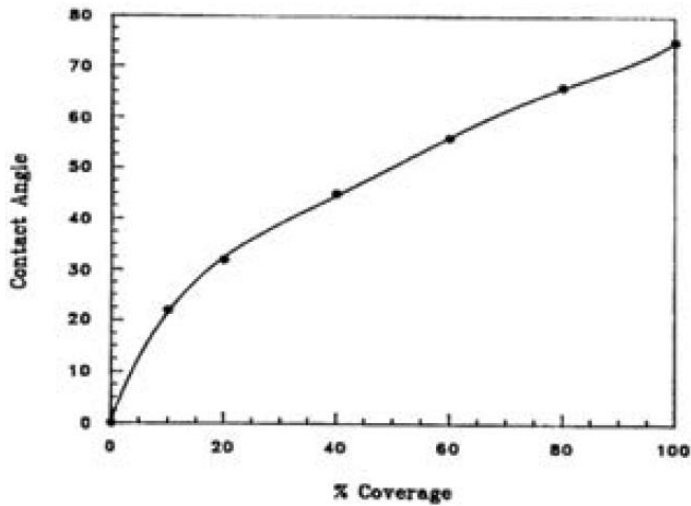


Figure 18 – Relationship between contact angle and surface coatings for polyethylene cold end coatings (Smay, 2017)

Because the material polyethylene is non-polar, the high amount of polyethylene can cause the surface to become more hydrophobic (Levene, 1989). Similarly, Smay (2017) mentions that high amounts of polyethylene can cause the surface of the bottle to show chemical behaviour similar to plastics rather than glass. Therefore, adhesives that have glass as intended substrates can have substandard adhesion. A contact angle of about 75 degrees refers to a completely covered surface (Smay, 2017) Likewise, Levene (1989) indicates that a contact angle in the range of 60 to 70 degrees refers to a surface completely covered with polyethylene.

4 Mechanical behaviour of individual glass bottles

In chapters 4 and 5, the goal is to answer the first sub-question of the thesis:

'What is the mechanical behaviour of an individual glass bottle subjected to vertical compressive load?'

This chapter is part of the literature study of the thesis and investigates existing literature on the mechanical behaviour of an individual glass bottle. This is important prerequisite information and knowledge for the failure tests of bottles that are performed at American Glass Research.

4.1. Surfaces and defects of glass bottles

Müller-Simon *et al* (1994) state that the strength of a container is not solely dependent on the stress distribution inside the container. Other than the before-mentioned coatings, the imperfections, flaws, inhomogeneities all play a key role in the strength of container glass. Müller-Simon *et al* (1994) found that each type of defect has their own individual distribution on a glass bottle. By testing the bursting pressure of a certain amount of beer bottles and plotting the fracture stress in Weibull-plot, a strange feature was found in the distribution. This distribution is shown in figure 19.

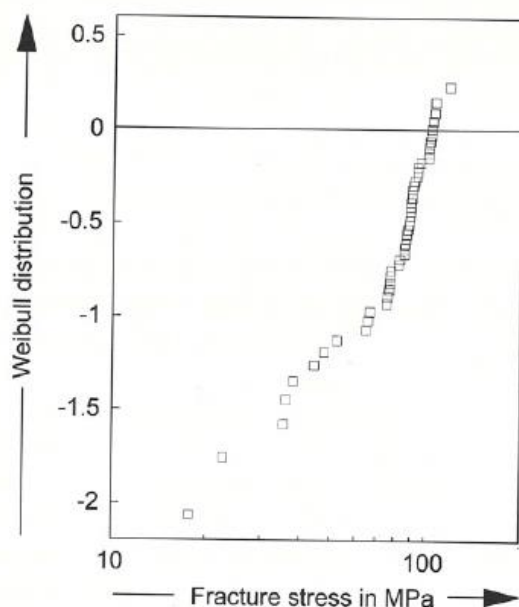


Figure 19 – Weibull distribution of the fracture stress of beer bottles (Müller-Simon, 1994)

The interesting feature is that the slope of the distribution changes at the tail of the distribution. Müller-Simon *et al* (1994) showed that this difference in slope has to do with the different types of defect and showed that this distribution is a characteristic of a certain defect. The separated curves are shown in figure 20. In their paper, a distinction is made between seed and blisters, inhomogeneities and sandblasted samples.

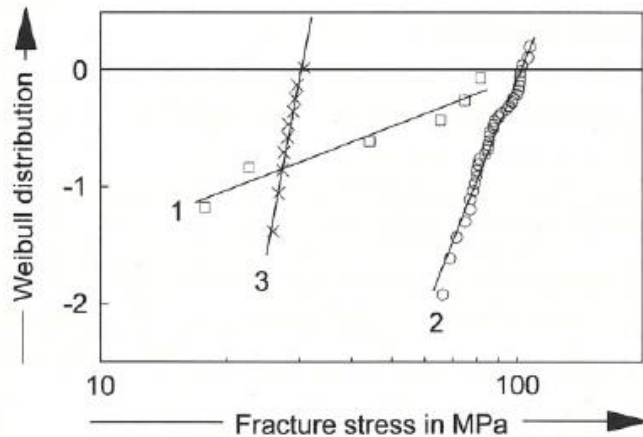


Figure 20 – Weibull distribution for the different types of defects (1 = seeds and blisters, 2 = inhomogeneities, 3 = sandblasted bottle) (Müller-Simon, 1994)

Thus, the strength of container glass is not only dependent on the presence of defects, but also the type of defect. It is therefore interesting to investigate in which regions of bottle certain defects might dominate. Müller-Simon et al (1994) concluded that fracture due to seed and bubbles mostly occurs in the side-wall of the bottle, whilst fracture due to stones and metal inclusions mostly occurs in the bottom of the bottle.

It is important to understand the possible defects that can originate during the manufacturing process of glass bottles. Aldinger & de Haan (2019) have summarized the defects in a glass bottle, which can either cause stress-increasing or strength-reducing effects. These defects are categorized under six sub-divisions: melting, dimensional, flaws, handling, ACL and tubing. The defects under the label ‘melting’ and ‘flaws’ will be covered:

- **Cord:** Inclusion of a glassy material inside the bottle with different properties (Stress-increasing)
- **Knots:** These fall under the term ‘stones’ and are also glassy inclusions on the inside surface (Usually stress-increasing)
- **Seeds and blisters:** Seeds are simply inclusions of gas inside the glass. Blisters are larger versions of seeds (Strength-reducing or critical)
- **Stone:** These are solid inclusions inside the glass (Strength-reducing).
- **Poor annealing:** Poor annealing can cause residual stresses to stay in the glass. (Stress-increasing)

Manufactures of glass bottles use an annealing lehr to cool down the bottles after the moulding process and application of the hot-end coating. The outer surface would cool much faster than the inner surface of the bottle without an annealing lehr, which would create tensile stresses on the inner surface of the bottle (Hann, 2013). Poor annealing can thus be a problem, because bottles would fail earlier due to the addition of these tensile stresses.

4.2. Finite-element modelling of glass bottles

Finite element models have been made to investigate the relations between the applied vertical load and the stresses inside the bottle. This has been done to understand the mechanical behavior of the glass bottle and to retrieve maximum principle stress values with the corresponding failure loads. The following plots have been made with a vertical load of 10 kN and the model contains the minimum thicknesses, as measured from samples at AGR. Figure 21 shows the vectors of the principal stresses (minimum and maximum) during

the application of vertical load. The red vector indicates principle tensile stresses and the blue vector indicates principle compressive stresses.

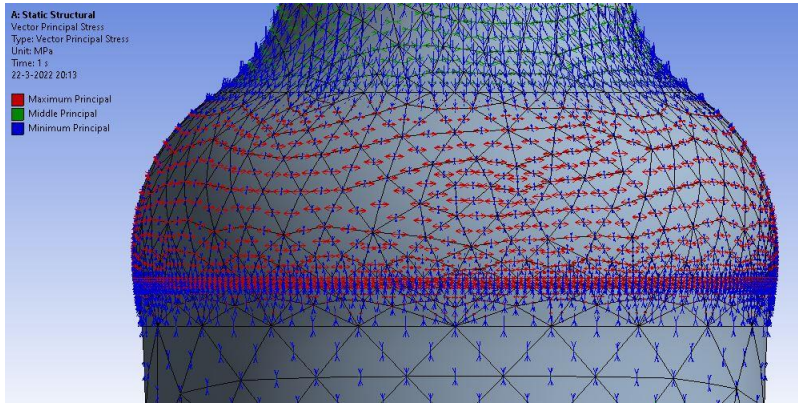


Figure 21 – Vectors of the maximum and minimum principle stresses in the shoulder region

The maximum principle stresses (σ_1) are of tensile nature in the shoulder region and they propagate in circumferential direction. It is important to check whether these stresses indeed propagate in circumferential direction.

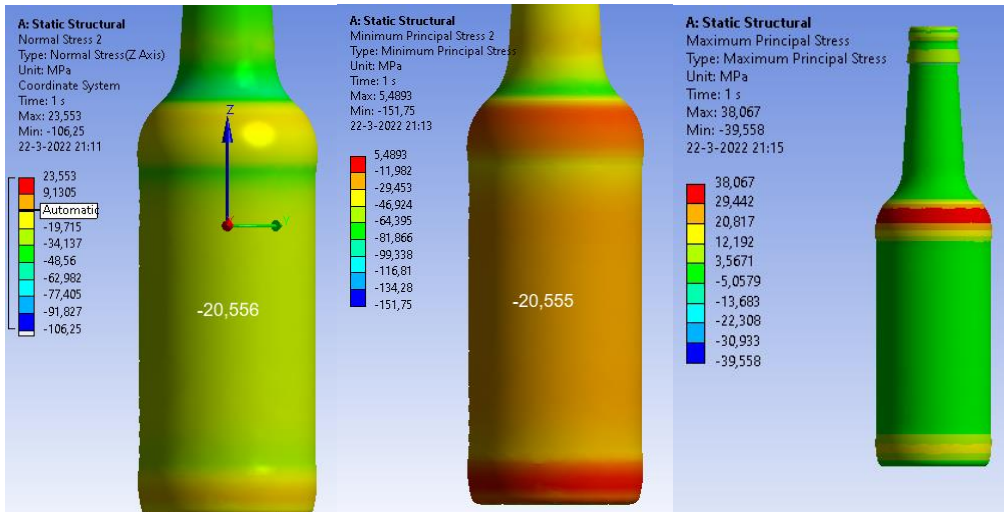
Kepple & Wasylyk (1994) mention the following on the mechanical behaviour of glass bottles under vertical loads:

- “The outside surface of the bottle will be in tension only in the heel and shoulder locations where the action of the load causes a bending of the container wall (Kepple & Wasylyk, 1994)”
- “The principal stress will be in circumferential direction, caused by the attempt of the vertical load to increase the diameter of the shoulder and heel (Kepple & Wasylyk, 1994).”
- “Typical vertical load fractures originate on the outside surface from tensile stresses oriented in the circumferential direction (Kepple & Wasylyk, 1994).”

These phenomena have been identified in both the model and the fracture of the bottles. A hand calculation can be made to check the model. For instance, the compressive stress in the body of the bottle can be calculated by using the applied vertical load, body diameter and the correct thickness. Figures 7 and 8 show values for the longitudinal stress and minimum principal stress σ_2 . This longitudinal stress can be calculated as follows with a vertical load of 10 kN.

$$\sigma_c = \frac{F}{A_{body}} = \frac{-10000}{\frac{1}{4}\pi d_{out,recess}^2 - \frac{1}{4}\pi(d_{out,recess} - 2 \times t_{body,min})^2} = \frac{-10000}{\frac{1}{4}\pi \times 58.9^2 - \frac{1}{4}\pi \times (58.9 - 2 \times 2.68)^2} = \frac{-10000}{473.343} = -21.13 \text{ MPa}$$

A value of -21.13 MPa is retrieved from the hand calculation. This comes very close to the longitudinal compressive stress and minimum principal stress retrieved from the finite element model. These are shown in figure 22 and 23.



Figures 22, 23 and 24 – Stress plots of the longitudinal stress, minimum principal stress (σ_2) and maximum principle stress (σ_2) from ANSYS

A relatively straightforward finite element model shows the phenomenon that was discussed by Southwick (1965). It was shown that under a vertical compressive load, tensile stresses will occur in and around the shoulder and heel region in both longitudinal and circumferential direction. When the results from the simple model and graphs of Southwick are compared, it showcases the two peaks in tensile stresses that are found in the shoulder and heel region. Figure 25 shows a 'vertical load stress index'-distribution against the height of the bottle.

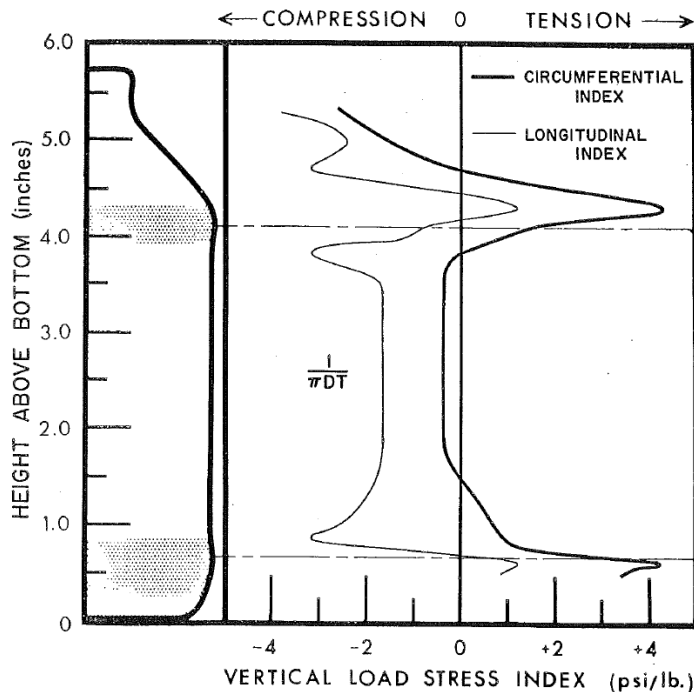


Figure 25 – Vertical load stress index against bottle height (Southwick, 1965)

B

B AGR Experiments

5 Fracture testing and FEM of individual bottles

The NEN2608 (2014) contains formulae for designing glass structures. The following formula is used for the tensile design strength for annealed glass:

$$f_{m;t,u;d} = \frac{k_a \times k_e \times k_{mod} \times k_{sp} \times f_{g;k}}{\gamma_{m,A}} \quad [1]$$

Equation 1 contains factors, such as k_a (the area factor), k_e (the edge factor), k_{mod} (the load-duration factor) and k_{sp} (surface factor). The problem is that this formula is based upon the structural use of float glass, which is different to container glass, as explained in the lab plan. The basis of these design strengths is the input of the characteristic strength. However, because the structural use of container glass is not widespread, there are no values for the characteristic tensile strength of container glass. To design structures with container glass, and more specifically in this thesis with columns out of glass bottles, characteristic tensile strength values have to be retrieved to design columns out of glass bottles.

This chapter contains experiments, finite element modelling and Weibull analyses to retrieve the characteristic tensile strength values for container glass. The retrieved values will then be discussed with existing literature wherein strength values for container glass are mentioned, but these are often ranges or averages and not characteristic. The characteristic strength is defined as the strength of the material, whereby 95% of the tested samples will surpass this threshold value.

The bottles that were used during the destructive testing were 330 ml longneck beer bottles. These were bought from *Brouwland*. The initial plan was to investigate three different bottles, each being from a different brand. However because of the difficulty of retrieving these samples and the allocated time for the thesis, the decision was made to focus on standardized bottles. Another benefit of investigating these standardized bottles is that they are not influenced by specific design features of a certain brand, for instance specific protuberances, logos etc. These standardized shapes are easier to model in a CAD program than a bottle from a specific brand. A technical drawing of the bottle is also available in combination with the bottles. This was handy for the creation of the geometry for the finite element calculations. The technical drawing is shown in Appendix A5.

Next to the measurement of the fracture loads, measurements of the dimensions, thicknesses and cold-end coating were also performed. Measurement of the cold-end coating was done to evaluate the difference in damaging between the line-simulated and manually abraded samples. The measurements were performed at American Glass Research in Delft under the guidance of dr. C. Justino de Lima. Moreover, the four weakest samples (i.e. the samples with the lowest failure load) were separated at the end for further fracture analysis under the microscope. This is done to compare the values retrieved from the finite element analysis with those from fracture analysis. These measurements were

performed at AGR. These experiments were performed to answer the first sub-question of the thesis:

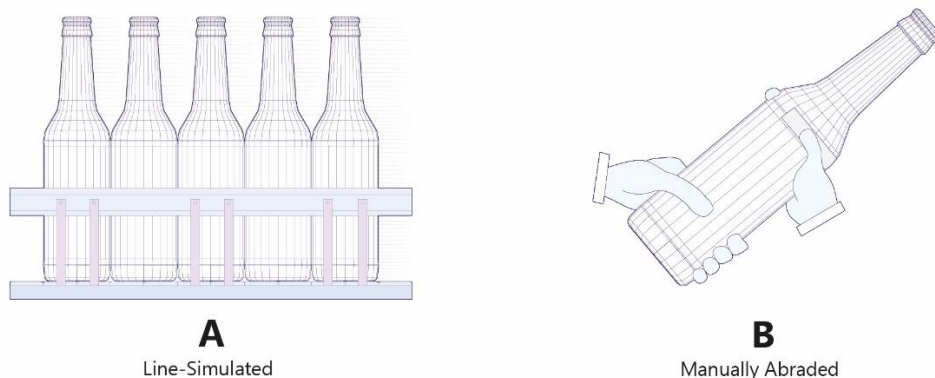
‘What is the mechanical behaviour of an individual glass bottle under vertical load’

5.1. Methodology of AGR Testing

The characteristic strength of container glass will be evaluated with the help of destructive testing and Weibull analysis. In the lab plan, it was shown that the characteristic strength of container glass has to be evaluated in order to design with the bottles. The destructive testing under which the bottles will fail is vertical load testing. This is done with the following arguments:

- Vertical load failure of standardized bottles can show the potential for vertical load carrying in structures. Other methods to test the strength of glass bottles is with the help of internal breaking pressure, but the bottles will be empty during construction. Furthermore, vertical load failure is more relevant for this thesis.
- Distinct areas with tensile principle stresses will develop in the bottles, specifically in the heel and shoulder region. Therefore, the areas of fracture can be found easily, especially in the shoulder region.
- The bottles are damaged before testing with either manually abrading the bottles or line-simulating the bottles. In both cases, the bottles are damaged in the shoulder contact and heel contact region and the damage is concentrated in those regions. This means that the bottles will fail due to a combination of damaging and mechanically applied stresses.

The destructive testing has been performed at the facility of American Glass Research in Delft. The sample size of the destructive testing is equal to 56 samples. These 56 samples are divided in two groups of 28 samples. This has to do with the fact that the maximum capacity for the line-simulator is equal to 28 bottles. The line-simulated bottles and manually abraded bottles are denoted with the index *A* and *B* respectively.



The interesting feature of the vertical load tester at AGR is that the result of the machine will show a converted value to an equivalent 3-second loading test. The manual for the vertical load tester mentions this as follows:

‘The actual force generated by the RPT2X is higher than indicated to provide an equivalent 3-second test. (AGR International, 2020).

The method to retrieve the fracture stresses for every single bottle is summarized in the diagram in figure 26.

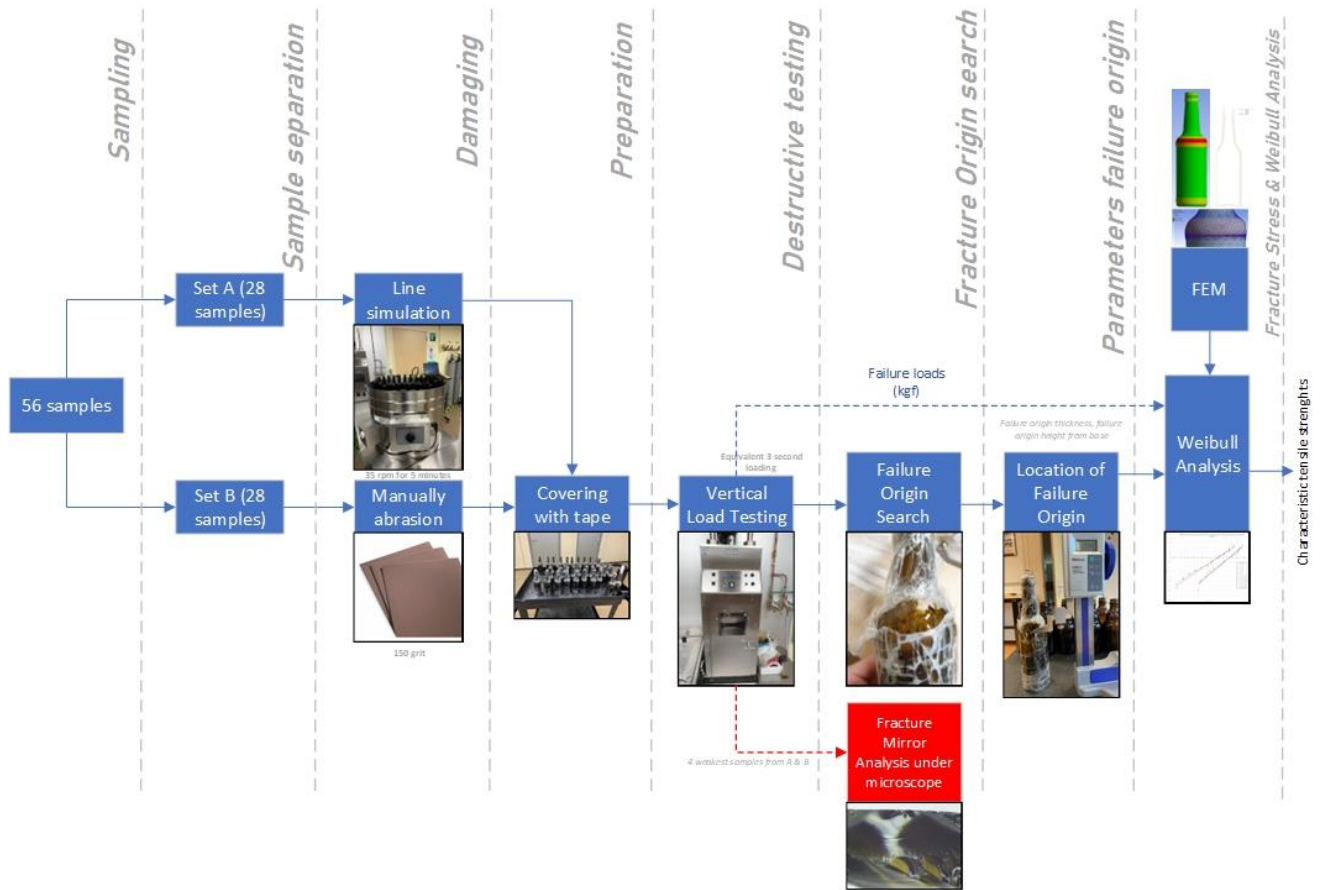
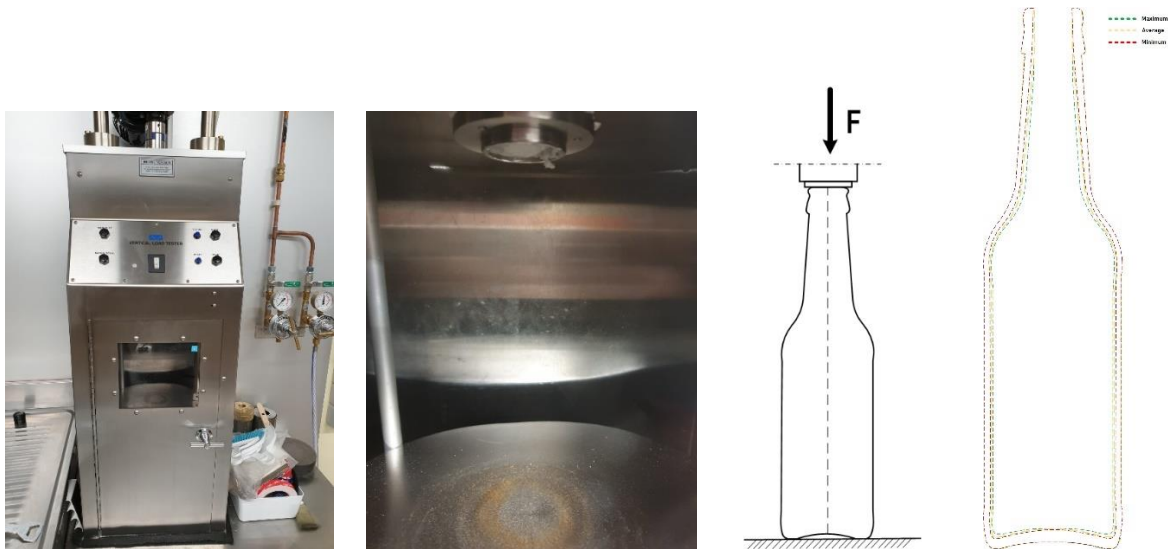


Figure 26 – Work-flow diagram of the AGR Experiments

The equivalent loading time of the machine will come in handy later on when the influence of load duration is taken into account. In the design of (glass) structures, this load duration factor is shown with the factor k_{mod} . This factor will be used when designs of the columns are made. This experiment however solely focuses on the retrieval of the characteristic strength. Figure 27 shows the machine used for the destructive vertical load testing. In addition, figure 28 shows the inside of the machine.

An important note to make is that the dimensions of the bottles cannot be measured before the destructive testing. This is due to the fact that measurements can induce damage on the surface of the bottle, which can cause a bias in the test results. Therefore, separate samples are used to measure the thickness at specific regions. This data will give minimum, average and maximum thicknesses of the bottle. These three different thicknesses are then used to create three different models, each with another thickness value. Figure 29 shows a schematic of the testing with the corresponding vertical load and boundary condition at the bottom. Figure 30 gives a visualization of the three different thickness distributions.



Figures 27, 28, 29 and 30 – The vertical load tester used at AGR, the inside of the vertical load tester, schematic of the vertical load testing on the used samples and the three different thickness distributions of the glass bottle

5.2. Damage evaluation of glass bottles

In addition to the destructive testing, the amount of surface coverage of the cold-end coating was measured on the damaged samples before testing. This was done to compare the amount of cold-end coating lost due to damaging by either line-simulated and manually abrading. This is done with contact angle measurement, with which a water droplet on the surface can indicate how much cold-end coating is present. Lower contact angles would indicate a smaller amount of cold-end coating left. Table 3 gives a summary of these tests, and it can be seen that the manually abraded samples have a smaller amount of cold-end coating left, which would indicate a higher degree of damaging. Therefore, the expectation is that the samples that are manually abraded should show lower fracture strengths than the line-simulated samples. The relation between contact angle and surface coverage of cold-end coating was made with the help of a graph in a study by Smay (2017).

Samples	Contact Region	Contact angle (degrees)	Surface coverage (%)
Line-simulated	Shoulder	45.22	44
	Heel	46.40	43
Manually abraded	Shoulder	23.55	12
	Heel	29.18	16

Table 3 – Measured contact angles on line-simulated and manually abraded and corresponding surface coverage of cold-end coating

5.3. Weibull Analysis

It was mentioned in the lab plan that the characteristic strength value of glass is the value where 95% of the samples would surpass this threshold value. In this report, the characteristic strength is noted with the symbol $\sigma_{0.05}$ (the stress at $P = 0.05$). Formally, the symbol f_k is used to denote the characteristic strength. The unit of these values in this report is in MPa.

The cumulative distribution function of the Weibull-distribution is formulated in the following formula (Kinsella & Persson, 2016) in equation 2:

$$F_x(x) = 1 - \exp \left[- \left(\frac{x}{x_0} \right)^m \right], x \geq 0 \quad [2]$$

In this case, x_0 and m are the Weibull parameters. Parameters for x_0 and m are also called the scale parameter and shape parameter. There are many ways to retrieve the values for these parameters, but in this report the parameters are found with the help of linear regression.

Datsiou & Overend (2018) use the following cumulative distribution function for the Weibull distribution of the fracture stress in equation 3:

$$P_f = 1 - \exp \left[- \left(\frac{\sigma_{f,60}}{\theta} \right)^\beta \right] \quad [3]$$

In this case, θ is the scale parameter and β is the shape parameter. Datsiou & Overend (2018) use the fracture stress $\sigma_{f,60}$, which is the fracture stress with a reference loading time of 60 s.

By rearranging equation 3 and by taking the natural log twice of both sides, equation 4 is found:

$$\ln \left(\ln \left(\frac{1}{1 - P_f} \right) \right) = \beta \cdot \ln \sigma - \beta \cdot \ln \theta \quad [4]$$

This equation is equivalent to a standard linear equation of $y = ax + b$. Microsoft Excel provides a feature with which the equation of a fitted linear line can be found and the corresponding goodness of fit can be found (R^2). The only unknown in this equation is the probability of failure P_f . However, this value can be estimated with the use of probability estimators. The data set is sorted in order from lowest fracture stress to highest fracture stress. The weakest value receives the index 1 and the strongest value will receive index n . The probability is then estimated with the help of four probability estimators. The standardized form of this probability estimator is as follows (Datsiou & Overend, 2018):

$$E_j = \frac{i - C_j}{n + 1 - 2C_j} \quad [5]$$

This standardized formula is used to develop four different probability estimators. This means that multiple Weibull plots are made and that a judgement is made based upon the goodness of fit.

$$E_1(\text{mean}) = \frac{i}{n + 1} \quad [6]$$

$$E_2(\text{Hazen's}) = \frac{i - 0.5}{n} \quad [7]$$

$$E_3(\text{median}) = \frac{i - 0.3}{n + 0.4} \quad [8]$$

$$E_4 (\text{small sample}) = \frac{i - 0.375}{n + 0.25} \quad [9]$$

Now that the fitted Weibull plot and the corresponding equation is known, estimations can be made of the average fracture stress $\sigma_{0.5}$ and the characteristic fracture stress $\sigma_{0.05}$.

5.4. Results of the AGR Tests

The results of the destructive testing have been summarized in table 4 for both the line-simulated and manually abraded samples. Failure loads are shown in kg_f (kilogram-force) in combination with the location of the fracture origin.

Line Simulated			Manually abraded		
Sample nr.	Vertical failure load kg_f	Fracture Origin Location	Sample nr.	Vertical failure load kg_f	Fracture Origin Location
A1	1825	Shoulder Contact	B1	1820	Heel Contact
A2	1790	Shoulder Contact	B2	1390	Shoulder Contact
A3	1835	Shoulder Contact	B3	1410	Shoulder Contact
A4	1865	Shoulder Contact	B4	1900	Shoulder Contact
A5	1885	Heel Contact	B5	1355	Shoulder Contact
A6	1460	Shoulder Contact	B6	2050	Heel Contact
A7	1555	Shoulder Contact	B7	1725	Shoulder Contact
A8	1450	Shoulder Contact	B8	2040	Shoulder Contact
A9	1845	Shoulder Contact	B9	nb (>2050)	No break
A10	1360	Heel Contact	B10	1515	Shoulder Contact
A11	1025	Heel Contact	B11	1370	Shoulder Contact
A12	1495	Shoulder Contact	B12	1950	Shoulder Contact
A13	nb (>2050)	No break	B13	1890	Shoulder Contact
A14	1545	Shoulder Contact	B14	2050	Shoulder Contact
A15	1770	Shoulder Contact	B15	1845	Heel Contact
A16	1815	Shoulder Contact	B16	1835	Shoulder Contact
A17	1765	Shoulder Contact	B17	1740	Shoulder Contact
A18	1795	Shoulder Contact	B18	1595	Shoulder Contact
A19	1870	Shoulder Contact	B19	2045	Heel Contact
A20	1015	Heel Contact	B20	1855	Shoulder Contact
A21	1970	Shoulder Contact	B21	1690	Shoulder Contact
A22	1970	Shoulder Contact	B22	2045	Heel Contact
A23	1670	Shoulder Contact	B23	1725	Shoulder Contact
A24	1560	Shoulder Contact	B24	1140	Heel Contact
A25	1590	Shoulder Contact	B25	1675	Shoulder Contact
A26	1155	Shoulder Contact	B26	1630	Shoulder Contact
A27	1630	Shoulder Contact	B27	nb (>2050)	No break
A28	1430	Shoulder Contact	B28	2000	Shoulder Contact
Summary			Summary		
Total samples:	28		Total samples:	28	
Shoulder Contact	23		Shoulder Contact	20	
Heel Contact	4		Heel Contact	6	
No break	1		No break	2	
Average	1643 kg_f (16.11 kN)		Average	1764 kg_f (17.30 kN)	
Minimum	1015 kg_f (9.96 kN)		Minimum	1140 kg_f (11.18 kN)	
Maximum	2050 kg_f (20.11 kN)		Maximum	2050 kg_f (20.11 kN)	

Table 4 – Summary of the failure loads of both line-simulated and manually abraded samples

Besides measuring the failure loads of every bottle, the location of the fracture origin and thickness of the fracture origin have to be measured. The failure loads themselves do not reveal the strength of the material used in the bottle, because the strength of the bottle is dependent on the thickness and possible defects. For instance, the minimum vertical load for the line simulated samples is equal to 1015 kg_f . The minimum vertical load of the manually abraded samples is equal to 1140 kg_f . This does not mean that the manually abraded samples are stronger, because the distribution of the thickness of the glass across samples can vary quite significantly. Therefore, the failure load has to be converted to a failure stress.

As mentioned before for the design of glass bottles, the stress and strength index are terms often used to describe the relation between the stress and applied load. Generally, this relation is formulated in the following manner:

$$SI = \frac{\sigma}{F} \quad [10]$$

Bottles that have a similar design and thickness distribution will reveal the same strength index. However, this strength index can change depending on the thickness. An example of the latter is shown in figure 31. This graph showcases the principal stress index for the finite element models in the shoulder region. The failure load that was applied to create this graph was equal to 10 kN. By dividing the principal tensile stress by the applied load, the strength index can be shown for different models (i.e. the same design with different thicknesses). The red line shows the principle tensile stresses with the minimum thickness of 2.18 mm and the blue line shows the principle tensile stress with the maximum thickness of 3.13 mm. Next to these two models, a third model was created that used an average thickness of 2.66 mm.

The data from the maximum and minimum thickness models are used to predict the principle stress for any other thickness. This is due to complex nature of the geometry of the shoulder. The principle stresses from the model with an average thickness of 2.66 mm is shown in light green, whilst the estimation of a bottle with a thickness of 2.66 mm by using the data from the two previous models is shown with the dotted dark green line. It shows that the estimation comes close to the values found in the model. The maximum difference between the estimation and the model values for average thickness was equal to 0.187 MPa/kN or in this case 1.87 MPa with a failure load of 10 kN.

The estimation is based upon linear interpolation between the two boundary values for minimum and maximum thickness. Formally, this estimation can be shown in the following formula:

$$SI_{estimation} = \frac{(SI_{t_{min}} - SI_{t_{max}})}{t_{max} - t_{min}} \cdot (t_{min} - t_{estimation}) + SI_{t_{max}} \quad [11]$$

This interpolation can help with finding the failure stress values for samples with different thicknesses.

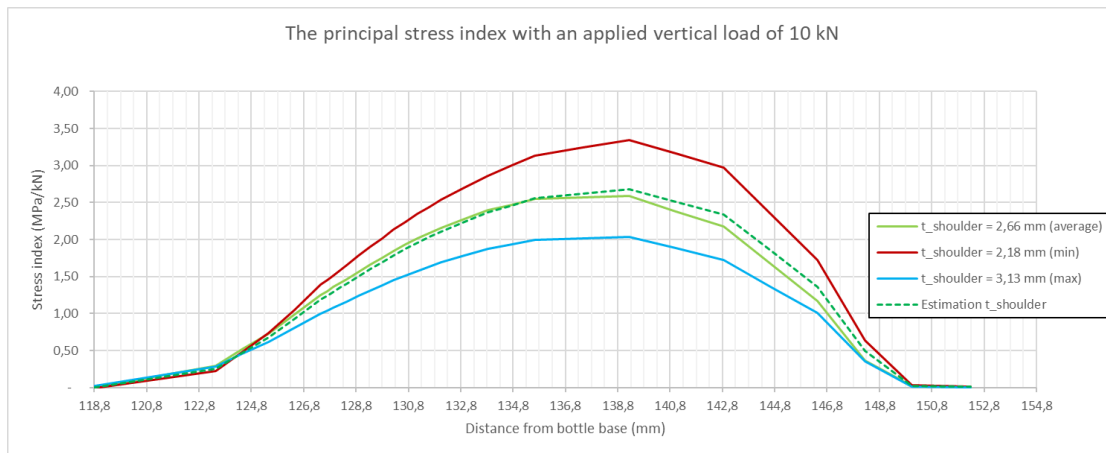


Figure 31 – The tensile principal failure stress from applied vertical load in the shoulder region for different shoulder wall thicknesses

From this stage, the samples with shoulder contact failure and heel contact failure are separated. Failure analysis on samples with heel contact failure is difficult, because the failure origin is difficult to find in the heel contact region and the heel region is often obliterated after destructive testing, which means that exact location of the failure origin is missing. The samples with shoulder contact failure are therefore used to analyse the strength of the material for both the line simulated and manually abraded bottles.

The values for the maximum principle stress at failure can then be sorted in order of lowest to highest stress. Four probability estimators are used to perform Weibull analysis. All four of them will provide different estimations for the failure probability, but a choice is made by observing the goodness of fit of the linearized Weibull plots.

The formulae that were mentioned before can be applied on the probability estimators and fracture stresses and they can be plotted in a Weibull plot. Microsoft Excel provides equations and goodness of fit for linear trendlines. This means that there are eight linear equations in total: four for the line-simulated samples and four for the manually abraded samples.

A horizontal shift between the line-simulated fracture stress data and the manually abraded data can clearly be seen in the combined Weibull plot. This horizontal shift is essentially the difference in fracture strengths between the manually abraded and line-simulated samples. This was expected, because the manually abraded samples have undergone more severe damage than the line-simulated samples. The results of the testing show a characteristic tensile strength of container glass for line-simulated samples of about **27 MPa** and for manually abraded samples of about **20 MPa**. The corresponding Weibull parameters, fitted line formulae and goodness of fit for different probability estimators are summarized in table 5 and 6.

Probability Estimators	Fitted line formula	Goodness of fit R^2	Weibull Parameters		Predicted fracture stress values	
			θ	β	$\sigma_{f,0.5} (MPa)$	$\sigma_{f,0.05} (MPa)$ $= f_{g;k}$
E_1	$y = 5.6256x - 21.679$	0.9689	47.164	5.6256	44.189	27.817
E_2	$y = 6.303x - 24.263$	0.9486	46.967	6.303	44.313	29.318
E_3	$y = 5.9919x - 23.076$	0.962	47.049	5.9919	44.258	28.660
E_4	$y = 6.1002x - 23.489$	0.956	47.018	6.1002	44.276	28.894

Table 5 – Predicted fracture stress values for different estimators in MPa for line-simulated samples

Probability Estimators	Fitted line formula	Goodness of fit R^2	Weibull Parameters		Predicted fracture stress values	
			θ	β	$\sigma_{f,0.5} (MPa)$	$\sigma_{f,0.05} (MPa)$ $= f_{g;k}$
E_1	$y = 4.4639x - 16.483$	0.987	40.146	4.4639	36.981	20.638
E_2	$y = 5.1401x - 18.944$	0.9789	39.866	5.1401	37.123	22.369
E_3	$y = 4.8252x - 17.798$	0.984	39.897	4.8252	37.062	21.606
E_4	$y = 4.934x - 18.194$	0.9826	39.944	4.934	37.084	21.878

Table 6 – Predicted fracture stress values for different estimators in MPa for manually abraded samples

Figure 32 shows the Weibull plots for the two datasets with different probability estimators.

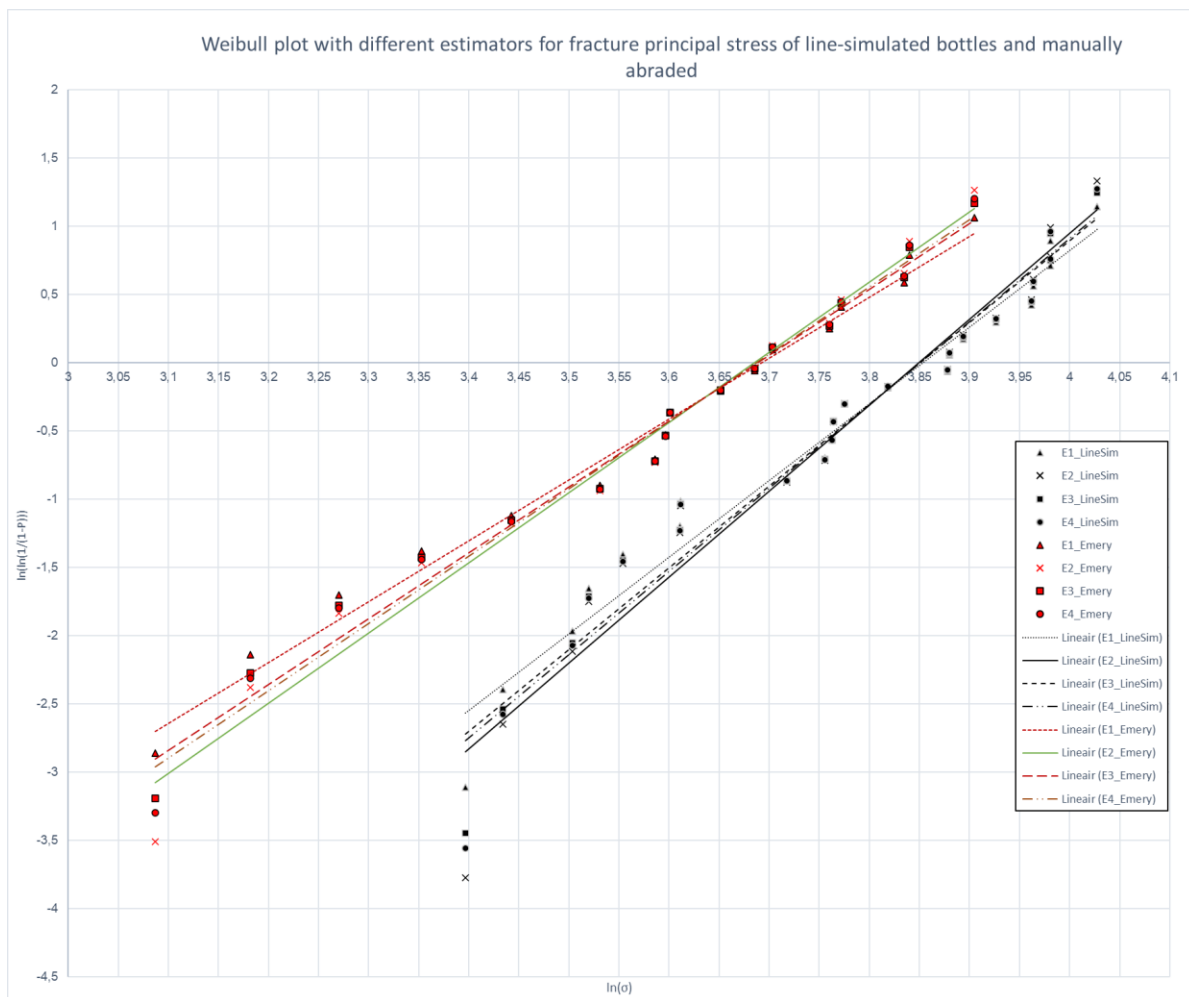


Figure 32 – Weibull plots for manually abraded (red) and line-simulated (black) samples

Similarly, a Weibull plot can be made with failure stress on the horizontal axis instead of the natural logarithm of the failure stress. This is shown in figure 33.

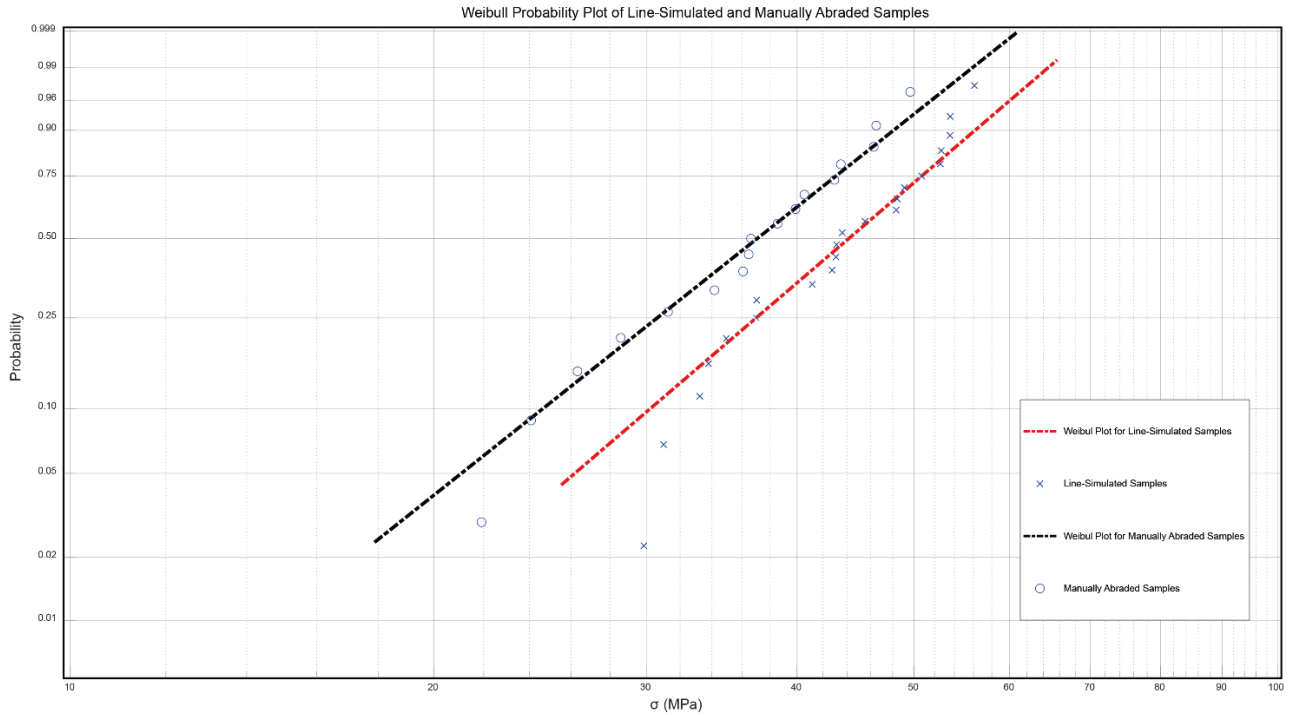


Figure 33 – Weibull plot with fracture stress on the horizontal axis from Matlab

5.5. Verification with second model in DIANA

Previously, the stress values were found by using models from ANSYS and linear interpolation with stress indices. DIANA FEA is used to check these stress values. Diana FEA works with regular curved shell elements which can be assigned a certain thickness. The input value for this thickness is the thickness of the fracture mirror from every sample. This is done and a comparison is made with the earlier found values. This is shown in table 7.

ANSYS+Interpolation				DIANA FEA				DIFFERENCES			
Line-simulated		Manually Abraded		Line Simulated		Manually Abraded		Difference Line Simulated	Error %	Difference Manually Abraded	Error %
Sample	Fracture Stress σ_1 (MPa)	Sample	Fracture Stress σ_1 (MPa)	Sample	Fracture Stress σ_1 (MPa)	Sample	Fracture Stress σ_1 (MPa)				
A1	43.077	B3	31.272	A1	38.551	B3	31.896	4.527	10.5	0.624	2.0
A2	53.556	B4	49.637	A2	51.867	B4	49.391	1.69	3.2	0.246	0.5
A3	48.325	B7	46.519	A3	52.291	B5	46.982	3.965	7.6	0.463	1.0
A4	52.660	B8	36.631	A4	55.273	B6	40.463	2.613	4.7	3.831	9.5
A6	36.997	B10	24.086	A6	36.797	B7	27.592	0.201	0.5	3.507	12.7
A7	49.091	B12	43.479	A7	46.623	B8	47.231	2.469	5.0	3.752	7.9
A8	33.785	B13	42.955	A8	34.700	B10	44.327	0.915	2.6	1.372	3.1
A9	53.573	B14	38.535	A9	54.089	B12	41.812	0.516	1.0	3.277	7.8
A12	33.226	B16	46.296	A12	35.167	B13	47.563	1.941	5.5	1.267	2.7
A14	43.132	B17	36.086	A14	43.221	B14	40.406	0.089	0.2	4.320	10.7
A15	48.422	B18	34.168	A15	48.373	B16	36.321	0.048	0.1	2.153	5.9
A16	45.539	B20	39.876	A16	46.0335	B17	42.168	0.495	1.1	2.292	5.4
A17	34.945	B21	26.313	A17	35.107	B18	30.461	0.157	1.7	4.149	13.6
A18	31.010	B23	36.471	A18	33.838	B20	38.589	2.828	8.4	2.118	5.5
A19	37.029	B25	28.576	A19	34.577	B21	31.884	2.452	6.6	3.308	10.4
A21	56.100	B26	21.910	A21	56.424	B23	26.941	0.325	0.6	5.031	18.7
A22	52.571	B28	40.565	A22	50.782	B25	44.943	1.79	3.4	4.378	9.7
A23	50.730			A23	49.873			0.857	1.7		
A24	41.179			A24	39.385			1.793	4.4		
A25	43.605			A25	42.695			0.911	2.1		
A27	42.766			A27	42.564			0.2017	0.5		
A28	29.865			A28	30.813			0.948	3.1		

Table 7 – Comparison of two models for stress evaluation and differences

It can be observed that the difference between the two methods depends on how close the thickness of the mirror is to the average thickness measured. The closer these values are, the better results from the estimation method. In the contrary, Diana FEA uses the exact thickness as input for the values. Therefore, Weibull plots are also made with the values from DIANA FEA and compared with those from ANSYS+Interpolation method.

5.6. Verification of Weibull parameters

An online tool (Timonpeters.de) exists to generate Weibull plots and parameters for a given list of numbers. This is used to verify the parameters that were previously found. This is shown in table 8.

	Excel method (best fit)		Timonpeters.de tool ($\frac{i}{n+1}$)	
	Line-Simulated	Manually Abraded	Line-Simulated	Manually Abraded
Linear equation	$y = 5.6256x - 21.679$	$y = 4.4639x - 16.483$	$y = 5.6256x - 21.679$	$y = 6.3030x - 24.263$
R^2	0.9689	0.987	0.9689	0.987
β	5.6256	4.4639	5.6256	4.4639
θ	47.164	40.146	47.161	40.145
$\sigma_{f,0.5}$	44.189	36.981	44.187	36.980
$\sigma_{f,0.05}$	27.817	20.638	27.816	20.375

Table 8 – Comparison between Excel method and Timonpeters.de tool for Weibull Parameters

5.7. Discussion of AGR Tests

The characteristic fracture stresses have been evaluated with the help of Weibull analysis. It is important to investigate whether these values are similar in order of magnitude to values from the literature. Because the literature for the strength of container glass does not specifically mention the *characteristic strength of container glass*, it is difficult to compare values exactly one to another. Firstly, in a study by Hu *et al* (2016), typical values for the surface strength of soda-lime glass have been mentioned. These are often used for proof-of-design of glass bottles. These values have been summarized for an equivalent reference time of 3 seconds, similar to the results from the Vertical Load Tester. These values are shown in table 9.

Surface state	Strength from 3 seconds loading $f_{t,surface,avg}$ (MPa)
<i>Pristine Inside</i>	424.0
<i>Pristine Molded</i>	169.6
<i>Mild/Moderate Abrasions</i>	42.4
<i>Moderately Severe Abrasions</i>	28.4

Table 9 - Typical surface strengths of soda-lime silica glass in MPa (Hu *et al*, 2016)

A tensile strength value of 42.4 MPa has been given for mild-moderate abrasions and a value of 28.4 MPa has been given for moderately severe abrasions. However, the term 'typical' in this case does not explain whether these values are average or minimum values. After some discussion with dr. C. Justino de Lima, it became clear that these values are average values based upon past experiments from AGR, which would resemble the $\sigma_{f;0.5}$ values (fracture at 50% of the samples). The line-simulated samples had a value of **44.189** MPa and the manually abraded had a value of **36.981** MPa. This comes close to the values mentioned by Hu *et al* (2016) for mild/moderate abrasions and moderately severe abrasions. Moderately severe abrasions can be created with the use of 150 grit emery paper, which was the case with the manually abraded-samples.

Similarly, a study from Müller-Simon *et al* (1994) shows ranges for the strength of container glass based upon finite element calculations, internal pressure testing and with the help of fracture mirror analysis. This has been done for different types of defects.

Type of defect	Strength f_t (MPa)	Determination method
<i>Sandblasted</i>	27 to 30	FEM
<i>Bubbles</i>	20 to 80	
<i>Inhomogeneities</i>	70 to 100	
<i>Bubbles</i>	40 to 220	Fracture Mirror Analysis
<i>Inhomogeneities</i>	130 to 220	

Table 10 - Strength values of container glass (Müller-Simon *et al*, 1994)

The range that is interesting in this case is for the sandblasted bottle, which would be similar to the manually abraded bottles with emery paper. The strength of container glass with this defect is between the 27 and 30 MPa, which again comes close to the values found in the results (i.e. 20.638 MPa characteristic fracture stress for manually abraded samples and an average value of 36.981 MPa). Jackson & Ford (1981) formulate a tensile strength range of glass containers between 30 and 40 MPa.

In another study from Davis (1994) the breaking stresses for a glass bottle were mentioned for specific areas of the bottle (i.e. shoulder contact, heel contact etc.). These are summarized in table 11.

Contact areas	Minimum breaking stress	Average breaking stress	Maximum breaking stress
	$\sigma_{f,min} (MPa)$	$\sigma_{f,avg} (MPa)$	$\sigma_{f,max} (MPa)$
Shoulder	48.27	96.52	186.16
Heel	48.27	96.52	172.37

Table 11 - Breaking stress from a typical glass bottles in MPa (Davis, 1994)

The values from this source are related to undamaged bottles. The minimum fracture stress in the shoulder contact region is typically 48.27 MPa, which is higher than the results found in this experiment. This is logical, because the samples used in these experiments have purposely been damaged before the destructive testing. The strength of the surface of glass is dependent on the degree of damage on that surface.

Finally, the graph previously shown in figure 19 with Weibull lines of different defects with the sandblasted bottles shows a fracture stress of about 20 MPa for a P_f -value of 0.05 on the vertical axis ($\ln\left(\ln\left(\frac{1}{1-0.05}\right)\right) = -2.97$).

5.8. Conclusion on AGR Tests

The goal of these experiments was to retrieve characteristic tensile strength values of container glass as input for design calculations in this thesis project. The bottles were purposely damaged before the destructive testing to resemble both the damage from a beverage factory with a line-simulator and the damage due to handling with manually abrading. Both these types of damage can give an estimation on the tensile strength of used or returnable glass bottles. The primary use of glass bottle is not being a construction material, but a beverage container. It is expected that the characteristic tensile strength of newly made bottles would be higher, but this is outside the scope of the thesis.

Results from these experiments show that the characteristic tensile strength ($\sigma_{f;0.05}$ or f_k) is equal to about 27 MPa or N/mm^2 for line-simulated bottles. These bottles resemble glass bottles which have gone through the production line of a beverage factory. The duration time of the simulation was 5 minutes. Manually abraded bottles had a characteristic tensile strength of about 20 MPa or N/mm^2 . The difference between these two values is due to the level of damage, and this can be seen in the horizontal shift in the Weibull plots.

Another goal of these experiments was to compare the characteristic tensile strength of float glass from the engineering codes with the characteristic tensile strength of container glass. NEN2608 (2014) mention a characteristic tensile strength for float glass of 45 MPa. The difference between these values can be explained with the purposely induced damage on the bottles to purposely weaken them. Moreover, the production processes are different to one another, which could explain the change in characteristic strength. However, the values from the experiments are in the right order of magnitude according to literature.

This report has introduced a method to analyse the strength of container glass with the help of finite element modelling, destructive vertical load testing and Weibull analysis. Further research has to be done on bottles from different manufacturers, because this experiment focused on a standardized 330 ml long neck beer bottle. This could help further investigation on the characteristic tensile strength of (damaged) container glass.



C

6 Connection concepts between glass bottles

As mentioned in chapter 2, contemporary examples of using glass bottles in structures can be found in different forms. In this thesis, three different connection concepts are formulated:

'How can glass bottles be connected to each other to resist applied vertical loads?'

The three different connection concepts are based upon real life examples and are elaborated further upon. At the end of this chapter, one of the three concepts is chosen to develop further into this thesis. The advantages and disadvantages of the three concepts will be highlighted

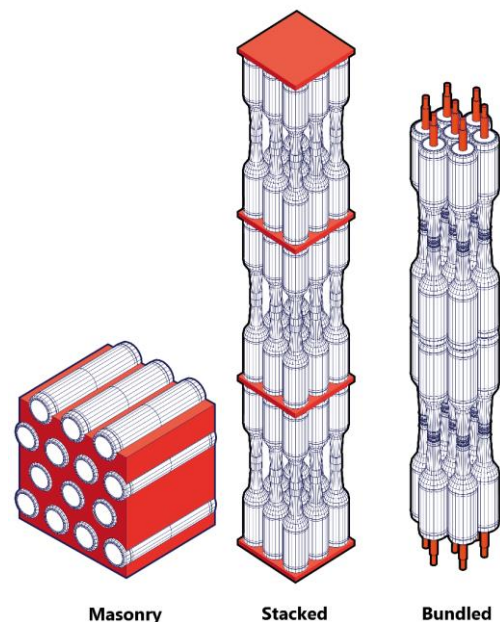


Figure 34 – Overview of the three connection concepts in this thesis

6.1. Masonry Concept

The first method of connecting bottles is by binding the bottles together with cement or mortar, in which the bottles behave like bricks in masonry. In chapter 2, many examples were shown that made use of this technique. The majority of examples contain this type of connecting bottles together. According to Fatima (2017), these masonry walls usually have a thickness of one or two bottles.

Bottles are either used in their existing geometry or they are cut apart. The cut bottles are then connected again with tape. The glass bottles can be placed in multiple directions: horizontal, vertical and even at an angle. Spasojevic-Stanic & Stanojlovic (2016) mention that these bottle walls are either built with or without a frame. Masonry elements can also be made with natural materials, such as adobe or cob (The Re:Generation Project, 2013). The elements can be built in-situ or blocks of bottle with adobe or mortar can be made, dried and then used (McFall, 2015). The three techniques are illustrated in figure 35.

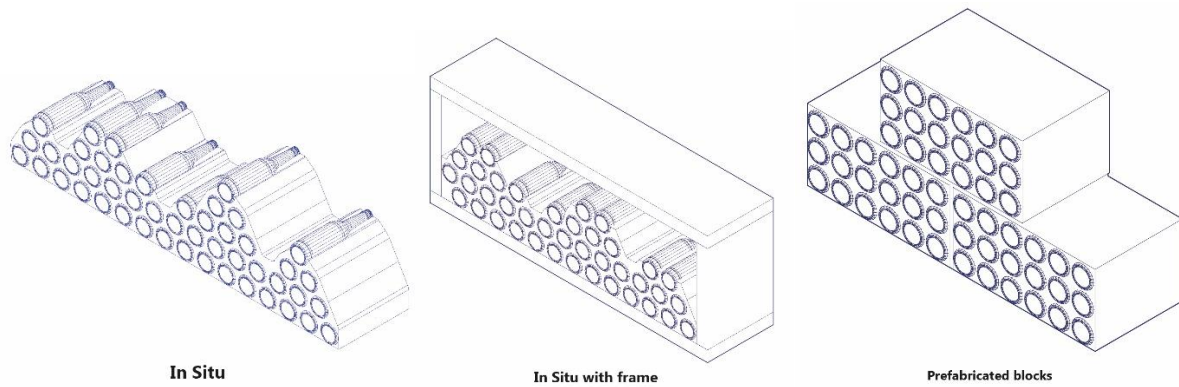


Figure 35 – Three techniques for the Masonry that are conventionally used

The advantages of the *Masonry* concept are as follows:

- Freedom in bottle orientation.
- Possible to use large array of different bottles to build with.
- Aesthetically pleasing structures with light influx.
- Simple construction method and the method is already widely used.

The disadvantages of the *Masonry* concept are as follows:

- The use of cement or mortar is not environmentally friendly.
- Reuse of the bottles could be difficult due to the cement or mortar.
- The construction with the bottle bricks can be time-consuming.
- Additional frames or moulds are necessary for a stable structure.

6.2. Stacked Concept

Another method of connecting the bottles is by stacking the bottles. Glass bottles are designed to withstand vertical loads due to self-weight of stacked bottles from above, such as in warehouses. These bottles either rest on pallets or special pads. An example of these pads is called 'Smartpad'.



Figure 36 & 37 – Smart pad (Loadhog, n.d.)

These 'Smartpads' are made out of polypropylene (Loadhog, 2017). These pads are only designed to bear the self-weight of the bottles, and thus not for structural purposes. Figures 36 & 37 show pictures of the Smartpad with stacked bottles in between.

Glass bottles do not have to be stacked vertically. In sub-chapter 6.1., it was explained that glass bottles are often used as bricks in combination with cement or mortar. However, bottles have been designed to be used as bricks, but these bricks use interlocking to connect to each other. An example of this is the WOBO-bottle designed by Heineken. The idea of the WOBO-bottle was that the bottle would receive another function other than its primary function of being a container. The purpose of this thesis is however to find solutions for

regular glass bottles that do not have intended features for reuse capabilities in them, such as the WOBO-bottle.

The advantages of the *Stacked* concept are as follows:

- The stacked option allows for demountable connections, which increases the reusability of glass bottles both a packaging container and construction material.
- Materials such as cement and mortar avoided, which makes it more sustainable. Glass bottles are the main load bearing elements.
- Easy to create height with the existing geometry of whole bottles
- Both cut and non-cut bottles can be used.
- Both mechanical and adhesive connections are possible with this concept.

The disadvantages to the *Stacked* concept are as follows:

- Possible stress concentrations near the finish due to small surface area.
- The same design of bottles needs to be used in one layer
- Connections between bottles and plates can be complicated.
- Difficult to create secondary load paths when a bottle in a layer breaks. More bottles have to be used to have a safety margin or additional measures need to be taken to protect the bottles or increase the post-breakage behaviour of the bottles.

6.3. Bundled Concept

The third and final concept for connecting glass bottles is the bundled concept. This concept is a mixture of the *Stacked* and the *Masonry concept*. The inspiration for this concept was gathered from fences made out of glass bottles. In these fences, a rebar is placed through glass bottles and then placed between timber elements. Holes have to be made through the bottoms of the glass bottles for a rebar to slide down. This is also similar to the C1-specimen designed by F. Oikonomopoulou *et al* (2017). A glass bundled column was developed with a steel post-tensioned tendon through the middle. The center hole of the bundled column had a diameter of 17 mm (Oikonomopolou *et al*, 2017). This is similar to the through-hole of most 330 ml glass bottles and the ones tested at AGR.

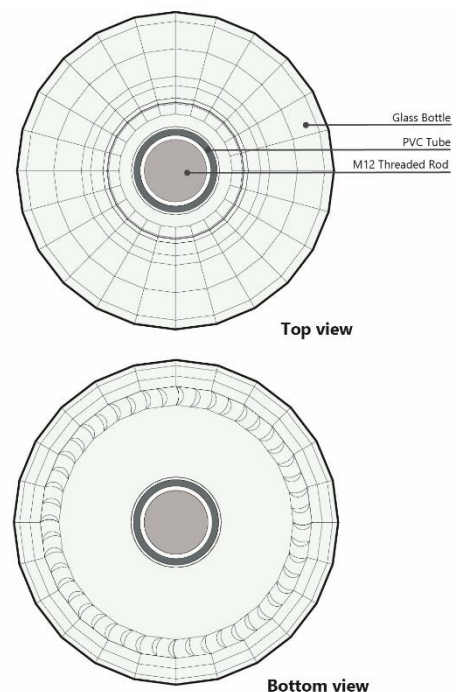


Figure 38 – Schematic of the bundled bottle concept

For the bundled column, a M12 threaded rod was used as a tendon (Oikonomopolou *et al*, 2017). The threaded rod and glass are not allowed to touch each other, and therefore a PVC tube with an outer diameter of 16 mm and inner diameter of 13.6 mm was used (Oikonomopolou *et al*, 2017). It is then possible to apply post-tensioning to the steel rod. The only difference with the bundled concept is that the bundled glass rods are substituted with glass bottles.

Another option would be to fill the remaining space inside the bottle with a material, such as cement or epoxy. The problem with that is that when the PVC tube is placed inside the bottle it is very difficult to then fill it with a material. Moreover, differences in thermal expansion can lead to internal pressure on the bottles. Especially when the material inside of the bottle tends to expand a lot with temperature increase, cracks can occur due to the high internal pressure. Glass bottles are however designed on internal pressure, especially bottles for carbonated drinks.

To summarize, the advantages of the bundled concept are as follows:

- Post-tensioning is possible with the addition of a steel tendon.
- Different designs of glass bottles can be used.
- The space inside the bottle is not used in the other concepts. Filling this space with a strong material can lead to a more space-efficient design than the other two.

The disadvantages of the bundled concept are as follows:

- Filling the bottles with a cementitious material can be a problem in the case of thermal expansion
- The concept requires holes to be made in the bottom of the bottles. This can be labour-intensive and complex.
- Threaded rods that are longer than 1 meter are hard to acquire. Especially when a column of 3 m long needs to be produced, there needs to be an opening in the PVC tube for a coupling nut.

6.4. Conclusion on connection concepts

By evaluating the advantages and disadvantages of the three concepts, a choice of concept can be made to further develop. The choice is also based upon comments given during intermediate meetings.

The choice of concept to further develop is the *Stacked* concept. This concept is chosen due to the following reasons:

- The *Stacked* concept comes closest to the loading condition of the individual bottles tested at AGR. It is easier to create parallels between the two rather than with the masonry and bundled concept.
- Vertical failure tests were already performed at AGR and thus a feeling of the vertical load capacity of an individual bottle was already gathered.
- Advice was given to focus on investigating the load carrying capability of the glass bottles. Introducing intermediate elements such as concrete or mortar would not show the full potential of the bottles themselves.
- Because the focus of the thesis is on columns, it is easier to create height with bottles by stacking them vertically rather than in the masonry concept.
- The bundled option is an interesting option to explore further down the line, but it is too advanced for exploratory research. However, it will be mentioned again during the *Design Explorations* in combination with the findings of this thesis.

7 Stacked Bottle Concepts

In chapter 6, the *Stacked* concept is chosen to develop further. Several configurations are designed to connect glass bottles together in a stacked manner. These configurations range from using whole bottles to cut bottles. Cut bottles are explored to see whether they are worth the time, money and effort over whole bottles. A few of these are then picked to be tested further in Stevinlab.

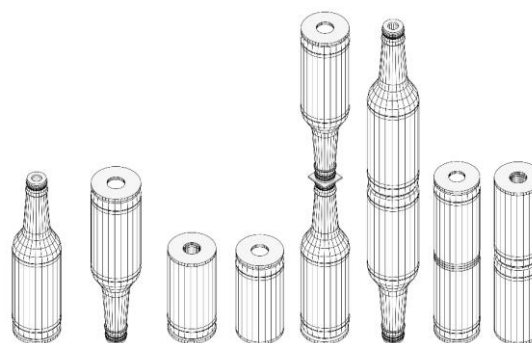


Figure 39 – Overview of the eight configurations

The eight configurations are compared with the help of six criteria: Price, Construction time, Complexity, Material use, Labour-intensity and Expected Capacity.

The eight configurations are scored with a score of 1 to 5, with 1 being the lowest and 5 being highest. Every score is supported with the appropriate argumentation. However, certain criteria outweigh other criteria, and therefore the weight factors of these criteria are supported with argumentation. For similar configurations under vertical loading (Whole-Up and Whole-Down, Cut-Up and Cut-Down) only one score is given per criteria. Prototypes were made for the configurations containing mechanical connections (i.e. Whole-FF and Cut-Double).

7.1. Weighing criteria for judgement bottle configurations

Firstly, the different criteria have to be weighed against each other. This results in the weight-factors calculated in table 12.

Criteria	Importance level (1-10)	Weight-factor	Argumentation
Price	10	0.196	The configuration should be as cheap as possible, so that it is available for a larger group of people.
Construction time	10	0.196	The configuration should be able to be built quickly.
Complexity	5	0.10	The importance of the criteria complexity lies somewhere in the middle. The configuration should not be too complex to the point that it is hard to replicate.
Material Use	8	0.157	The material use is of high importance for sustainability and re-usability reasons. However, if it turns out that by removing certain parts of the bottle it would result in more capacity, then that would be something to consider.
Labour-intensity	8	0.157	Labour-intensity is of high importance, because if too much effort needs to be put in just one configuration, it would be difficult to replicate for an entire building.
Expected Capacity	10	0.196	The configuration should be strong, stable and stiff enough to carry vertical loads.

Table 12 – Weight factor for different criteria

7.2. Configurations with whole bottles

The configurations with whole bottles can be classified into two categories: single bottles between plates or multiple bottles between plates. The first option has one bottle between clamping points. The second option has two bottles stacked on each other between clamping points. The configurations are called *Whole-Up*, *Whole-Down*, *Whole-FF* and *Whole-BB* respectfully.

7.2.1. Single bottles

Configurations with whole single bottles are the simplest configurations of glass bottles in a stacked formation. The bottles are simply clamped with plates with intermediate material between the glass and plates. The corresponding configurations are called *Whole-Up* and *Whole-Down*. Up and down refer to the direction of the finish. In a specimen under pure compression, there is no difference between the two configurations. There is however a difference when a bending moment is applied on the boundaries of the bottle. The bottom of the bottle is usually thicker and has a larger diameter than the finish of the bottle, which means that the bending stiffness at the bottom is higher. For compression tests in the Stevinlab laboratory, these configurations are combined as one. The *Whole-Up* and *Whole-Down* are also the cheapest options, because no additional cutting or gluing has to be done.

Criteria	Score	Argumentation
Price	5	The <i>Whole-Up</i> and <i>Whole-Down</i> are the cheapest options across the eight configurations. Most of the material costs is covered by the M20 and M12 nylon rings at the boundaries. The labour costs are also estimated to be relatively low compared to the others.
Construction Time	4	Because this configuration does not involve a lot of preparation, the construction time is the lowest of all the configurations.
Complexity	5	The idea of the configuration is based upon clamping bottles together with intermediate plastic rings (i.e. nylon)
Material Use	5	This configuration uses whole bottles and makes use of all the glass available.
Labour-Intensity	5	Because the complexity and construction time are both low, the labour-intensity will also be relatively low.
Expected Capacity	3	The shoulder and heel have been shown to be the weakest areas under vertical compressive loading. These areas still remain in the bottles, which means that the bottles only have a limited capacity determined by the geometry of the heel and shoulder.

Table 13 – Scores given for *Whole-Up* and *Whole-Down* concept with argumentation

7.2.2. Multiple bottles

Configurations with multiple whole bottles are more complex than the single bottles, because there has to be a connection between the glass bottles themselves. These connections can either be made with adhesives or mechanically. This lead to the configurations *Whole-FF* and *Whole-BB*. The abbreviation ‘FF’ refers to ‘finish-finish’, meaning that the finish of the bottle is connected to another finish of a bottle. Similarly, the abbreviation ‘BB’ refers to ‘bottom-bottom’, meaning that the bottom of one bottle is connected to the bottom of another bottle. The *Whole-FF* configuration uses plugs to plug the bottles against each other with the use of rubber. These plugs are made to prevent sideways movement when stacking. Buckling problems would arise if the finishes of two bottles are connected together with an adhesive, because of the smaller cross-section. On the contrary, the *Whole-BB* configuration makes use of an adhesive connection between the bottom of glass bottles. Earlier in the thesis, the potential for an adhesive connection in the push-up of the bottle with interlocking knurling was discussed. This was inspiration for the *Whole-BB* configuration.

Criteria	Score	Argumentation
Price	2	The Whole-FF is much more expensive than the two previous configurations. To illustrate: The price to build the Whole-Up and Whole-BB is about 1.40 euros. The price to build the Whole-FF concept is about 10.09 euros. This is mainly due to the fact that specific items with the correct dimensions have to be bought (i.e. rubber rings). For instance, the gummi-rings cost about 4.18 euros per connection, which is 41% of the total price. Solutions need to be found to lower this price.
Construction Time	3	This configuration needs a lot of preparation, which mainly consists of building the plugs. Plugging the bottles onto the plates is fairly straightforward, but when a lot of bottles need to be plugged on one plate, it can become quite tedious and time-consuming.
Complexity	3	The Whole-FF configuration is more complex than the previous two, because it involves a mechanical connection between two glass elements.
Material Use	5	This configuration also makes use of all the glass available.
Labour-Intensity	3	The plugging of all the bottles can be quite labour-intensive, especially if the plugs are too tight. It has been noticed from experience that it can take several tries to plug the bottle onto the plate.
Expected Capacity	3	It is expected that the capacity is somewhat similar to what is found for the Whole-Up and Whole-Down concept. However, a reservation is made for the imperfections that can occur due to insignificant plugging or height differences.

Table 14 – Scores given for Whole-FF concept with argumentation

Criteria	Score	Argumentation
Price	3	The Whole-BB concept is fairly cheap considering the amount of bottles that are used. The price of this concept mainly depends on the type of adhesive that is used between the glass bottles. The goal therefore is to choose a cheap adhesive, but an adhesive that has a sufficient gap-filling capability and compressive strength.
Construction Time	1	The low score for the construction time for the most part comes from the setting time of the adhesive. Moreover, this concept takes a lot of preparation, which consists of creating moulds for the bottles to be glued in and cleaning of the glass surfaces.
Complexity	3	This configuration has a little complexity as a result of the gluing process of the bottles. For instance, the right amount of adhesive needs to be applied, safety measures need to be taken in terms of gloves and/or masks and the bottles need to be as straight as possible when being glued.
Material Use	5	This concept makes use of all the glass available.
Labour-Intensity	2	The preparation work and gluing can be labour intensive. Especially when a large column needs to be created, most of the time is dedicated towards cleaning and gluing rather than stacking.
Expected Capacity	3	It is expected that the capacity is somewhat similar to what is found for the Whole-Up and Whole-Down concept. However, a reservation is made for the imperfections that can occur due to insignificant gluing or height differences.

Table 15 – Scores given for Whole-BB concept with argumentation

A prototype was made of the Whole-FF configuration with recycled bottles. Figures 40 and 41 show pictures of this prototype.



Figures 40 and 41 – Pictures of a prototype of the Whole-FF configuration

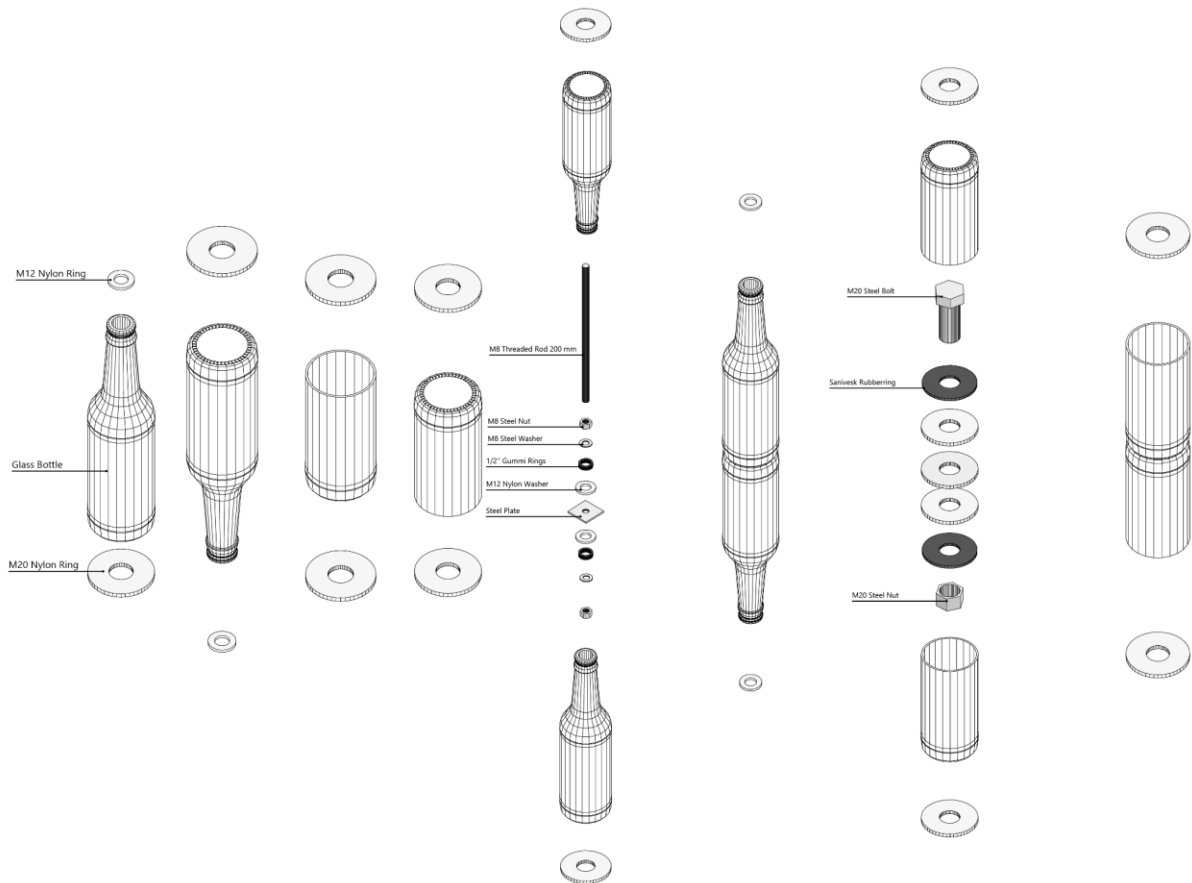
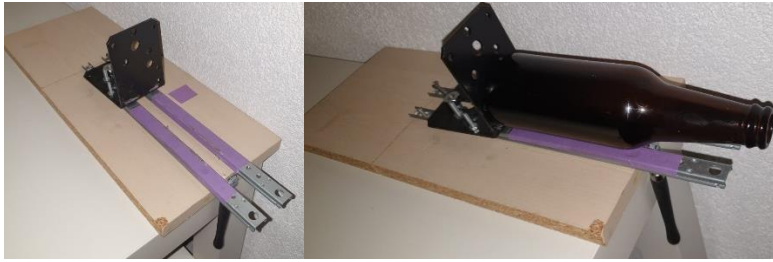


Figure 42 – Exploded view of the eight configurations (f.r.t.l. Whole-Up, Whole-Down, Cut-Up, Cut-Down, Whole-FF, Whole-BB-, Cut-Double, Cut-Double-BB)

7.3. Configurations with cut bottles

Besides whole bottles, the potential of cut bottles are also examined. FEM-models, a literature study and the AGR results have shown that rings of tensile stresses form in the shoulder and heel under a vertical load. It was discovered that the largest principle stresses are formed in the shoulder of the bottle. It is investigated whether the shoulder can be removed to increase the capacity of the bottle. At the end of the Stevinlab tests, a conclusion can be made on whether cut bottles show more potential than whole bottles. If not, solutions can be provided on how to improve the vertical load capacity of cut-bottles. The configurations that will be discussed in this thesis for cut bottles are as follows: *Cut-Up*, *Cut-Down*, *Cut-Double* and *Cut-Double-BB*.

Several recycled bottles were cut to experiment with different cutting techniques. A home-made bottle cutter was made from ordinary materials, such as rails from a drawer and a steel L-bracket. By pressing the bottle down and simultaneously rotating the bottle, a carved line is created. The technique that worked the best was heating this carved line up with a candle. Then, the bottle is put in a bucket of cold water. This will lead to the bottle separating at the carved line. Figure 43 and 44 show pictures of the home-made bottle cutter.



Figures 43 and 44 – Pictures of the home-made bottle cutter (left without bottle, right with bottle)

7.3.1. Single bottles

The cut single bottles are divided into two configurations: *Cut-Up* and *Cut-Down*. The single cut bottles are a bit more expensive than the cut whole bottles, because these involve more effort to be accurately prepared, cut and sanded.

Criteria	Score	Argumentation
Price	3	The costs for this concept mainly arise from the costs of cutting the bottles and sanding them. Moreover, larger nylon rings have to be used on both sides rather than on just the bottom.
Construction Time	2	The cutting and sanding can take a long time to remove all the imperfections from the surfaces.
Complexity	3	The complexity in this configuration mainly arises from the accurate cutting and sanding, which have to be done very precisely to get satisfactory results.
Material Use	2	Large part of the bottle is cut off and thus not all glass is being re-used as a building material.
Labour-Intensity	2	The cutting, cleaning, and sanding can be quite laboursome to execute. This is especially the case when an entire column needs to be made out of the <i>Cut-Up</i> or <i>Cut-Down</i> configuration.
Expected Capacity	4	Because the shape of the bottle would be more closer to a cylinder rather than the shape of a bottle and because the shoulder area is removed, it is expected that the cut bottle would behave better under vertical compressive loading.

Table 16 – Scores given for *Cut-Up* and *Cut-Down* concept with argumentation

7.3.2. Multiple bottles

The configurations with multiple cut bottles are divided into two configurations: *Cut-Double* and *Cut-Double-BB*. The term ‘*Double*’ refers to the stacking of two cut bottles between plates. A distinction is made between stacking the cut surfaces of two bottles together (*Cut-Double*) and stacking the bottom of two cut bottles together (*Cut-Double-BB*). Similarly to the multiple whole bottles, the *Cut-Double* configuration consists of a mechanical connection between the two cut bottles, whereas the *Cut-Double-BB* configuration contains an adhesive connection between the two cut bottles. These are the configurations that would be the most laboursome.

Criteria	Score	Argumentation
Price	1	The <i>Cut-Double</i> configuration was the most expensive configuration to build by far. The total costs of one configuration is equal to about 18 euros, where a large amount of it, 7.18 euros, was reserved for large rubber rings.
Construction Time	2	The construction time depends on the speed of the cutting and sanding. This can take a long time, especially when certain bottles have to be redone.
Complexity	1	This configuration is dependent on the accuracy of the sanding and cutting, because the cut surfaces are connected to each other with nylon rings and a steel ring. If the cutting or sanding have not been accurate enough, a lot of stress concentrations can occur in the connection. Moreover, if the cut surface is not exactly straight, deviations in the verticality of the configuration can occur,

		<i>which means that additional bending stresses can occur under a vertical compressive load.</i>
<i>Material Use</i>	<i>1</i>	<i>Large part of the bottles are cut off and thus not all glass is being re-used as a building material.</i>
<i>Labour-Intensity</i>	<i>2</i>	<i>The cutting, cleaning, and sanding can be quite laboursome to execute. This is especially the case when an entire column needs to be made out of the Cut-Up or Cut-Down configuration.</i>
<i>Expected Capacity</i>	<i>4</i>	<i>Because the shape of the bottle would be more closer to a cylinder rather than the shape of a bottle and because the shoulder area is removed, it is expected that the cut bottle would behave better under vertical compressive loading.</i>

Table 17 – Scores given for Cut-Double concept with argumentation

<i>Criteria</i>	<i>Score</i>	<i>Argumentation</i>
<i>Price</i>	<i>1</i>	<i>The Cut-Double-BB is cheaper than the Cut-Double configuration, because the bottom are simply glued together.</i>
<i>Construction Time</i>	<i>1</i>	<i>The construction time depends on the speed of the cutting and sanding. This can take a long time, especially when certain bottles have to be redone. Additionally, the bottles have to be glued and need time to set appropriately.</i>
<i>Complexity</i>	<i>2</i>	<i>This configuration has a little complexity as a result of the gluing process of the bottles. For instance, the right amount of adhesive needs to be applied, safety measures need to be taken in terms of gloves and/or masks and the bottles need to be as straight as possible when being glued. The latter can be difficult if the bottles are not cut straight enough.</i>
<i>Material Use</i>	<i>1</i>	<i>Large part of the bottles are cut off and thus not all glass is being re-used as a building material.</i>
<i>Labour-Intensity</i>	<i>1</i>	<i>This configuration involves the most work of all the configuration and is therefore scored with the lowest value.</i>
<i>Expected Capacity</i>	<i>5</i>	<i>Because the shape of the bottle would be more closer to a cylinder rather than the shape of a bottle and because the shoulder area is removed, it is expected that the cut bottle would behave better under vertical compressive loading. Moreover, the glued connection is expected to lead to a better stress distribution and reduce the amount of stress concentrations at the bottom of the bottles.</i>

Table 18 – Scores given for Cut-Double-BB concept with argumentation

A prototype of the Cut-Double configuration was created. Figures 45 and 46 show pictures of this configuration. The picture shows three steel rings. In reality, the upper and lower ring should be made out of nylon, but for modelling purposes, steel rings were used here. The bottles were cut with the home-made bottle cutter.



Figure 45 and 46 – Pictures of a prototype of the Cut-Double configuration

7.4. Comparison of bottle configurations

The strong and weak points of the eight configurations have been discussed together with appropriate scoring. These scores and weights do not determine the eventual look of the design, but they do determine which configurations are most suitable for lab-testing at the Stevinlab. This is due to the limited amount of time and money that is allocated for the testing, which means that a very time consuming, labour-intensive and expensive configuration is not suitable for testing in this thesis.

In table 19, the scores for every criteria for every configuration is multiplied by the weight factor. Then, the weighted scores are added up and reveal which configurations would be the best ones to test.

Criteria	Whole-Up & Whole-Down	Whole-FF	Whole-BB	Cut-Up & Cut-Down	Cut-Double	Cut-Double-BB
Price	0.980	0.392	0.588	0.784	0.196	0.392
Construction Time	0.784	0.588	0.196	0.588	0.392	0.196
Complexity	0.490	0.294	0.294	0.294	0.098	0.196
Material Use	0.784	0.784	0.784	0.314	0.157	0.157
Labour-intensity	0.784	0.471	0.314	0.314	0.314	0.157
Expected Capacity	0.588	0.588	0.588	0.784	0.784	0.980
Total	4.412	3.118	2.765	3.078	1.941	2.078

Table 19 – Weighted scores for all the configurations with corresponding criteria and total scores

7.5. Investigation on stress distributions of different configurations

Simplified models were made to investigate the differences between stress distributions of the eight configurations. The result of these models and hand calculations showed that the Cut-Double-BB option would perform the best, mainly due to large cross-sections at the boundaries and the cylindrical shape of a cut bottle. This is however without any imperfections in mind on the cut-surface in mind. This configuration will therefore be tested to see if it still behaves the best in real life. Moreover, the use of whole-bottles for columns that have to take up large bending moments is not advised, due to the fact that the finish of

the bottle is a fairly small cross-section to take up the bending moment, compared to a cut-bottle or the bottom of a bottle.

Lastly, the configurations could then be compared based upon the maximum principle tensile stresses in the bottles. The configurations are compared with fixed and hinged connections, as well as the application of external tension elements (i.e. threaded rods or cables). This is shown in figure 47. The full calculation of these stresses with models and hand calculations is shown in Appendix A2.

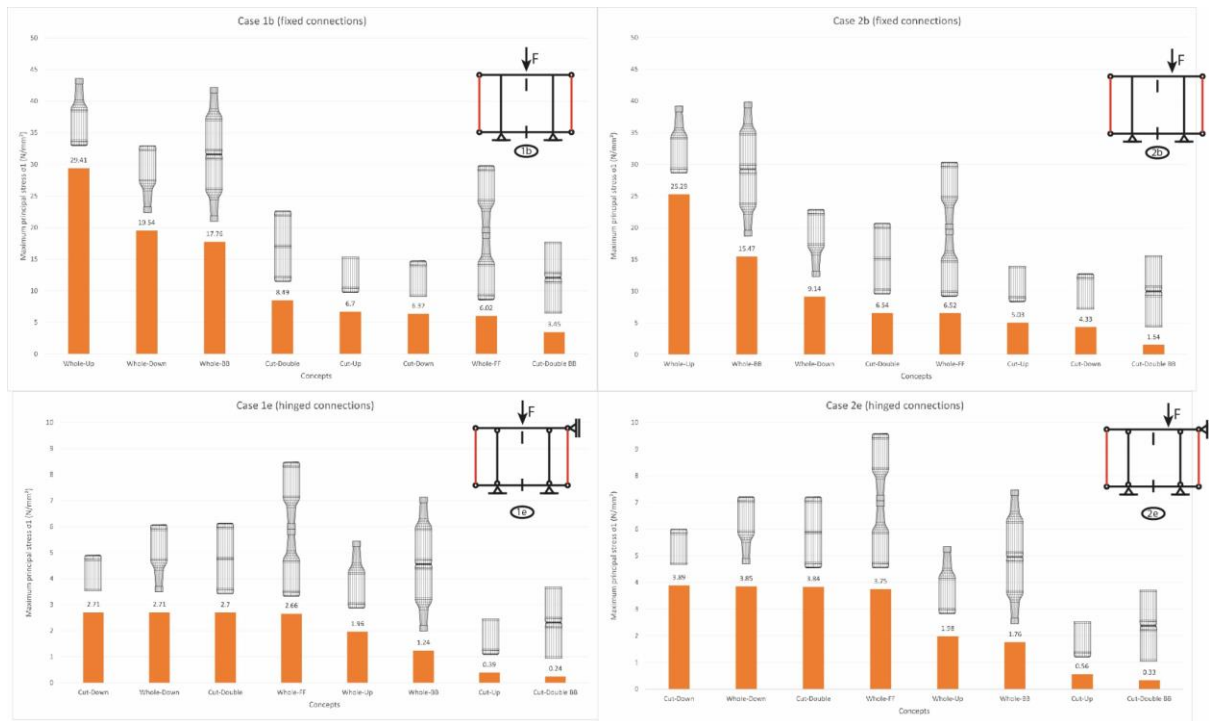


Figure 47 – Summary of maximum principle stresses for every concept and case

7.6. Conclusions on bottle configurations and choices for testing

The results from the weighted scores in table 19 shows that the Whole-Up & Whole-Down configurations are the best to test at Stevinlab. These are followed in order from highest to lowest scores: Whole-FF, Cut-Up & Cut-Down, Cut-Double-BB and Cut-Double. The advice from the lab assistant was that only about 10-15 tests could be performed with the allocated time available. This meant that for a sufficient set of results per configuration, it was decided that only four configurations would be tested.

This would include the following four concepts:

- **Whole-Up & Whole Down:** This was the best option from weighted scores table and is the simplest of all the configurations. This configuration is also the most similar to the loading configuration of the individual bottles at AGR. From this point onwards in the thesis, this configuration is simply denoted as *Whole-Up*
- **Whole-FF:** This was the second highest configuration. It also involves a mechanical connection with plugs that are interesting to test at Stevinlab.
- **Whole-BB:** The *Whole-BB* configuration is the fourth highest scoring, but it is preferred over *Cut-Up* & *Cut-Down* configurations, because the latter two configurations are fairly short, which is not beneficial for building a tall structural

element like a column. It is also interesting to see how an adhesive connection would compare to a mechanical connection by comparing *Whole-FF* with *Whole-BB*.

- Finally, at least one cut configuration is chosen to see whether it is worth the time, money and effort to cut the bottles. It is investigated whether the cut bottles would lead to a significant increase in capacity. The best scoring of the multiple cut bottles is the **Cut-Double-BB** sample. By choosing Cut-Double-BB, the only difference between the Cut-Double-BB and Whole-BB is the change in geometry of the substrate (i.e. whole or cut bottle).

D

D Stevinlab Experiments

8 Compression Tests of Bottle Configurations

In this chapter, four different configuration concepts are tested on their vertical load carrying capacity with whole and cut bottles. These configuration concepts were chosen in the previous chapter with the help of a scoring system. Moreover, due to a limited amount of money and time available with the lab assistant, only four configurations could be built and tested. In short, these configuration concepts are:

- Whole Up
- Whole-FF
- Whole-BB
- Cut-Double-BB

In this chapter, information is gathered to answer the third sub-question:

‘Which configurations of glass bottles in a structural column are most sufficient in terms of resisting tensile stresses?’

In the previous chapter, multiple criteria were investigated per configuration. This chapter focuses more on the capacity of the configurations with the help of compression tests. Firstly, the reasoning and the methodology behind the failure tests will be explained, including necessary materials and equipment. Next, the results of the failure tests are presented in the form of force-displacement graphs, box-plots and tables. Afterwards, the results are discussed and a hand-calculation of the axial stiffness of one concept is made. Lastly, a conclusion is made on these tests and a recommendation of the useful concepts is made for a final design.

8.1. Previous experiments with glass columns in Stevinlab

Practical experiments on glass columns have been performed before in master theses at TUDelft. To gain inspiration and insight on the testing procedure, it is important to summarize a few of these.

In a study by Oikonomopoulou et al (2017) about bundled columns, steel caps with milled conveces and half spheres were used to create pinned connections at both ends of the column. The top pressing plates is then lowered until slight contact is made. According to Oikonomopolou et al (2017), this initial force is negligible in the results.

A few test samples used by Oikonomopoulou et al (2017), more specifically test specimen A1 and A2, had heights of 500 and 470 mm respectively. These heights are similar to the heights of some of the combined concepts, Whole-FF and Whole-BB. The experiments that were performed in this study were compression tests where the maximum normal force was retrieved. The results were plotted in a force-displacement graph.

Likewise, Veenstra (2021) performed compression tests on tubular glass elements with a height of 300 mm. These tests were performed at Stevinlab II. In that project, a hydraulic

displacement-controlled compression machine was used. Plexiglass panels were used for safety purposes (Veenstra, 2021). Also in this project, force-displacement curves were produced. Furthermore, strain sensors were placed on the inside and outside of the tubes to record strain values during the compression tests.

Verleg (2019) also used displacement-controlled compression tests to validate glass bundled columns. A test rate of 1 mm/min was applied and a total of 20 tests were performed. GoPro cameras were used to capture the failure mode of the bundled elements. Force-displacement graphs were produced from these tests.

8.2. Methodology of compression tests of bottle configurations

Firstly, the methodology of the tests is discussed. This includes the approach of the tests, the necessary materials, preparation work and safety measures.

8.2.1. Approach

It was told that only about 14 to 16 tests could be completed due to the large amount of preparation time and time available with the lab assistant. Due to the amount of whole and cut samples available, the decision was made for the following number of tests per configuration:

- Whole-Up: 4 tests
- Whole-FF: 4 tests
- Whole-BB: 4 tests
- Cut-Double-BB: 3 tests

This resulted in a total of 15 tests that had to be carried out. The tests are performed in collaboration with lab-assistant G. Stamoulis.

The bottom-to-bottom connection can be realised with the help of adhesive connections. Because the bottom of the bottle is essentially concave, two bottles together would create a cavity similar to the shape of a biconvex lens. In this cavity, adhesive can be placed to bind the two bottles together.

Because the push-up of the chosen bottle is about 3 mm, the gap filling capability of the adhesive is of much importance. Moreover, ease of assembly is favoured and the adhesive needs to have a reasonable compressive strength. The tests will be performed at room temperature and the curing time of the adhesive should not be long. Lastly, it is desired to not use additional scaffolding.

A study from Oikonomopoulou & Bristogianni (2022) showed that flexible adhesives, cement-based mortars and tile adhesives showed great gap filling capability, ranging from 1 to 10 mm and even higher in other cases. The anticipated load for flexible adhesives is shear, whilst for cement-based mortars and tile adhesives the anticipated load is compressive and shear. Because the elements between the plates are essentially loaded in compression, cement-based mortars and tile adhesives could be of interest. However, Oikonomopoulou & Bristogianni (2022) state that the latter options could have a slow setting-time. All in all, the following five options are considered for adhesive connections between the bottoms of glass bottles:

- Tile adhesives

- Mortar (Cement-based)
- Silicone
- MS Polymer
- Polyurethane

The cheapest option in this case is tile adhesive. The set-up of the tests is shown in schematic drawings in figure 48.

The displacement rate that is chosen is equal to 0.005 mm/s. The displacement had to be as slow as possible to stop the machine after fracture, but not too slow so that the tests would take too long.

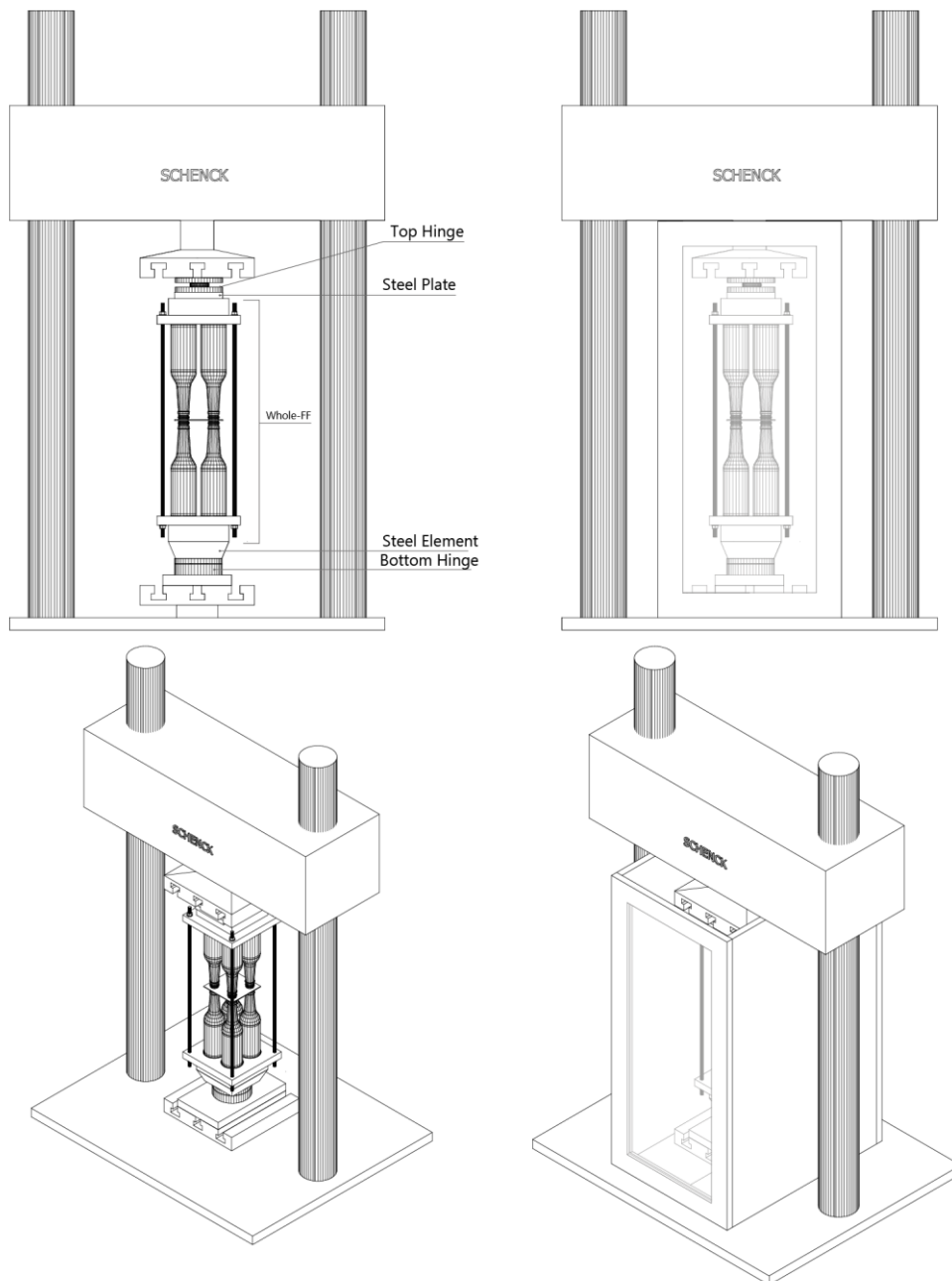


Figure 48 – Set-Up of the experiments (top left and bottom left: Whole-FF set-up without safety casing, top right and bottom right: Whole- FF set up with safety casing)

8.2.2. Materials

The materials necessary for the tests are summarized in a list in table 20. These varied from the actual samples to MDF Plates for the safety casing. Several items were available at the Stevinlab, which helped cutting down on costs. Most of the material costs were spent on buying the bottles and element for the safety casing.

<i>Use</i>	<i>Material</i>	<i>Store/Webshop</i>	
Safety-Casing	3x MDF Plates t = 20 mm	GAMMA	
	Polycarbonate plate t = 5 mm (890x390mm)	Kunststofplatenshop.nl	
Samples	Glass Bottles 6x24 Longneck beer bottles 33cl. Brown <i>Of which:</i> - 32 bottles cut at the shoulder contact area	Brouwland	
	Steel Plate S235 (125x125 mm) with t = 2 mm)	DEMO	
	40x Rubber Gummi rings (d = ½")	GAMMA	
	4x M8 Threaded rods (L = 200 mm)	GAMMA	
	80x POM Rings t = 4 mm and d = 30 mm <i>Of which:</i> - 32 POM Rings with M8 holes in the center	DEMO	
	80x M20 Nylon Rings of d = 60 mm and t = 4 mm	TechniekWebshop.nl	
	1x Bison Tile Adhesive	Praxis	
	8x S235 Steel Disks t = 4 mm and d = 30 mm	DEMO	
	8x Steel M20 Rings of d = 60 mm and t = 4 mm	Wildkamp	
	Plates	4x Timber Plates of 145x145 mm of t = 41 mm	Stevinlab
		4x MDF Plates of 200x200 mm with t = 22 mm <i>Of which:</i> - 2 plates with 4 holes of d = 65 mm. See Appendix A6 for the corresponding drawings - 2 plates with 4 holes of d = 30 mm. See Appendix A6 for corresponding drawings	DEMO
Rods	8x Steel M8 Threaded Rods	Stevinlab	
Other	1x Bison Degreaser	Praxis	

Table 20 – Necessary materials for concept failure tests

8.2.3. Equipment and tools

The machine that was used for the compression tests is a hydraulic displacement-controlled compression machine by Schenck in room 0.27 of Stevinlab. The machine includes two pressure plates, of which the bottom plate would move up to create a compression load on the specimen. A picture of room 0.27 with the machine is shown in figure 49.

A rotating diamond sanding disk was used to smoothen the surface of the cut-bottles and to remove as many imperfections as possible at the surface. Pads of 60, 200 and 400 grit were used respectively to smoothen the surface. Additional, a Dremel with a rotating bit was used to smoothen the inside edge of the cut bottles. The sanding machine is shown in figure 50. Molds were made out of scrap timber plates and plastic rods to glue the bottles together.

These molds made sure that the bottles would be aligned with each other as much as possible. These molds are shown in figure 51.



Figures 49, 50 and 51 – The allocated lab room with machine, sanding machine for the cut-bottles, molds for gluing the samples

8.2.4. Preparation phase and safety measures

The glass bottles had to be cleaned before they could be glued. This was done with a degreaser from Bison to remove potential grease on the surface and to further enhance the adhesion of the glue. Earlier in the thesis, it was explained that there could be adhesion issues due to the properties of the glass surface and coatings. After the bottles were cleaned, adhesive was applied on both bottoms of two bottles. Afterwards, the glass bottles were pushed together with the help of the rails to straighten them out. Excess tile adhesive was wiped away with a paper towel. Every glued sample set for a minimum of 24 hours, as recommended by the product label. Figure 52 shows picture before and after gluing the samples.



Figure 52 – Pictures of the bottles after cleaning and gluing

Four timber plates of size 145x145 and about 40 mm thick were acquired. Moreover, four MDF plates were provided by DEMO with different sizes of holes for the glass bottles.

The steel rings and steel disks were double-taped on the timber plates and the plastic materials were double taped on the steel rings and disks. This way, the POM disks and nylon rings could easily be changed after testing.

The glass bottles were cut at AGR with the help of a diamond blade. Because there is a possibility of pieces of glass chipping off the cut-surface, the recommendation was made to cut the bottle a little bit higher, after which the remaining part had to be abraded away. A top view of the abraded cut bottles is shown in figure 53. This last part took the most effort. The interesting thing about the Whole-FF connection is that it could be re-used for multiple tests (i.e. the steel plate, threaded rods and rubber rings). It was easy to remove the POM rings in this connection as well if necessary.



Figure 53 – Top view of the cut Bottles after sanding

For safety purpose, a safety casing had to be built from scratch to protect from flying shards after failure. MDF plates were bought from the GAMMA with the correct sizes and a polycarbonate plate was bought from kunststofplatenshop.nl. This polycarbonate plate was then screwed on the MDF casing, which could easily be removed and reattached between testing. The safety casing is shown in figure 54.

Before the bottles could be tested, the bottles were labelled appropriate, so that it was easy to find the corresponding bottles of certain test afterwards. After the bottles were labelled, the bottles were surrounded by transparent tape, so that it was possible to inspect the bottles after failure and to prevent an explosive failure as much as possible. The inspiration from this came from the tests performed at American Glass Research.



Figure 54 – Safety casing made from MDF surround the pressure plates

Figure 55 shows a picture of the set-up with the Whole-Up configuration before testing. A bubble level is used to check the levelness of the elements (i.e. top of the bottom hinge, bottom MDF plate, top MDF plate).



Figure 55 – Whole-Up configuration set-up before testing

8.2.5. Failed test trial and solution

A preliminary test was completed to observe possible irregularities in the test results. A set-up of the Whole-Up configuration was created, which initially had nylon M12 rings on the finishes of the bottles instead of POM rings. During the testing, sounds of the glass crushing were noticed and the force-displacement graph did not show the expected curve. The bottles seemed to crush instead of failing either in the heel or shoulder, as expected from the literature study. As soon as the test was completed and the top plate was removed, the problem was very evident.

Pictures in figure 56 show the nylon rings that were ripped apart due to plastic deformation and figure 57 show the crushed finishes of the bottles. The reason for the crushing of the finishes was that the rings had either a surface area that was too small to take up the vertical force, or the nylon used was not stiff enough to resist such large deformations. The finishes of the bottles were then crushed due to stress concentrations, because the nylon rings could not uniformly distribute the force to the glass. This problem was solved by using a stiffer plastic, such as POM. Moreover, disks with a diameter of 30 mm were used instead of rings to increase the surface area. Crushing of the finishes was not seen again in the remaining tests.



Figure 56 and 57 – Torn nylon rings after failed test. Picture showing crushed finishes of the bottle, indicating a fault in the test procedure.

8.3. Results of the compression tests of configurations

8.3.1. Collected data from compression tests of configurations

The results of the tests show the vertical force recorded by the machine versus the vertical displacement of the pressure plate. This is the displacement of the whole unit. Firstly, the four concepts are placed in a combined graph to showcase the difference between the concepts. Pictures of the fractured bottles are shown in Appendix A7.

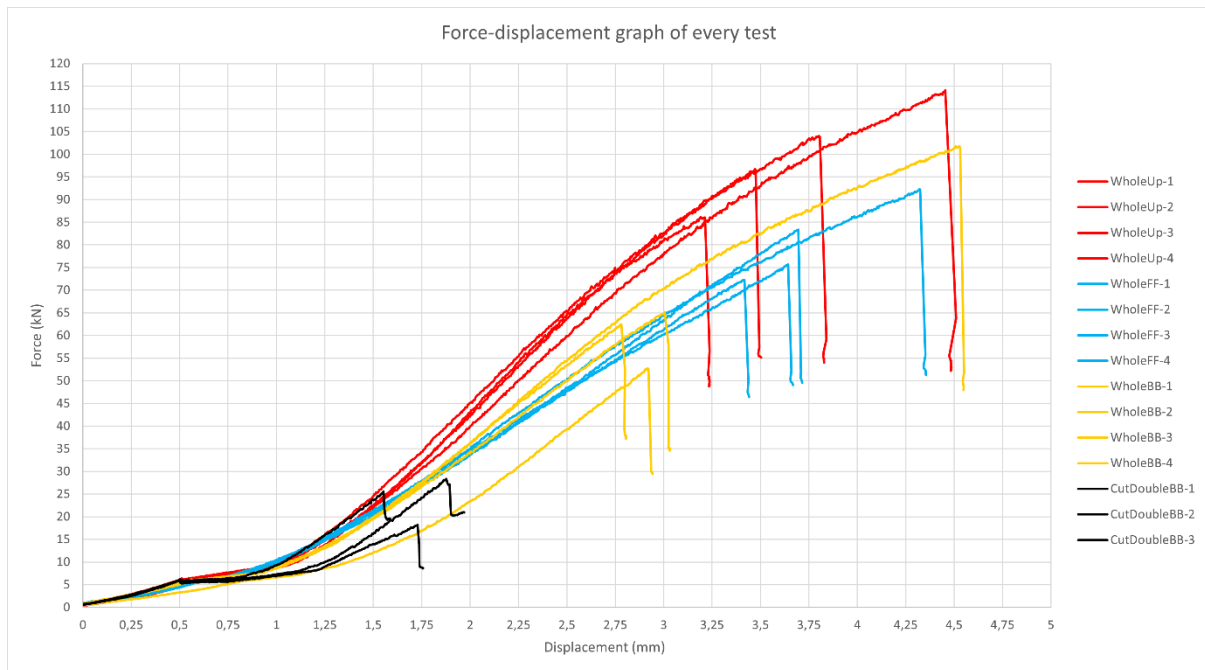
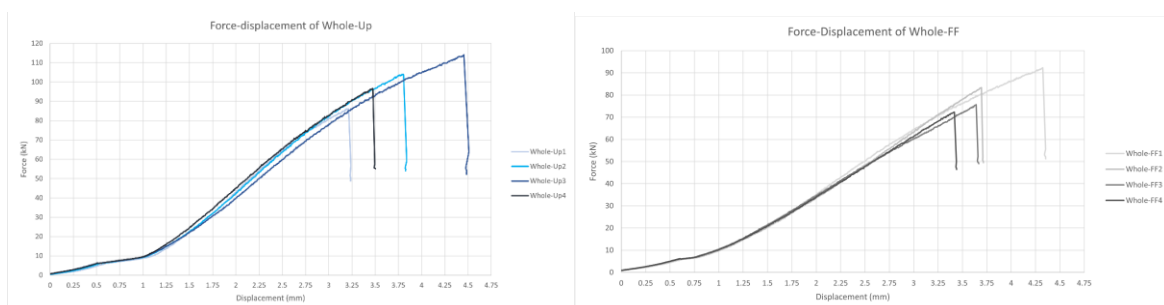
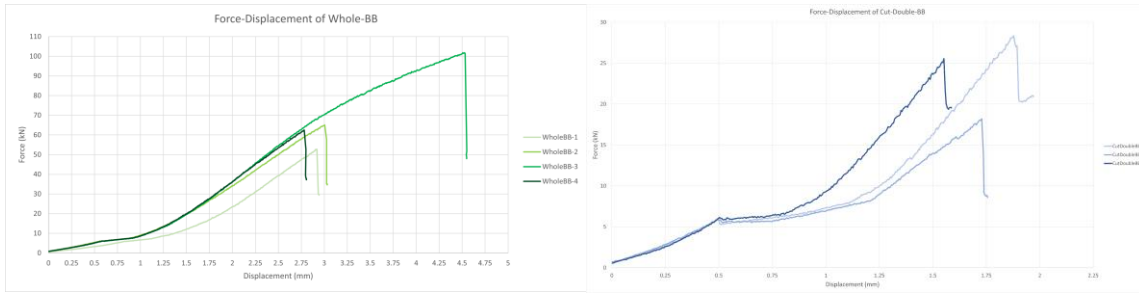


Figure 58 – A graph of all failure tests with color-coded lines (red: Whole-Up, blue: Whole-FF, yellow: Whole-BB, black: Cut-Double-BB)

The most basic concept, the Whole-Up, is shown in red and shows on average the highest failure load. The Whole-FF concept, the concept with the demountable plug, is shown in blue and has on average a slightly lower failure load than the Whole-Up concept. The Whole-BB concept is shown in yellow and has on average an even lower failure load than the Whole-Up concept, but an outlier was recorded. The Cut-Double-BB recorded a far lower failure load than the other three concepts.

The four concepts are also displayed in four separate graphs, which are shown in figures 59 till 62.





Figures 59, 60, 61 and 62 – Force-displacements graph of the Whole-Up, Whole-FF, Whole-BB and Cut-Double-BB respectively

The Cut-Double BB concept was unique in the sense that progressive cracking could be heard during the test. The time stamps of the audible cracks were recorded and are displayed in a larger version of figure 62 in figure 63. The location of the cracks in figure 63 seem to correspond with the zig-zag behaviour of the graphs. There is a difference of when the first crack appears in the unit.

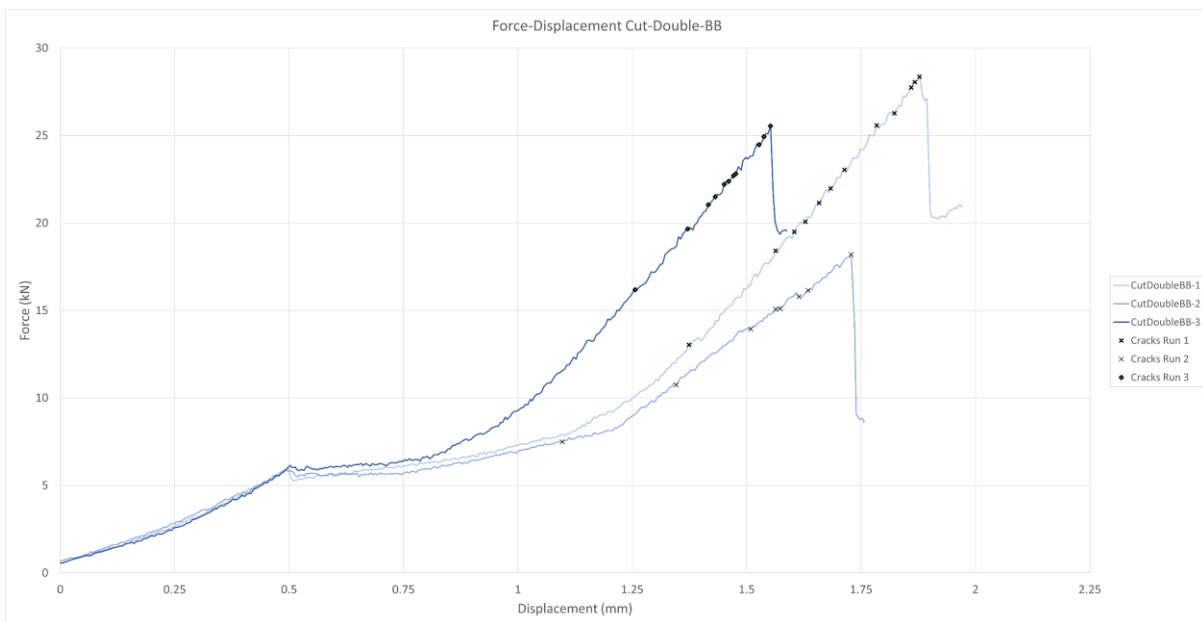


Figure 63 – Force-displacement graphs of the Cut-Double BB samples with moments of audible cracks.

The difference between the concepts can also be shown in the form of boxplots. This is displayed in figure 64. The statistical data of these boxplots is shown in table 21.

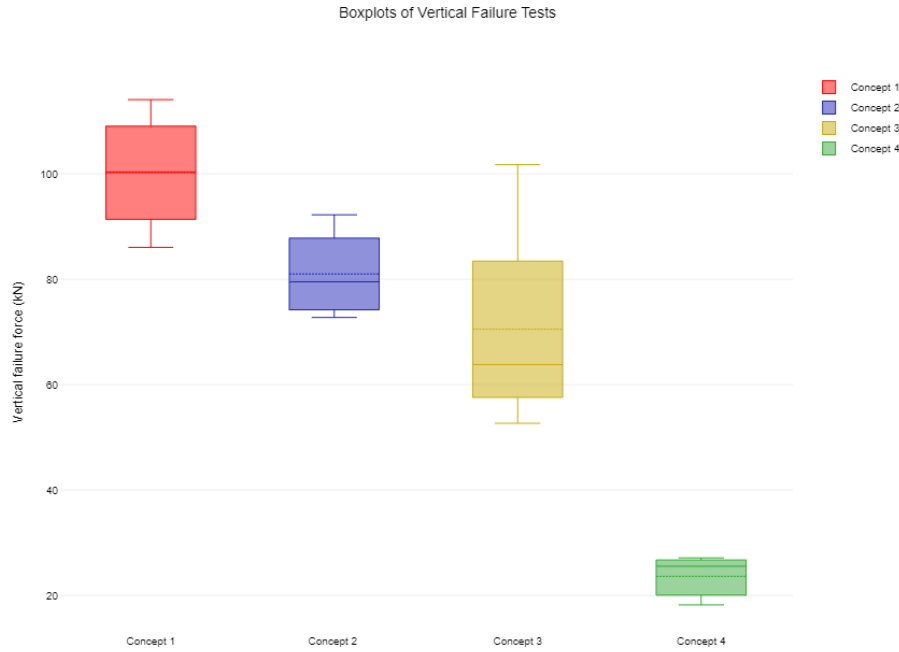


Figure 64 – Boxplots of the acquired data from the four different configurations

Concepts	Minimum [kN]	Q1 [kN]	Median [kN]	Q3 [kN]	Maximum [kN]	Mean [kN]	IQR [kN]
1	86.05	91.38	100.38	109.07	114.10	100.23	17.69
2	72.75	74.21	79.525	87.81	92.24	81.01	13.60
3	52.67	57.58	63.81	83.45	101.76	70.51	25.87
4	18.20	21.87	25.54	26.33	27.12	23.62	4.46

Table 21 – Statistical data of the boxplots in figure 62

Finally, table 22 gives an overview of every tested configuration with their respective failure loads and their failure mechanism.

Configuration	Failure load [kN]	Failure mechanism
Whole-Up 1	86.05	Heel failure
Whole-Up 2	104.03	Heel failure
Whole-Up 3	114.10	Heel failure
Whole-Up 4	96.72	Heel failure
Whole-FF 1	92.24	Shoulder failure
Whole-FF 2	83.38	Heel failure
Whole-FF 3	75.67	Heel failure
Whole-FF 4	72.25	Heel failure
Whole-BB 1	52.67	Heel failure
Whole-BB 2	65.14	Heel failure
Whole-BB 3	101.76	Heel failure + collapse
Whole-BB 4	62.48	Heel failure
Cut-Double-BB 1	27.12	Progressive cracking until heel failure
Cut-Double-BB 2	18.20	Progressive cracking until heel failure
Cut-Double-BB 3	25.54	Progressive cracking until heel failure

Table 22 – Configurations with respective failure loads and failure mechanisms

8.3.2. Hand-calculation Whole-Up axial stiffness

A separate hand-calculation was made to investigate the slope of the force-displacement graphs, which depicts the stiffness of the **system**. A hand-calculation was made for the Whole-Up set-up. A hand-calculation was made based upon a model of springs in parallel and series. The slope of the Whole-FF graph was equal to about 4×10^4 N/mm and the simplified hand-calculation found a value of about 7.9×10^4 N/mm. The main difference between these values are the assumptions taken for the stiffness of the timber plates, the stiffness of the plastic elements and the stiffness of the bottles. The full calculation of the axial stiffness is shown in Appendix A3.

8.4. Discussion of the compression tests of configurations

First of all, the slopes of the different runs in a single concept seem to be equal for every concept, except for the Cut-Double-BB concept. This could be down to slight differences between the heights of the cut-bottles from sanding. Also, it could be that the differences in cracking has an effect on the stiffness of the unit. The second run of the Cut-Double-BB differs the most from the other two and the first crack is recorded much earlier than in the other two samples.

The differences between slopes of the different concepts can be explained due to the fact that different amount of plastic and types of plastic are used in the unit. For example, the Whole-Up concept contains POM rings at the top and nylon rings at the bottom. The Whole-FF concept contains twice as many POM rings and Nylon Rings. The Whole-BB concept contains twice as many POM rings than the Whole-Up concept, but no nylon rings.

Moreover, a slightly stiffer wood-type was used for the plates connected to the finish of the bottle. This was due to the fact that force would be transferred to a much smaller area than the bottom of the bottle. This could have an effect on the differences between the concepts.

The spread in failure loads in a single concept has to do with the characteristics of glass bottles themselves, i.e. differing flaws, thicknesses etc. The difference between concepts can be explained as follows:

- The Cut-Double-BB concept has much lower failure loads than the other three. This seems to be because of the initial imperfections that are induced on the cut surface of the bottle. Even after sanding with 60, 200 and 400 grit, there are still small imperfections left on the cut surface. Vertical cracks could be seen either emanating or travelling towards these imperfections.
- The Whole-Up concept seems to have higher failure loads than the Whole-FF and Whole-BB concept. This could be down to the fact that the Whole-FF and Whole-BB uses twice as much glass than the Whole-Up concept. This means that there is a larger area of glass with tensile stresses, and there could be a larger chance of a weak governing flaw in those areas. Another explanation is that the Whole-FF and Whole-BB concepts simply have more connection points than the Whole-FF concept, i.e. eight instead of four. This means that there could be a slight difference in how the forces flow through the unit, which could lead to earlier failure compared to the Whole-Up concept.

On the test procedure itself, the cracks, especially from the Cut-Double-BB samples, were hard to see on video and by eye after the testing. This was due to the transparent tape that was attached on the bottles for safety purposes.

8.5. Conclusion on the compression tests of configurations and answering third sub-question

It can be concluded from the results of the Stevinlab tests and the discussion following these results that the Whole-Up concept would behave the best according to the minimum, maximum and mean values. However, the Whole-FF and Whole-BB concept can create a much larger height and needs less plate material.

Generally, the Cut-Double-BB concept behaves worse than expected due to the imperfections at the cut surface. It is not beneficial to remove the shoulder area by cutting the bottles for the capacity of the column. The Cut-Double-BB is therefore not very practical, because the bottles have to be cut and sanded. The bottles need to be cut and sanded at the same height and one has to be careful not to damage the bottles while performing these actions. The Cut-Double-BB concept needs too much labour, time, money, tools and precision to work well. Whole bottles are a better option to build with costs, labour-intensity capacity in mind.

The third sub-question of this thesis was formulated as follows:

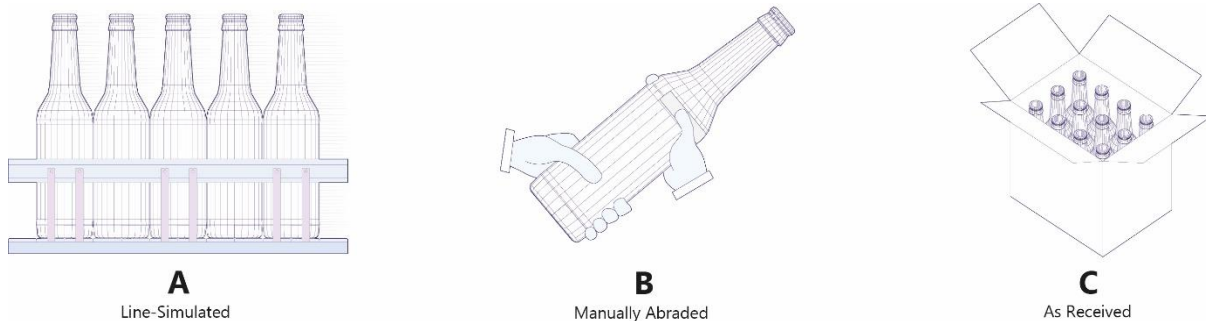
'Which configurations of glass bottles in a structural column are most sufficient in terms of resisting tensile stresses?'

The answer to that question is the Whole-Up concept, followed by the Whole-FF concept and the Whole-BB concept. The Cut-Double-BB concept did not show competitive results. However, the option is still open for future researches with better cutting and sanding of the bottles for testing.

9 Relation between individual bottle tests and configuration tests

The failure tests at Stevinlab were done with so-called ‘as received bottles’. Their respective failure loads were presented in the previous chapter. However, it will be unlikely that glass bottles for construction purposes will be in their ‘as received’ state. This is the reason why tests with damaged samples were carried out.

In this chapter, a relation is made between the tests carried out at AGR with damaged samples and the tests at Stevinlab with ‘as-received’ samples in the configurations. These samples are marked with the letter ‘C’. The result of this chapter is a proposal for a vertical load resistance formula for a bottle column.



9.1. Characteristic tensile strengths of manually abraded and line-simulated bottles

In chapter 5, the following characteristic failure stresses were found for both line-simulated samples and manually abraded samples:

$$\sigma_{f;0.05;MA} = f_{k;MA} = 20 \text{ MPa}$$

$$\sigma_{f;0.05;LS} = f_{k;LS} = 27 \text{ MPa}$$

As a reminder, the values for the line simulated samples are representative for bottles that are found in shops after filling in a beverage factory. Manually abraded samples are representative for bottles that have been damaged due to handling. These values relate to each other in the following manner:

$$f_{k;MA} = f_{k;LS} \times \phi_{MA-LS} \quad [12]$$

The factor ϕ_{MA-LS} is a reduction factor to the strength of the samples with handling damage in mind. This is equal to:

$$\phi_{MA-LS;Weibull} = \frac{f_{k,MA}}{f_{k,LS}} = \frac{20}{27} = 0.74$$

This can be done because:

- The same design of glass bottles was used for both the manually abraded samples and line-simulated samples. The only differences between these bottles are the thickness at the origin, the damage state and the already existing flaws i.e. bubbles, stones etc.
- A large sample of equal size was taken for both categories to get a balanced reading of the data. The strength values are both the characteristic strength values where 95% of the samples are predicted to pass this value.

This means there is about a 26% strength loss that has to be taken into account when designing columns out of used glass bottles. Moreover, in previous chapters it has been noticed that bottles in different damage states cannot be compared solely with vertical failure load values.

In addition, 28 ‘as received’ samples were tested on their vertical failure capacity at AGR. This was due to the fact that the bottles tested at Stevinlab were ‘as-received’ bottles. In total, only two out of these 28 bottles broke, because the maximum capacity of the machine is equal to 2050 kg_f or 20.1105 kN. The two broken bottles had vertical failure loads of 18.79 and 19.47 kN respectively. This means that about 93% of the samples had a higher vertical failure load than 20.1105 kN. The assumption is that the load is equally distributed across the bottles in the Whole-Up concept such that:

$$F_{v;bottle} = \frac{F_{v;total}}{4} \quad [13]$$

Runs	Vertical failure load concept (kN)	Vertical failure load per bottle at failure (kN)
1	86.05	21.51
2	104.03	26.01
3	114.10	28.525
4	96.72	24.18

Table 23 – Vertical failure load for the Whole-Up concept and average failure load per bottle

These values are higher than the ones recorded for the line-simulated and manually abraded samples.

The mirror radii of the weakest samples of the three different groups were measured after testing at AGR. Pictures of the fracture mirrors are shown in Appendix A1. The fracture stress at the mirror can then be calculated. This is not equal to the applied stress, but it is a very localized stress or stress concentration due to the flaw in the glass. These stresses should be higher than the ones found in the FEM model. By comparing these values, a ratio between the damage states can be estimated.

Manually Abraded			Line Simulated			As Received		
Sample nr.	Mirror radius r_m (mm)	Breaking stress σ_f (MPa)	Sample nr.	Mirror radius r_m (mm)	Breaking stress σ_f (MPa)	Sample nr.	Mirror radius r_m (mm)	Breaking stress σ_f (MPa)
B24	2.742	50.31	A10	1.896	60.51	C1	1.315	72.67
B2	2.086	57.66	A11	1.243	74.73	C12	1.504	67.96
B11	2.882	49.03	A26	1.5	68.06			
B5	2.323	54.62						
Average		52.91			67.76			70.31

Table 24 – Breaking stresses at the fracture mirror from the weakest samples

Interestingly, the ratio between manually abraded samples and line-simulated samples is as follows:

$$\phi_{MA-LS;FractureMechanics} = \frac{\sigma_{f;MA,avg}}{\sigma_{f;LS,avg}} = \frac{52.906877}{67.764} = 0.78$$

This value comes close to the earlier mentioned value of 0.74. The ‘average’ values in table 24 is not the average across 28 samples, but the weakest two (as received), three (line-simulated) and four (manually abraded) respectively. There is not a large difference between the values of the line-simulated and as received bottles, but a large difference can clearly be seen between these two and the manually abraded samples. Based upon this, an estimation can be made for a strength reduction factor between as-received bottles and manually abraded bottles:

$$k_{dmg} = \phi_{MA-AR;FractureMechanics} = \frac{\sigma_{f;MA}}{\sigma_{f;AR}} = \frac{52.906877}{70.3137} = 0.75$$

Another way of taking into account the damaged state of the bottle is to design with a characteristic tensile strength of 20 MPa. This will be done in this thesis.

9.2. Load duration factor for glass strength

Because glass is susceptible to static fatigue, a load duration factor has to be included in the design strength of the bottles. The following formula is provided in the NEN2608 (2014) for a load-duration factor. This is shown in equation 14.

$$k_{mod} = \left(\frac{5}{t}\right)^{\frac{1}{c}} \quad [14]$$

A value for c, the corrosion constant, of 16 is usually taken. The parameter ‘t’ is the loading time or load duration in seconds. For example, a column that has to be in use for 5 years:

$$5 \text{ years} = 157788000 \text{ seconds}$$

$$k_{mod} = \left(\frac{5}{157788000}\right)^{\frac{1}{16}} = 0.34$$

The NEN2608 (2014) uses a 5 second reference duration or t_0 (Meyland *et al*, 2021). This is where the value of 5 originates from. However, the tests that were done at AGR were equivalent to a 3 second test as described in chapter 5. For a constant stress, the relationship between fracture stresses at different times is given in equation 15 (Meyland *et al*, 2021):

$$\frac{\sigma_{f,s,2}}{\sigma_{f,s,1}} = \left(\frac{t_{f,s,1}}{t_{f,s,2}}\right)^{\frac{1}{n}} \quad [15]$$

The parameter 'n' is the same as the corrosion constant c, and so a value of 16 is taken. The load-duration factor is a ratio between the stress at failure after a specific time and the characteristic strength of the glass (Meyland *et al*, 2021). This is shown in equation 16.

$$k_{mod} = \frac{\sigma_f}{f_k} \quad [16]$$

The value for $\sigma_{f,s,1}$ is the characteristic tensile stress found with a reference time of 3 seconds with the AGR tests. The value for $\sigma_{f,s,2}$ is the characteristic tensile stress after a period of $t_{f,s,2}$ seconds. This gives equation 17.

$$\frac{\sigma_{f,s,2}}{\sigma_{f,s,1}} = \left(\frac{t_{f,s,1}}{t_{f,s,2}}\right)^{\frac{1}{n}} = \left(\frac{3}{t_{f,s,2}}\right)^{\frac{1}{n}} = k_{mod} \quad [17]$$

According to the AGR test results, the load-duration factor is as follows with the same load-duration:

$$k_{mod} = \left(\frac{3}{157788000}\right)^{\frac{1}{16}} = 0.33$$

There is therefore a slight difference between the load-duration factor calculated with the NEN2608 (2014) and the load-duration factor calculated with a reference time of 3 seconds.

9.3. Calculating the tensile design strength of container glass

Therefore, the design tensile strength of the bottle can be calculated in the following manner:

$$f_{mt;u;d} = \frac{k_{dmg} \times k_{mod} \times f_{g;AR;k}}{\gamma_{m;A}} = \frac{k_{mod} \times f_{g;MA;k}}{\gamma_{m;A}} \quad [18]$$

$$f_{g;MA;k} = 20 \text{ MPa}$$

NEN2608 (2014) gives a value for $\gamma_{m;A}$ of 1.8. This is a material factor for float glass. For example, the design strength of a manually abraded bottle after 50 years can be calculated:

$$k_{mod} = \left(\frac{3}{365 \times 50 \times 24 \times 3600}\right)^{\frac{1}{16}} = 0.285$$

$$f_{mt;u;d} = \frac{0.285 \times 20}{1.8} = 3.167 \text{ MPa}$$

For safety purposes, this is the value that cannot be exceeded in the glass bottles. A method needs to be created to transfer this design strength to the allowable vertical load on any glass bottle. The tests at AGR and Stevinlab were performed with standardized 300 ml longneck beer bottles.

9.4. Calculating the vertical load resistance of an individual bottle

From the data simulated in ANSYS earlier on, a relation was estimated between the thickness of the shoulder of broken AGR samples and the maximum strength index in MPa/kN with a R^2 of 0.999. This relation is shown in equation 19.

$$SI_{max} = 10.335e^{-0.519 \times t}$$

[19]

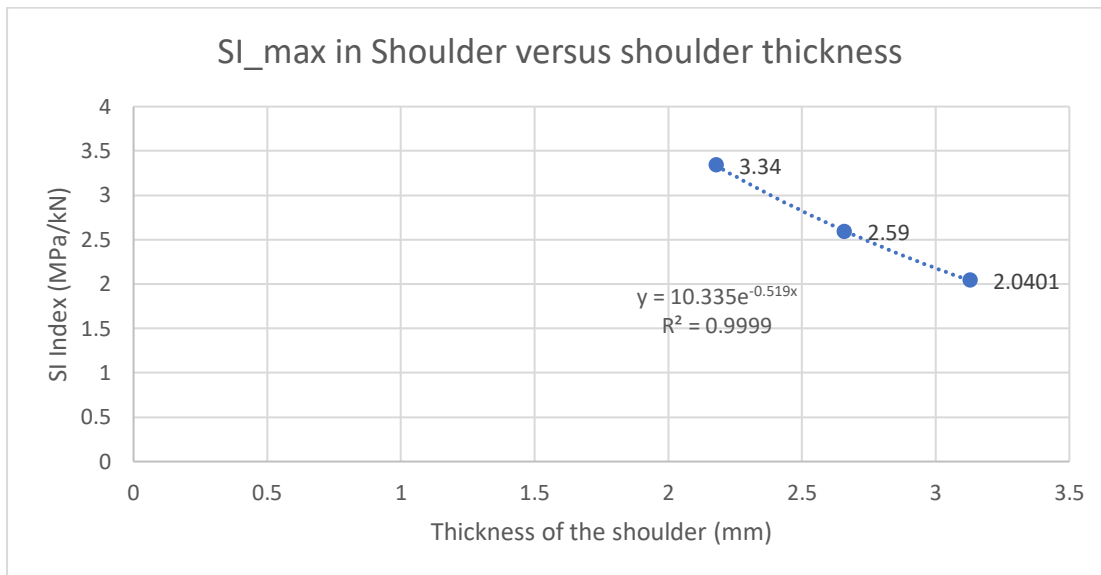


Figure 65 - Relation of the stress index versus the shoulder thickness at the origin based upon the ANSYS+Interpolation data

This empirical relation can be used to predict the vertical load resistance of an individual bottle based upon the thickness. However, DIANA FEA has an useful feature where the thickness of the shell can easily be changed, which is not possible in ANSYS. Therefore, this empirical relation is checked with a DIANA model. The input for the DIANA model is a vertical load of 1 kN. The maximum principle stress in the shoulder is then equal to the stress index in the shoulder, because the vertical load is equal to 1 kN.

Shoulder Thickness (mm)	SI_max formula (MPa/kN)	SI_max DIANA (MPa/kN)
1.5	4.74	4.63
1.75	4.17	3.96
2	3.66	3.43
2.25	3.21	3.02
2.5	2.82	2.68
2.75	2.48	2.39
3	2.18	2.16
3.25	1.91	1.96
3.5	1.68	1.79

Table 25 – Comparison between stress indices from the empirical formula and a second model in DIANA

Table 25 shows that the stress indices of the empirical formula are slightly higher than the ones from DIANA. In other words, the empirical formula slightly overestimates the maximum principle stress in the shoulder. The empirical formula is however based on the design of the bottle that is tested at AGR and in Stevinlab. Extensive research should follow to investigate this relation across a multitude of bottles designs. This empirical formula is useful to quickly transfer the design strength to a vertical load resistance due to the complex geometric nature of the bottle.

By assuming a thickness of the shoulder of 2.5 mm and a $f_{mt;u;d}$ of 3.22 MPa after 50 years, the vertical load capacity on the bottle can be estimated:

$$N_{Rd} = \frac{f_{mt;u;d}}{SI_{max}(t)} = \frac{3.167}{10.335e^{-0.519 \times 2.5}} = 1.12 \text{ kN}$$

[20]

The value of 1.12 kN is then used in a FEM program and the maximum principle stress in the shoulder is collected. A shell thickness of 2.5 mm is used.

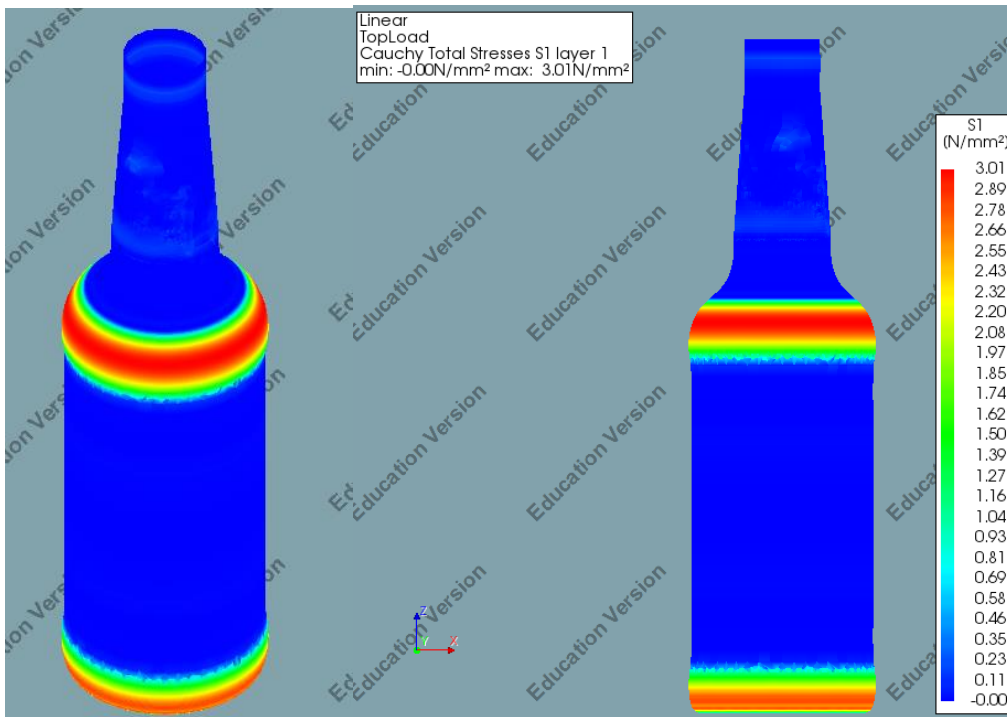


Figure 66 – FEA output in DIANA – Bottle with 2.5 mm thickness, $E = 70 \text{ GPa}$ and a top load of 1.12 kN

The largest principle tensile stress in the bottle is $\sigma_{1,max} = 3.01 \text{ N/mm}^2$.

$$\text{Accuracy: } \frac{|3.01-3.167|}{3.167} * 100 = 4.96\% \text{ difference}$$

9.5. Influence of intermediate connections on the vertical failure loads

The results from the Stevinlab tests have shown lower values for the Whole-FF and Whole-BB concept than for the Whole-Up concept. The mean values of the Whole-FF and Whole-BB values show a decrease of 19.2% and 29.5% respectively compared to the Whole-Up samples. This has to be taken into account when creating prototypes with these two configurations. The difference between the configuration is not the glass itself, so the calculated design strength value does not change. This has to do with the fact that some bottles end up taking more vertical load than others. This is captured with a tolerance factor called k_{system} . For a system with Whole-FF configurations, a factor of 0.8 is applied.

$$N_{Rd,system} = N_{Rd,bottle} \times n_{bottle} \quad [21]$$

$$N_{Rd,system,reduced} = k_{system} \times N_{Rd,system} \quad [22]$$

There is however an uncertainty as to how large this k_{system} is for a larger amount of bottles (i.e. more tolerance issues). This is something that has to be investigated in the future.

9.6. Design formula for vertical load resistance of a bottle column

The combination of the data acquired from the AGR and Stevinlab tests and the relation between two tests led to the proposal of a formula in equation 23 for the vertical load resistance of a bottle column:

$$N_{Rd,system,reduced} = k_{system} \times n_{bottle} \times \frac{f_{mt;u;d}}{10.335e^{-0.519 \times t}} \quad [23]$$

k_{system} = factor taking into account the tolerances of the system leading to a non-uniform load distribution: 0.8 for Whole-FF. 0.7 for Whole-BB. When applying both configurations, choose the lowest value for k_{system} .

n_{bottle} = number of bottles per layer

$f_{mt;u;d}$ = the tensile design strength of container glass in (N/mm²)

t = thickness of the shoulder of the bottle (in mm)

$N_{Rd,system,reduced}$ = the vertical load resistance of a bottle column (in kN)

This design formula takes the following points into account:

- *The tensile design strength of abraded container glass.* The value for $f_{mt;u;d}$ is based upon the **characteristic** tensile strength of abraded container glass. The load-duration effect is taken into with the k-mod factor. Moreover, a material factor γ_M is used.
- *The effect of bottle thickness on the vertical load resistance.* It was noticed during the AGR tests that the thickness of the bottle had a large effect on the vertical load resistance of the bottle. The thickness of the bottle is added as a parameter into this formula.
- *Tolerance factor.* When the Whole-FF configuration is used, there could be issues due to different tolerances (f.e. slightly different bottle lengths, the plugs, thickness of the plastic elements, verticality of the bottles). A factor is therefore applied to reduce the resistance of the column to take into account the non-uniform loading of the bottles (i.e. one bottle takes up more load than the others leading to early failure).

This formula is a concept and this needs to be validated with a large bottle column.



E

E Column Design

E

10 Column Designs and Limitations

In this chapter, a column design is made from glass bottles based upon the information gathered in earlier tests and studies. A case study will be used to evaluate the vertical design load on the column. The retrieved strength values and reduction factors will be used to validate the design.

It is important to choose the right configurations of bottles for the column. In the thesis, the options are limited to symmetrical bottle patterns in equilateral polygons. These polygons range from a triangle to higher orders of polygons. On top of that, the option of eight bottles is also considered in a square pattern.

10.1. Bottle Patterns

The choice of the desired glass bottle pattern mainly depends on the necessary capacity of the column i.e. how many bottles are needed to resist the vertical load. Moreover, a choice can also be made for the type of plates, which are either square or circular. In figure 67, the used area of the cross section from the bottles compared to the plates is given in percentages. It can be seen that some configurations are more space efficient with square plates than with circular plates, and vice versa. The square plates are therefore more efficient than circular plates for bottle counts of 4, 8, 16, 24, 36 etc.

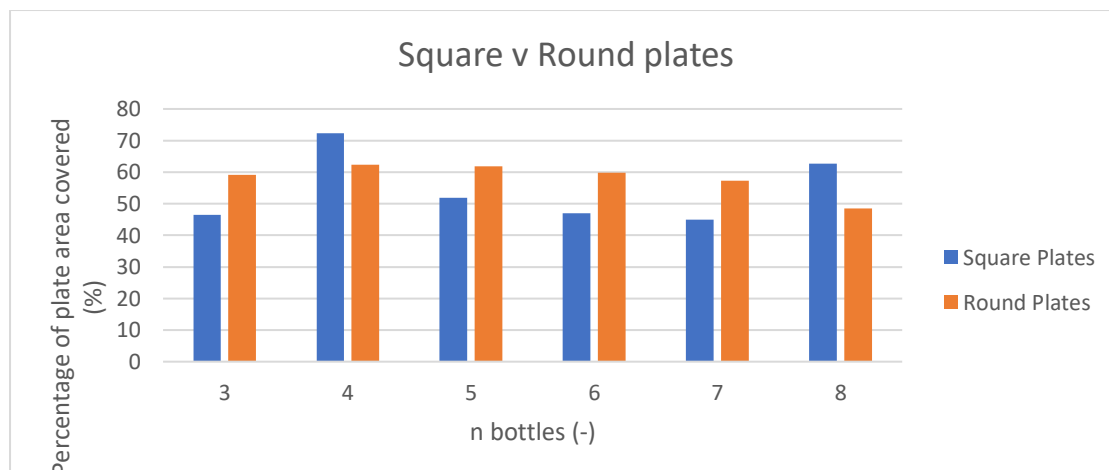
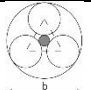
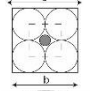

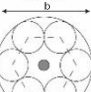
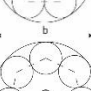
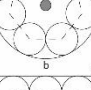
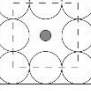
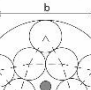
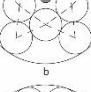
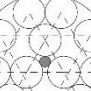


Figure 67 – Percentage of area covered in cross-section by bottles with a bottle diameter of 60 mm and a clearance of 5 mm

Graham *et al* (1998) investigated the dense packing of equal circles in a larger circle. This is similar to the problem of densely packed glass bottles on a circular plate, although the problem in the paper of Graham *et al* (1998) is in 2D. The patterns found by Graham *et al* (1998) are however not all symmetrical and not all have space left in the centre for a threaded rod. A catalogue of patterns for square and circular plates is therefore created for the purpose of packing glass bottles, whilst being symmetrical and having space for a

threaded rod in the centre. The intention is then that a designer picks a pattern from this catalogue closest to the necessary amount of bottles to resist the compression load. The minimum width of the plate is also given in this catalogue. The proposed formula is used to calculate the estimated vertical compressive load resistance after 50 years.

$$N_{Rd,system,reduced} = k_{system} \times n_{bottle} \times \frac{f_{mt;u;d}}{10.335e^{-0.519 \times t}}$$

Number of bottles	Shape plate	Top-view	Width	Minimum Plate Area	Estimated Design Compression load Capacity after 50 years N_{Rd} (kN)
n (-)			b (mm)	A_{min} (mm ²)	
3	Circular		$2.15 \times d_{bottle,max}$	$1.16\pi \times d_{bottle,max}^2$ $\approx 3.63 \times d_{bottle,max}^2$	2.69
4	Square		$2 \times d_{bottle,max}$	$4 \times d_{bottle,max}^2$	3.59
5	Circular		$\approx 2.70 \times d_{bottle,max}$	$\approx 1.82\pi \times d_{bottle,max}^2$ $\approx 5.72 \times d_{bottle,max}^2$	4.49
6	Circular		$3 \times d_{bottle,max}$	$2.25\pi \times d_{bottle,max}^2$ $\approx 7.07 \times d_{bottle,max}^2$	5.39
7	Circular		$\approx 3.30 \times d_{bottle,max}$	$\approx 2.73\pi \times d_{bottle,max}^2$ $\approx 8.58 \times d_{bottle,max}^2$	6.29
8	Square		$3 \times d_{bottle,max}$	$9 \times d_{bottle,max}^2$	7.18
10	Circular		$\approx 4.10 \times d_{bottle,max}$	$\approx 4.20\pi \times d_{bottle,max}^2$ $\approx 13.19 \times d_{bottle,max}^2$	8.98
12	Circular		$\approx 4.22 \times d_{bottle,max}$	$\approx 4.46\pi \times d_{bottle,max}^2$ $\approx 14.01 \times d_{bottle,max}^2$	10.78
15	Circular		$\approx 4.532 \times d_{bottle,max}$	$\approx 5.13\pi \times d_{bottle,max}^2$ $\approx 16.12 \times d_{bottle,max}^2$	13.47
16	Square		$4 \times d_{bottle,max}$	$16 \times d_{bottle,max}^2$	14.37

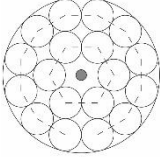
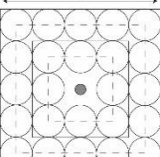
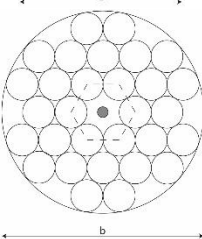
18	Circular		≈ 4.86 $\times d_{bottle,max}$	$\approx 5.91\pi \times d_{bottle,max}^2$ $\approx 18.57 \times d_{bottle,max}^2$	16.17
24	Square		$5 \times d_{bottle,max}$	$25 \times d_{bottle,max}^2$	21.55
30	Circular		≈ 6.296 $\times d_{bottle,max}$	$\approx 9.91\pi \times d_{bottle,max}^2$ $\approx 31.13 \times d_{bottle,max}^2$	26.94

Table 26 – Catalogue of bottle patterns that can be used for efficient spacing

The parameter $d_{bottle,max}$ is the largest diameter of the bottle. These options for patterns are rotational symmetric and the glass bottles are evenly spread over the plates. The grey dots indicate the necessary space for a threaded rod. The square options are more space-efficient compared to the circle options, but symmetrical square options are only possible for a certain amount of glass bottles (i.e. 4, 8, 16 etc.). These options will be used for a case-study calculation.

10.2. Design options glass bottle columns

From the investigated concepts tested at Stevinlab, two main design options are looked at for creating a column out of glass bottles:

- Option A: Combining Whole-FF with Whole-BB. Column with glued connections and demountable connections
- Option B: Fully demountable column, combining Whole-FF with Whole-Up.

Figures 66 and 67 show the building steps for Option A and Option B respectively. Both options have advantages and disadvantages. Table 27 gives a concise summary of the advantages and disadvantages.

Advantages and disadvantages Option A	Advantages and disadvantages Option B
- Glued connections (+/-)	- Demountable connection (++)
- Hard to build in stages (--)	- Easy to build in stages (++)
- Less plastic material (+)	- More plastic material (--)
- Less plate material (+)	- More plate material (+/-)
- Lower tolerance factor (--)	- Higher tolerance factor (++)
- Long preparation and setting time (--)	- Lower preparation time (+)

Table 27 – Advantages and disadvantages of both options

Figures 70 and 71 show side view and details of the connections of both options. Option B is built as a prototype mainly due to the demountable connection, quick building time and higher tolerance factor.

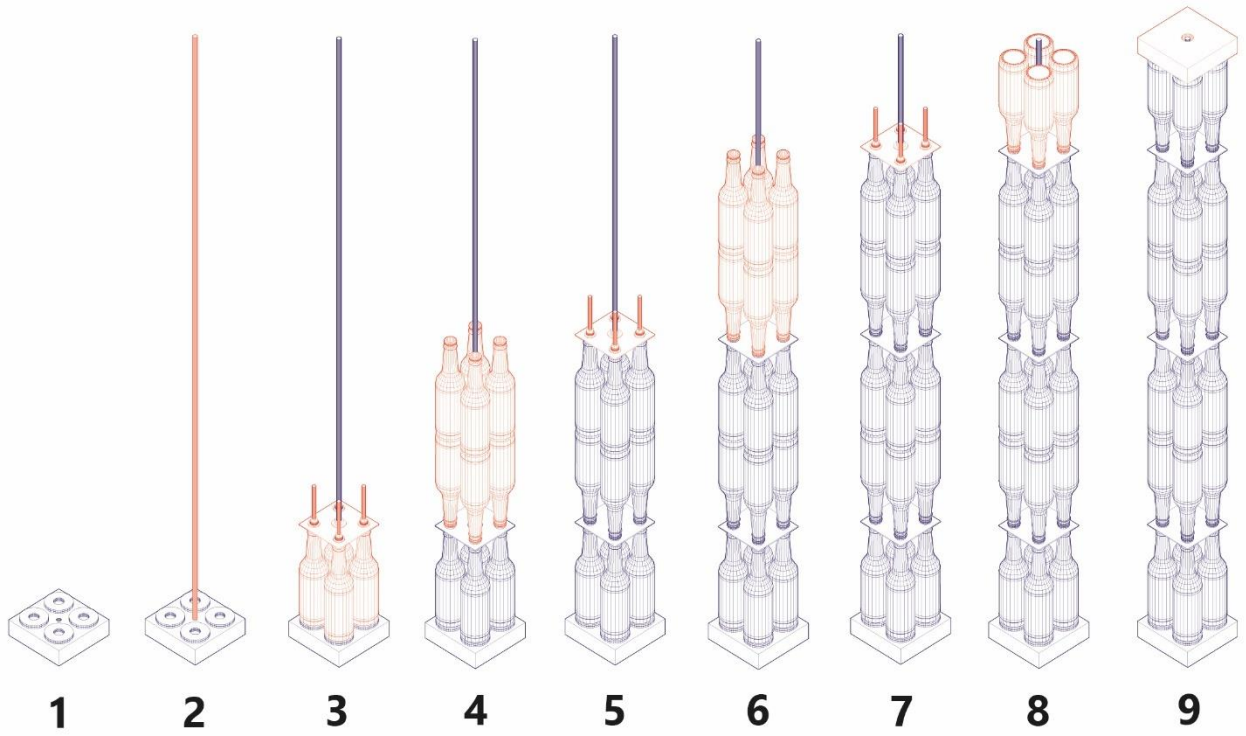


Figure 68 – The building steps for Option A

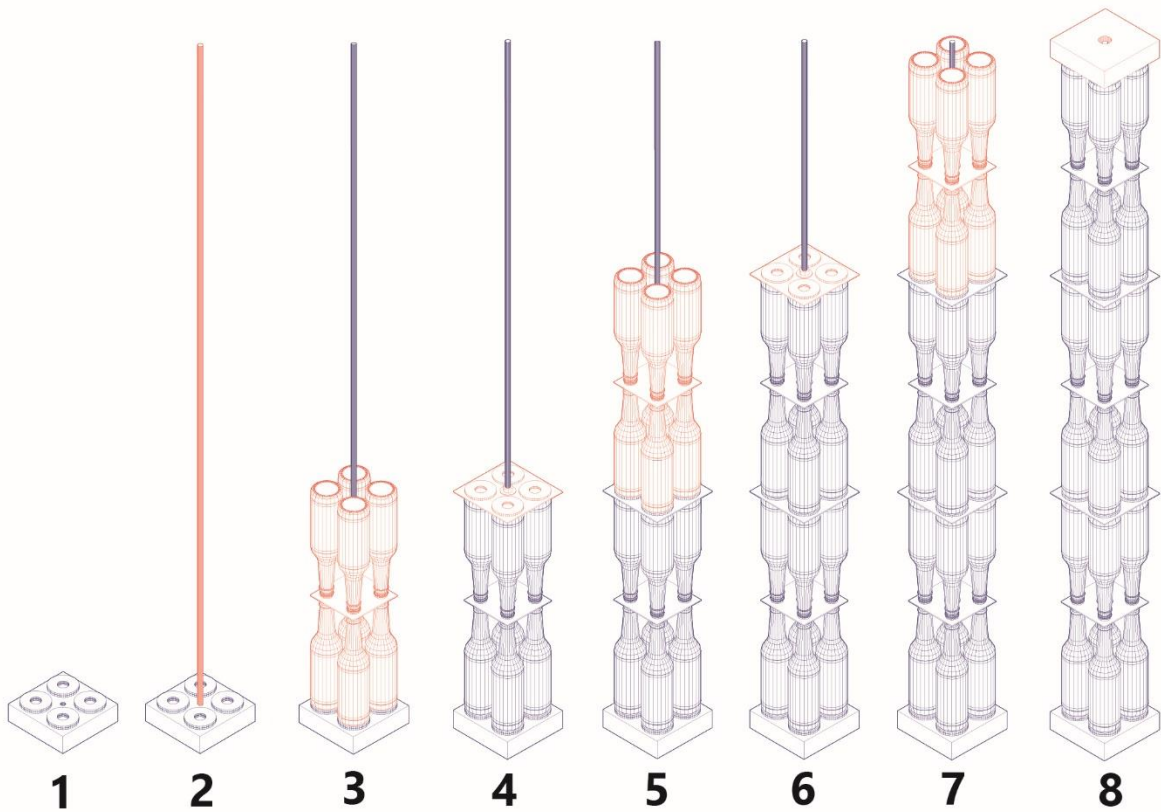


Figure 69 – The building steps for Option B

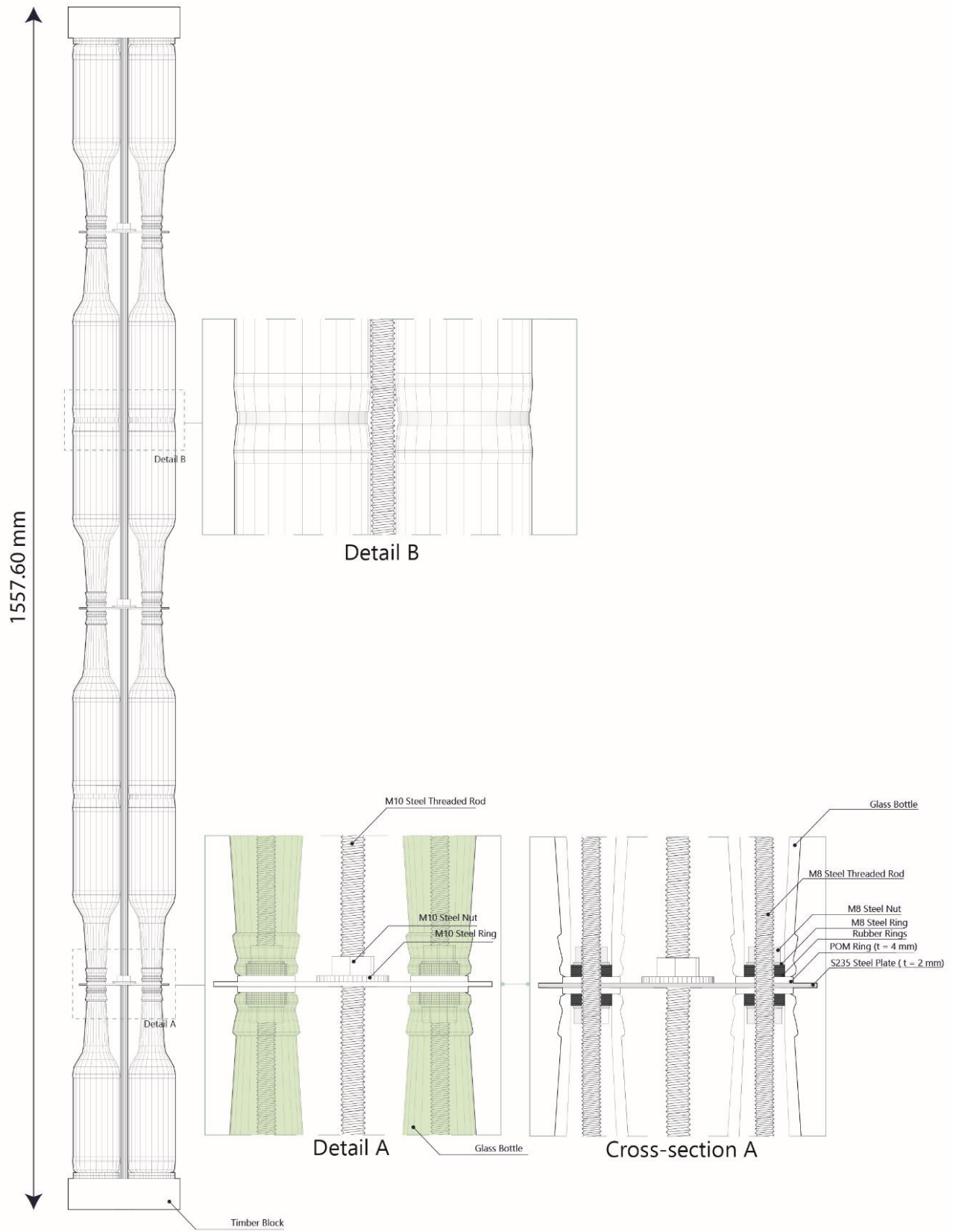


Figure 70 – Side-view and details of Option A

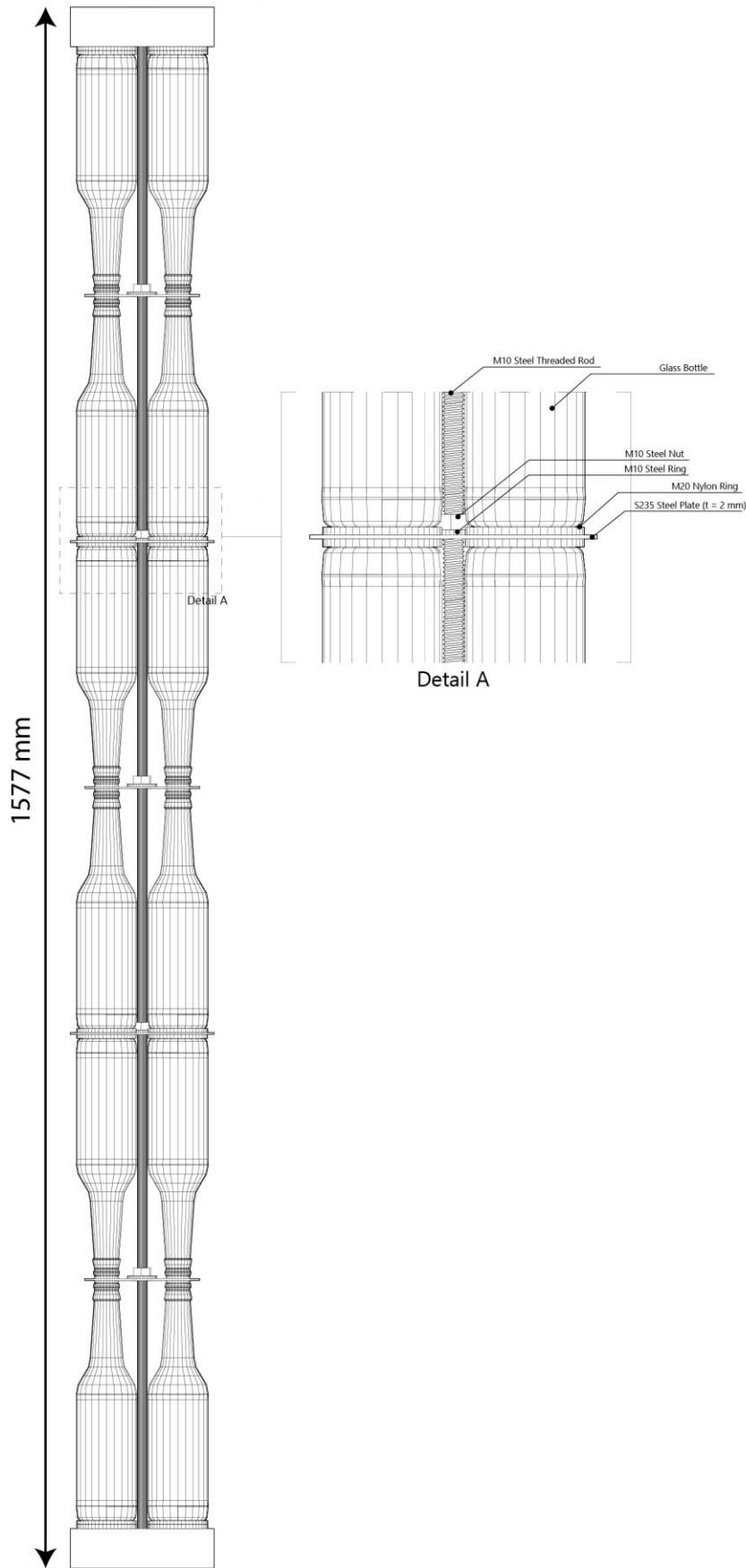


Figure 71 – Side-view and detail of Option B

10.3. Case study calculation for a bottle column

A case-study calculation is made to understand the amount of bottles one needs to construct a column to resist the applied vertical compressive load.

For the case-study calculation, the following things are assumed:

- The service life of the building is 50 years. A bottle thickness of 2.5 mm is assumed.
- The building is a one-story building.
- The column is three meters long and is simply supported on both edges.
- The calculation will be a unity-check on the vertical compressive force on the column due to variable and permanent loads.
- The building is classified as CC2-building.
- The columns need to be fully demountable to recycle the building materials. Therefore, option B is chosen from the design alternatives.

Figure 72 shows a drawing of a sketch of the column location in the building.

Firstly, the load factors are defined for permanent and variable loads. This is based upon the CC2 construction class.

$$\gamma_G = 1.2 ; \gamma_Q = 1.5 ;$$

Because the location of the building is not known, the following value for $q_{Q,wind}$ is assumed:

$$q_{Q,wind} = 1 \text{ kN/m}^2$$

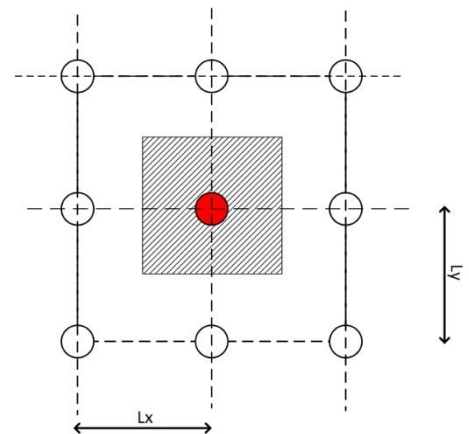


Figure 72 – Sketch of the investigated column in red.

The permanent loads of the structure resting on the column are retrieved from the Quick Reference by L.A.G. Wagemans (2014).

$$q_{G:roofing+insulation} = 0.15 \text{ kN/m}^2$$

$$q_{G:beams+purlins} = 1 \text{ kN/m}^2$$

$$q_{G;k,roof} = q_{G:roof;sheeting;steel} + q_{G:roofing+insulation} + q_{G:beams+purlins} = 1.15 \text{ kN/m}^2$$

The other remaining permanent load is the weight of the column itself. The glass bottles that were used during the testing had a weight of about 300 grams or 0.0029 kN. The column length is equal to 3 meters. The bottles that were used were 238 mm long. This means that a total of 12 layers can fit in this 3 meters.

$$F_{G,k,bottle} = 12 \times 0.0029 = 0.035 \text{ kN}$$

It can be seen that the order of magnitude of the self-weight of the column is much lower than the permanent load from the structure above. It is therefore neglected in this hand-calculation.

The total distributed design load is then equal to:

$$q_{Ed} = \gamma_G \times q_{G,k} + \gamma_Q \times q_{Q,k}$$

$$q_{Ed} = 1.2 \times 1.15 + 1.5 \times 1 = 2.88 \text{ kN/m}^2$$

For a column in the center of the grid plan, the vertical load on that column is then:

$$N_{Ed} = q_{Ed} \times L_{span,x} \times L_{span,y}$$

Suppose that the span in both direction is equal to 3 meters.

$$N_{Ed} = 2.396 \times 3 \times 3 = 25.92 \text{ kN}$$

For the calculation of the resistance part, the following formula is used:

$$N_{Rd,system,reduced} = k_{system} \times n_{bottle} \times \frac{f_{mt;w,d}}{10.335e^{-0.519 \times t}}$$

$$k_{system} = 0.8 \text{ (Whole - FF configurations)}$$

$$k_{mod} = \left(\frac{3}{365 \times 50 \times 24 \times 3600} \right)^{\frac{1}{16}} = 0.285$$

$$f_{mt;w,d} = \frac{0.285 \times 20}{1.8} = 3.17 \text{ MPa}$$

Suppose 24 bottles are used per layer:

$$N_{Rd,system,reduced} = 0.8 \times 24 \times \frac{3.17}{10.335e^{-0.519 \times 2.5}} = 21.554 \text{ kN}$$

Unity check on vertical load:

$$U.C. = \frac{N_{Ed}}{N_{Rd,system,reduced}} = \frac{25.92}{21.554} = 1.2$$

Increase the number of bottles to lower the unity check:

$$n_{bottle} = 30$$

$$N_{Rd,system,reduced} = 0.8 \times 30 \times \frac{3.17}{10.335e^{-0.519 \times 2.5}} = 26.94 \text{ kN}$$

$$U.C. = \frac{N_{Ed}}{N_{Rd,system,reduced}} = \frac{25.92}{26.94} = 0.96$$

According to the table, the width of the column needs to be about $6.296 \times d_{bottle;max}$. Assume a $d_{bottle;max}$ of about 61 mm. This means that circular plates with a width of about 384.1 mm are necessary. The total amount of bottles that one needs to construct in column is then equal to 360. Figure 73 shows a context drawing of the case study.

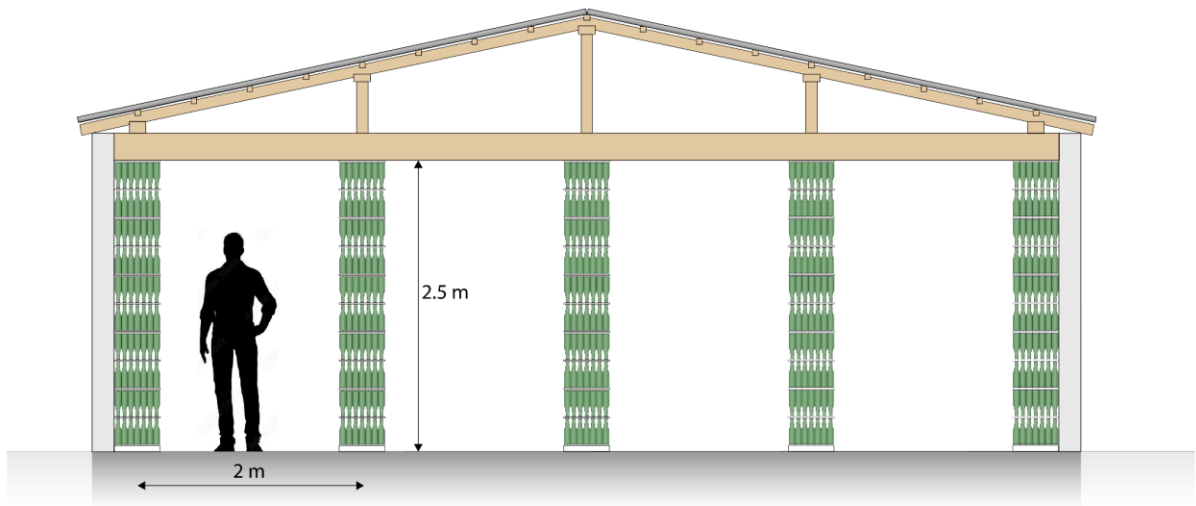
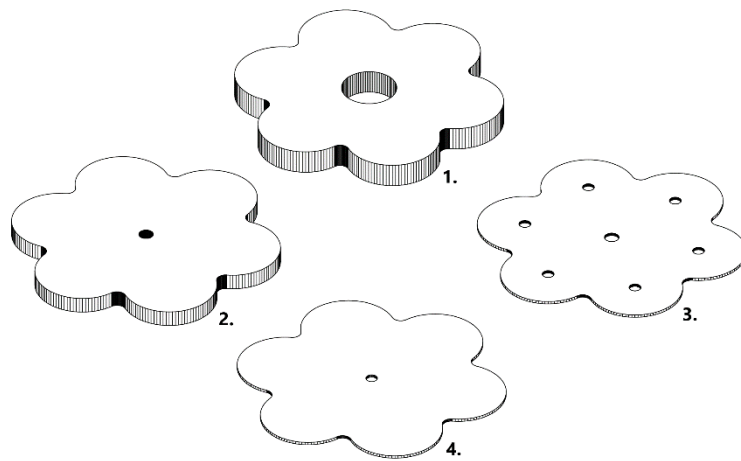


Figure 73 – Context drawing of the case study

10.4. Prototype of a bottle column

A prototype of the bottle column was created in Stevinlab from left over bottles of the testing and recycled bottles from a restaurant. The bottom and top layer contain bottles that were left over from the fracture tests, the rest of the bottles are all recycled. Furthermore, the connections were made with left over pieces from the testing. In the prototype, the POM disks are modelled with M12 Nylon rings for visual purposes. Moreover, the steel plates are modelled with MDF. Figure 74 shows a 3D render of how the column was planned to look like. Figure 75 shows the design of the plates that were laser-cut and CNC-milled at the faculty of Architecture of TU Delft. A choice was made for a hexagon pattern.



MDF Plate 18 mm - 2x

MDF Plate 12 mm - 2x

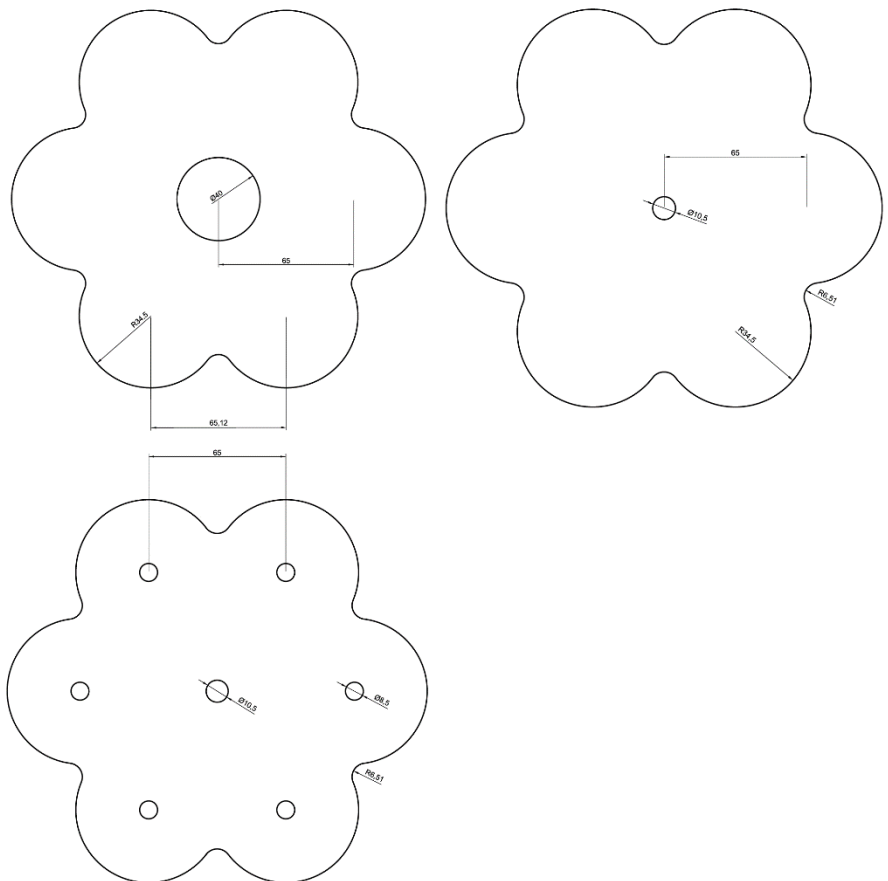
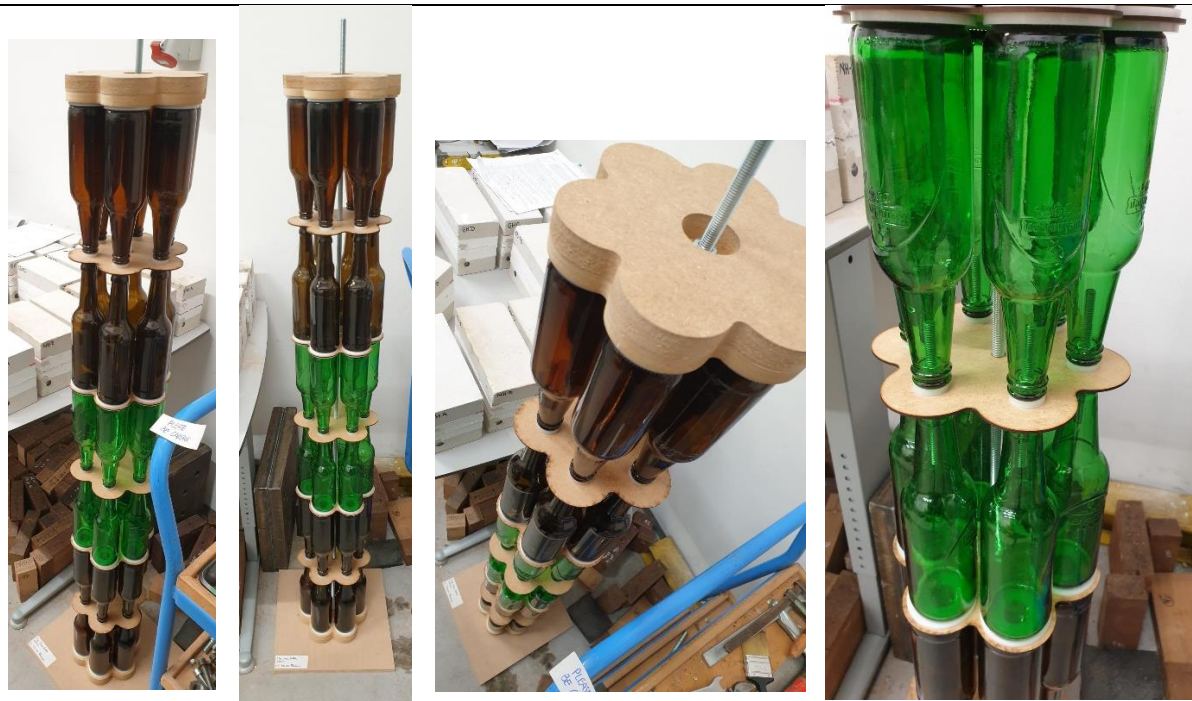


Figure 74 and 75 – Left: 3D render of the prototype. Right: Top views and 3D views of the plates to be laser-cut and CNC-milled at the Faculty of Architecture (1. = Boundary Plate 1, 2. = Boundary Plate 2, 3. Finish Plate, 4. Bottom Plate)



3D-View Front View Top View Close-Up Connection

Figure 76 – Pictures of the prototype of the stacked bottle column

Figure 76 shows pictures of the prototype. The following things were noticed when building the prototype:

- There were a few air gaps between the bottom of the glass bottles and the large nylon rings, especially at the top of the column. This could be either due to the slight difference in heights of the glass bottles.
- Some rubber rings were a bit oversized, which means they had to be cut down slightly for the glass bottle to fit. This could also have had an effect on the verticality of the bottles.
- Because the connections are tied to the plates, this can lead to the thin MDF plates bending ever so slightly. In reality, stiffer plates or thicker plates should be used with the final connection.
- To improve the verticality of the bottles, a solution can be found by putting the threaded rods through the whole column, rather than just at the connection. This will be elaborated upon in the design explorations.

10.5. Comparison bottle column with conventional materials

It is interesting to show the comparison of the bottle column with other alternatives. Hand calculations are made to give an indication of the difference between more conventional options and the bottle column. The hand calculations are made based upon rules for buckling stability of the different materials. The unknown in these calculations is the design load that can be put on the column.

The following values are considered:

- The same design of the bottle column is used for the hand calculation
- For the concrete column:
 - A circular concrete column with a diameter of 200 mm.

- Concrete class C30/37
- For the steel column:
 - A hollow steel column CHS193.7 with a wall thickness of 6.3 mm
 - Strength class S235
- For the timber column:
 - A square timber column of 140x140 mm
 - The material C24 (Solid timber) is used.

The columns have lengths of 3 meters. The hand calculations are limited to first order stability calculations.

10.5.1. Concrete option

For the hand-calculations of the concrete option, rules from the NEN-EN 1992-1-1+C2 (2011) are used. For the concrete column, a few things are assumed:

- All column types are compared with axial compressive buckling. The reinforcement in concrete has an influence on the stability of the column. Because the reinforcement properties are not known, they are left out.
- Second order effects do not have to be analyzed when:

$$\frac{n_{knik}}{n_{knik} - 1} \leq 1.1 ; n_{knik} = \frac{N_{knik}}{N_{Ed}}$$

In the Eurocode, this is put into a slenderness criterium:

$$\lambda \leq \lambda_{lim} = \frac{20 \times A \times B \times C}{\sqrt{n}}$$

In this hand-calculation, $\lambda = \lambda_{lim}$. The unknown is the value n , which includes N_{Ed} . The factor A takes into account the time-dependent behavior of concrete with the creep factor φ_{eff} .

$$A = \max\left(\frac{1}{1 + 0.2 \times \varphi_{eff}}; 0.7\right)$$

Assumption: φ_{eff} (creep factor) = 1.2

$$A = \max\left(\frac{1}{1 + 0.2 \times 1.2}; 0.7\right) = 0.81$$

The factor B takes into account the amount of reinforcement in the concrete with the parameter ω . This parameter is set to zero.

$$\omega = \frac{A_{s,tot} \times f_{yd}}{A_c \times f_{cd}}$$

$$B = \max(\sqrt{1 + 2 \times \omega}; 1.1) = 1.1$$

The factor C takes into account the first order load distribution with additional bending moments on the boundaries. The r_m value is set to zero.

$$r_m = \frac{M_{01}}{M_{02}}$$

$$C = \max(1.7 - r_m; 0.7) = 0.7$$

The slenderness of the column is calculated as follows:

$$\lambda = \frac{l_{buc}}{i}$$

$$i = \sqrt{\frac{I}{A}} = \sqrt{\frac{\frac{\pi}{64} d^4}{\frac{\pi}{4} d^2}} = 0.25d = 50 \text{ mm}$$

$$\lambda = \frac{3000}{50} = 60$$

$$\frac{l_{buc}}{i} = \frac{20 \times A \times B \times C}{\sqrt{n}}$$

$$60 = \frac{20 \times 0.81 \times 1.1 \times 0.7}{\sqrt{n}}$$

$$\sqrt{n} = 0.2079 ; n = 0.456$$

$$n = \frac{N_{Ed}}{A_c \times f_{cd}}$$

$$f_{cd} = \frac{f_{ck}}{\gamma_c} = \frac{30}{1.5} = 20 \text{ MPa}$$

$$N_{Ed} = n \times A_c \times f_{cd} = 0.456 \times \frac{\pi}{4} \times 200^2 \times 20 = 286488.45 \text{ N} = 286.49 \text{ kN}$$

10.5.2. Steel Option

For the steel column, the procedure from the Eurocode is used. The document that has been followed is NEN-EN 1993-1-1+C2+A1:2016 (2016). The cross-section class has to be decided first for round hollow profiles:

$$\frac{d}{t} = \frac{193.7}{6.3} = 30.75$$

The criterium for cross-section class 1:

$$\frac{d}{t} \leq 50 \varepsilon^2$$

$$30.75 \leq 50$$

The buckling resistance of a column with cross-section class 1 is calculated as follows:

$$N_{b,Rd} = \frac{\chi A f_y}{\gamma_{M1}}$$

$$N_{cr} = \frac{\pi^2 EI}{L_{buc}^2}$$

$$I_{column} = \frac{\pi}{64} \times (193.7^4 - (193.7 - 2 \times 6.3)^4) = 16300455.56 \text{ mm}^4$$

$$E_{steel} = 210 \times 10^3 \text{ MPa}$$

$$N_{cr} = \frac{\pi^2 \times 210 \times 10^3 \times 16300455.56}{3000^2} = 3753844.452 \text{ N}$$

$$\bar{\lambda} = \sqrt{\frac{A f_y}{N_{cr}}} = \sqrt{\frac{(\frac{\pi}{4} \times 193.7^2 - \frac{\pi}{4} \times (193.7 - 6.3 \times 2)^2) \times 235}{3753844.452}} = 0.482$$

CHS profiles are round, hollow and hot-rolled, which means that buckling curve a needs to be chosen. This comes with an imperfection factor α of 0.21.

$$\Phi = 0.5[1 + \alpha(\bar{\lambda} - 0.2) + \bar{\lambda}^2] = 0.5 \times [1 + 0.21 \times (0.482 - 0.2) + 0.482^2] = 0.646$$

$$\chi = \frac{1}{\Phi + \sqrt{\Phi^2 - \bar{\lambda}^2}} = 0.93$$

$$N_{b,Rd} = \frac{0.93 \times \left(\frac{\pi}{4} \times 193.7^2 - \frac{\pi}{4} \times (193.7 - 6.3 \times 2)^2\right) \times 235}{1} = 810607.88 \text{ N} = 810.61 \text{ kN}$$

10.5.3. Timber Option

The hand-calculations for the timber option are made with the help of the NEN-EN 1995-1-1 (en) (2005).

$$C24: f_{c,0,k} = 21 \text{ N/mm}^2$$

$$E_{0.05} = 7400 \text{ N/mm}^2$$

For a permanent load and service class 2 a k_{mod} of 0.6 is used.

$$I = \frac{1}{12} \times b \times h^3 = \frac{1}{12} \times 140 \times 140^3 = 32013333.33 \text{ mm}^4$$

$$i = \sqrt{\frac{I}{A}} = \sqrt{\frac{32013333.33}{140 \times 140}} = 40.41$$

$$\lambda = \frac{l_{buc}}{i} = \frac{3000}{40.41} = 74.23$$

$$\lambda_{rel} = \frac{\lambda}{\pi} \times \sqrt{\frac{f_{c,0,k}}{E_{0.05}}} = \frac{74.23}{\pi} \times \sqrt{\frac{21}{7400}} = 1.26$$

With $\beta_c = 0.2$ for solid timber:

$$k_y = 0.5 \times (1 + 0.2 \times (1.26 - 0.3) + 1.26^2) = 1.39$$

$$k_{c,y} = \frac{1}{k_y + \sqrt{k_y^2 - \lambda_{rel}^2}} = 0.51$$

$$f_{c,0,d} = k_{mod} \times \frac{f_{c,0,k}}{\gamma_M} = 0.6 \times \frac{21}{1.3} = 9.69 \text{ N/mm}^2$$

$$N_{Rd} = f_{c,0,d} \times A_{column} \times k_{c,y} = 9.69 \times 140 \times 140 \times 0.51 = 96861.24 \text{ N} = 96.86 \text{ kN}$$

10.5.4. Glass Bottle Option

The proposed formula is used to calculate the vertical compressive resistance of the bottle column with six bottles, an assumed thickness of 2.5 mm, Whole-FF connections and a design life of 50 years.

$$N_{Rd,system,reduced} = 0.8 \times 6 \times \frac{3.17}{10.335e^{-0.519 \times 2.5}} = 5.38 \text{ kN}$$

These four values are put in table 28 for comparison.

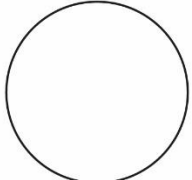
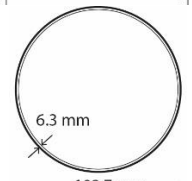
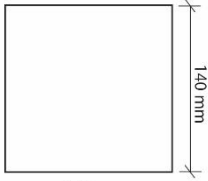
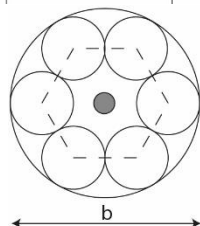
Material	Cross-section shape	Design compression load in kN
Concrete (no-rebar)		286.49
Steel CHS-profile		810.61
Square timber		96.86
Glass Bottle Column (n=6) with b = 199 mm		5.38 (after 50 years)

Table 28 – Comparison between design compression loads

It is shown with hand calculations that the design compression load is much higher with materials such as concrete, steel or timber. It is therefore advised to use the application of glass bottles in a column in a stacked manner for small buildings for now.

However, the steel and timber option are both options that need to be prefabricated in a factory, which includes a high amount of fabrication costs and transport costs, especially to very remote areas. Concrete itself is known to be a high contributor to the world's greenhouse gas emissions and is not a very sustainable option. The bottle column can therefore still be a viable option for smaller projects. The biggest contributor to the large differences in resistance is the time-dependent behavior of the glass strength and the fact that abraded bottles are used.

10.6. Limitations of the stacked glass bottle column

The gathered information in this chapter has contributed to answering the final sub-question of this thesis:

‘What are the limitations of columns out of glass bottles?’

10.6.1. Height tolerances

The bottles that were used for the experiments did have a technical drawing included with them. The drawing is shown in Appendix A5. The technical drawing shows a total height of about 238 mm, but with an error margin in mind. The height of ten bottles were also measured. This is shown in Appendix A4.5. The highest measured height was equal to 238.3 mm and the lowest was equal to 237.8 mm, a difference of 0.5 mm. This may not seem as much, but when a stacked column is made, these errors can build up when stacking multiple layers. This slight difference in bottle height can cause some bottles to take up more load than others.

After building the prototype, very small air gaps were observed between some bottles and nylon rings at the top.

10.6.2. Bottle designs

When working with a stacked bottle column, one can only use the same design of bottles per layer. If there is a high diversity between bottle designs collected, it can become difficult to construct such a column.

10.6.3. Bottle patterns

Earlier in this chapter, several patterns of glass bottles were provided. These are symmetrical patterns. This limits the amount of bottles that can be used per layer. On the other hand, one has to build with the next highest pattern, but that means that more bottles are being used per layer than that are necessary, which does not create an economical design.

10.6.4. Connection costs

The costs for these columns are mainly derived from the connections. To make this option even more accessible to individuals, solutions need to be made for more readily-available materials.

10.6.5. Vertical load resistance compared to conventional materials

On the basis of hand-calculations, it can be derived that the design vertical load resistance of the bottle column is not very competitive with more conventional materials. However, if the connections of the bottle column can be made cheaper, then the bottle column would be more economical, especially for smaller projects such as single story houses.

10.6.6. Post breakage behavior and safety

Glass columns are often designed with post-breakage behavior and rest capacity in mind if a part would break. This could be an issue for bottle columns. Solutions to tackle this are to apply a coating on the inside of the bottles to increase the post-breakage behavior, integrate the column in the building envelop or to build a safety structure around the column. Another solution could be to use more bottles than that are necessary to have some rest capacity.

11 Design explorations

A few design explorations are considered for subsequent research studies on using glass bottles in columns. These design explorations are based upon the proposed design, but contain additions that were not able to be investigated in this thesis. These explorations merely give the reader different pathways the topic can branch into. Two of these design explorations will be highlighted.

11.1. Combining Whole-FF with bundled option

In chapter 6, three concepts of connecting glass bottles were elaborated upon. One of these concepts, the bundled concept, explored an integrated approach where the threaded rods would be placed through the bottles rather than around them. There are arguments as to why the bundled option could be integrated into the proposed design:

- The Whole-FF connection concept already requires the use of threaded rods to clamp the rubber and POM to the plates.
- This solution is more space-efficient, because glass bottles contain a large volume of air. Threaded rods can be passed through this space instead of the space around the bottles.
- As a result of the second argument, a threaded rod through the middle is not required. Threaded rods through the bottles can be used to clamp all the bottles and plates together.
- The removal of the threaded in the middle can facilitate for another glass bottle, which can increase the capacity of vertical compressive loading.
- Threaded rods with a lever arm from the center can take up some bending moments instead of a threaded rod through the center point.
- The large nylon rings under the bottles already have holes in them.

The additional action that has to take place is creating holes in the bottom of the bottles. These holes are usually made with a diamond drill bit. The effect that this might have on the strength of the bottle has to be further investigated. A illustration of this option is shown in figure 77.

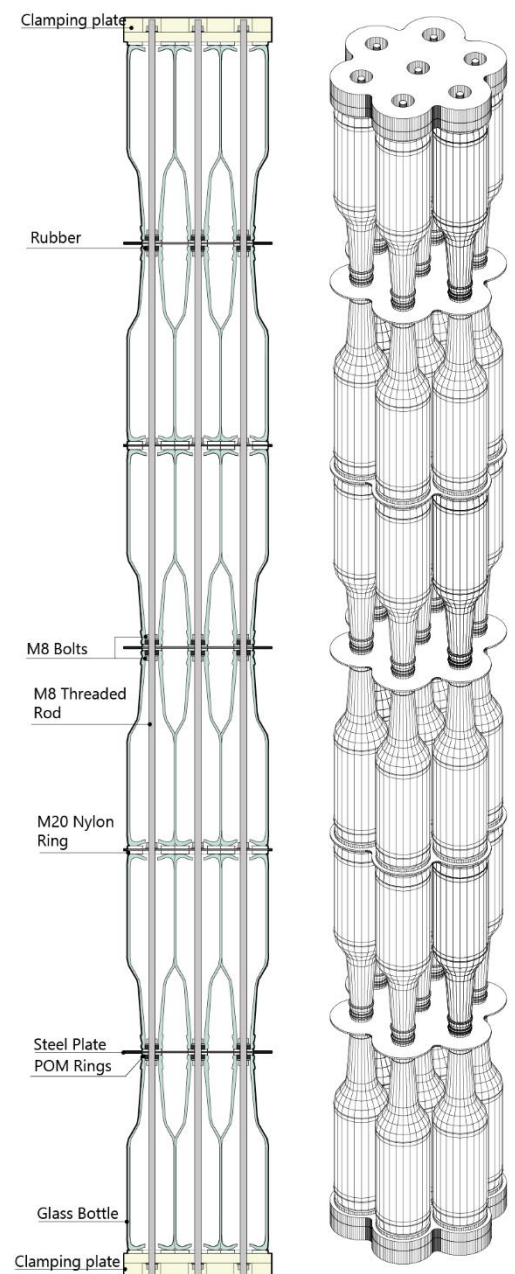


Figure 77 – Schematic and 3D Drawing of the Bundled+Whole-FF Option

An obvious downside to this is that it would demand more work than the previous option.

The inspiration for this design exploration comes from creations individuals often build called '*bottle fences*'. A picture of such a bottle fence is shown in figure 78.



Figure 78 – Fence made out of glass bottles (Livingston, n.d.)

11.2. External tension element around bottle column

The second design exploration is the addition of an external tension element around the bottle column, such as a rope lattice of cable net. This mesh of external tension elements could take up a tension load and also a bending moment. The inspiration for this design exploration is the analogy with an outrigger system in a high rise building. When a building with an outrigger system has a bending moment applied, one side of the building is under tension and the other side is under compression. These tension and compression loads due to a bending moment are taken up by exterior columns, or in the case of the bottle column by a rope lattice or cable net. The majority of the vertical compression load is still taken up by the core of the building, or in this case the glass bottles.

The cables or ropes on the outside could also provide slight protection to the bottles. Inspiration is also derived from a master thesis study on a filament wound column by P.N. Mossert (2015). However, in that design, the individual filaments take up the compression load of the pedestrian bridge. In a dual-system with a core of glass bottles and an external tension element, both system can work together to resist the applied loads. A sketch of how such a column might look like is shown in figure 79.

11.3. Overview of other design explorations

Other than the two previously mentioned design explorations, the following points are suggested:

- Using more readily available materials for the Whole-FF connection. This could be for instance by replacing the nylon rings by thick cardboard rings.
- The expensive rubber rings can be replaced with more conventional recycled rubber, such as from old tires.
- The tests for the Whole-FF concept were performed with a steel plate. However, there was no deformation of the steel plate after the fracture of the glass. Therefore, research needs to be done for more cheaper materials such as aluminum or MDF.

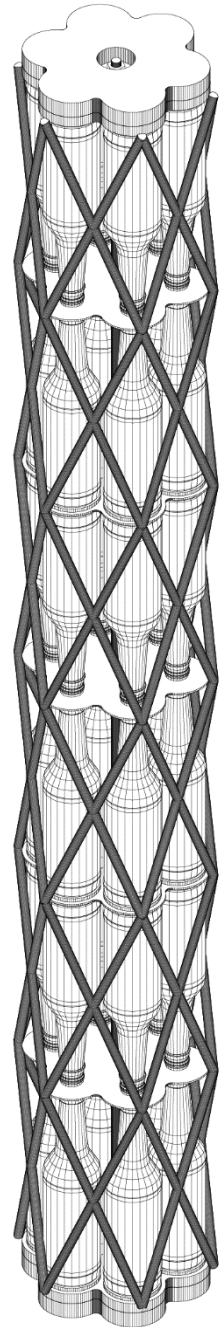


Figure 79 – Sketch of a dual-system between a core of glass bottles and an external wound tension element



F

F Discussion, Conclusion and Recommendations

12 Thesis Discussion and Conclusion

The four sub-questions that were stated at the start of the thesis can now be answered with the collected information. The answers from these sub-questions are then used to answer the main question of the thesis.

12.1. Thesis Discussion

12.1.1. Mechanical behavior of glass bottles under vertical load

The first sub-question of this thesis is:

'What is the mechanical behaviour of an individual glass bottle subjected to vertical compressive load?'

This sub-question was made with the intention of getting a better understanding of the mechanical behaviour of glass bottles when being compressed vertically. The combination of AGR experiments and finite element modelling have shown that under vertical compressive load, rings of tensile principle stress form in the shoulder of the bottle and in the heel of the bottle. Consequently, the bottles always failed either due to fracture in the shoulder of the bottle or fracture in the heel of the bottle. The results and models were validated by information from relevant literature.

The strength of the container glass was also evaluated. It was concluded that abraded container glass has a characteristic tensile strength of about 20 MPa, whilst line-simulated container glass has a characteristic tensile strength of about 27 MPa. Both values were retrieved with Weibull analysis. In the end, two different methods were used to evaluate the stresses in the bottles under corresponding loads, ANSYS+Interpolation and DIANA FEA. Both methods showed very similar results.

Parameters from Weibull Analysis were also found with two methods: Excel and an online tool from timonpeters.de. Similarly, the results were closely matched. Two methods were used in both cases to see how much uncertainty there was between different models or calculation methods.

The idea of evaluating the tensile strength of the container glass is to create a value to calculate with, rather than using the characteristic tensile strength of float glass of 45 MPa.

The coatings on the outside surface and damage state of the bottles did have an effect on the vertical load capacity of the bottles.

During the testing, it was found that the thickness of the tensile stressed areas had a significant effect on the failure load of the bottles. The bottles could thus not be compared solely on failure load, but the thickness of the failed samples had to be taken into account.

The gap between the Weibull lines of both groups is something that is expected. The difference in damage state leads to a difference in recorded strengths. The combination of variability of glass strength due to inherent imperfections or stones and the large difference in recorded thicknesses led to a large spread between failure loads. For sample group C, as-received bottles, the lowest recorded failure load was equal to about **20 kN**.

12.1.2. Connection between glass bottles

The second sub-question of this thesis is:

How can glass bottles be connected to each other to resist applied vertical loads?

There were three concepts of bottle connections that were analysed in this thesis:

- Masonry Concept
- Stacked Concept
- Bundled Concept

The Masonry concept has the benefits of ease of construction and it has been used all over the world already. However, the use of concrete is not very sustainable. The Stacked Concept allows for creating a lot of height quickly. Furthermore, it allows for the freedom of creating both adhesive and mechanical connections, which is not possible with the masonry concept. Also, the Stacked Concept allows for full use of the bottles. It is uncertain with the masonry concept how much the bottles contribute to the strength of the element.

The Bundled Concept is an option similar to the post-tensioned option in the study on bundled columns. This option was however deemed too advanced for the current knowledge on these structures, but it should definitely be an option to be analysed further.

12.1.3. Configurations of glass bottles

The third sub-question of this thesis is:

Which configurations of glass bottles in a structural column are most sufficient in terms of resisting tensile stresses?

In total, eight configurations were developed for the Stacked Concept. Afterwards, the four best configurations were picked out to be analyzed further in Stevinlab. The tests in Stevinlab showed that the Whole-Up concept behaved the best under vertical loads, followed by the Whole-FF and Whole-BB concept. The Cut-Double-BB configuration performed worse than expected, which is probably due to the imperfections that were still present on the cut-surface, even after sanding. This led to progressive cracking of the cut-bottle, eventually leading to a much lower failure load of around 28 kN for 4 bottles, almost as much as one whole bottle. The Whole-Up Concept has a minimum failure load of 86.05 kN, the Whole-FF has a minimum failure load of 72.75 kN and the Whole-BB has a minimum failure load of 52.67 kN. All configurations were performed with either four bottles (Whole-Up) or eight bottles (Whole-FF and Whole-BB).

The Whole-FF and Whole-BB concepts had lower failure loads than the Whole-Up concept, which was probably due to the higher number of connections points. Together with the tolerances of all the connections and bottles, this can lead one bottle taking more vertical load than expected, leading to a lower failure load of the system. Almost every configuration

failed in the heel of the bottle, which is a known failure mechanism that was recorded in the answering of the first sub-question. The advice is thus to use whole bottles in configurations for stacked columns to avoid the effort, time and money with cut-bottles.

12.1.4. Limitations of glass bottles

The final sub-question of this thesis is:

'What are the limitations of columns out of glass bottles?'

Several limitations of the bottle column were noticed during the thesis and are summarized in sub-chapter 10.6. In short, the limitations of the column are as of now the costs of the connections, the tolerances of the height of the bottles and the connections, the freedom in choice of bottle designs per layer, the freedom in pattern choice and the vertical load resistance compared to conventional materials.

The tests at AGR and Stevinlab showed maximum failure loads for individual bottles and configurations respectively. However, these are not the vertical loads that function as design values. Therefore, a design formula had to be proposed for a design compression resistance of the column, which takes the following into account:

- The damaged and abraded state of glass bottles
- The load-duration effect on glass
- The characteristic tensile strength of glass
- Material factor
- Tolerance factor
- Thickness of the bottle

The column is thus only limited to potentially temporary or small projects for now, for instance single storey buildings as demonstrated with a hand calculation. Full scale columns of glass bottles should therefore be tested to compare it to the design formula.

Lastly, solutions need to be found for adequate safety of these columns, either by integrating the columns in the building envelope, creating a safety structure around the columns or by introducing more bottles for rest capacity.

12.2. Thesis Conclusion

The goal of this thesis is answering the main question:

'How can structural columns be constructed out of glass bottles?'

Structural columns can either be created out of whole bottles or cut bottles. Whole bottles can either be clamped between intermediate plates, plugged onto a plate or glued together with an adhesive with high gap filling capability (i.e. tile adhesive). The bottles can be cut with either a home-made bottle cutter or a saw with a diamond blade. Other than stacking glass bottles, they can be used as substrate with concrete or either used in a bundled concept, similar to the bundled glass column.

The columns should be designed with a characteristic tensile strength of 20 MPa in mind. Furthermore, a slight change in the formula of the load-duration factor is taken into account due to different in the reference time t_0 .



The columns should be constructed with the damaged state of the bottle in mind, the load-duration effect on glass and a tolerance factor due to the proposed connections. These tolerance factors are 0.8 when using the Whole-FF configuration and 0.7 when using the Whole-BB configuration. Other limitations that one might come across are the current costs of the connections, the height tolerances of the bottles themselves and the competition with more conventional materials.

Figure 80 – Front view of the prototype of the bottle column concept

13 Research Recommendations

Finally, recommendations can be made for further research on glass bottle columns, which are mainly derived from the limitations of the column. This chapter gives a concise selection of research options that can follow from this thesis.

- Investigate and test a bottle column of several layers in a compression machine.
 - Individual bottles and configurations of bottles have now been tested and a design formula has been proposed. This has to be validated with a bottle column.
- Investigate the influence of the number of bottles on the system factor.
 - In this thesis, a system factor was used to reduce the capacity of the column due to tolerance issues that might arise. This is based upon experiments with four bottles in a square pattern. It would be interesting to investigate whether this factor changes when more bottles are used in a layer for the same configuration.
- Investigate the shear and bending resistance of the column with the aforementioned design explorations (external tension element or the bundled option compared to the proposed design).
 - In this thesis, research is limited to the compression resistance of the column. Therefore, additional research needs to be done for shear and bending resistance.
- Collect glass bottles from a waste plant and validate the characteristic tensile strength for abraded bottles.
 - The damage on manually abraded bottles was simulated with emery paper. It is interesting to investigate whether the same strengths can be found in bottles that are retrieved from a recycling centre or waste plant.
- Re-evaluate the use of cut-bottles in a column, but with a better cutting and sanding technique.
 - The cutting and sanding technique used in this thesis led to some imperfections at the cut surface of the bottle, which could lower the compression capacity of the bottles. Previously in this thesis, bottles were cut with a home-made bottle cutter and by using sudden temperature changes on the glass to cut the glass. Other cutting techniques for glass cutting already exist, such as laser cutting, however this can be too expensive.
- Introduce a coating on the inside of the bottle for better post-breakage behaviour and investigate the post-breakage behaviour.
 - Sprayable coatings exist which can be sprayed on the inside of the bottle. These coatings enhance the post-breakage behaviour of the bottles and make sure that the shards stay together, which improves the safety of the column.

- Investigate a zero-waste design.
 - The thesis has proposed solutions to create columns out of waste glass bottles. Investigate whether large portions of the connections elements could be made from waste materials (cardboard, old tires etc.).
- Re-evaluate the bundled option and compare it to the bundled glass columns.
 - The bundled option is an interesting option to further evaluate, because it does not involve any intermediate plates.
- Re-evaluate the Masonry option, but try and use a cementitious material that is sustainable, such as cob.
 - The masonry option does allow for bottles with different designs to be combined. However, instead of using materials such as concrete or mortar, scientific research needs to be done on making structural elements out of cob and glass bottles.

Bibliography

References

Afvalfonds Verpakkingen. (2018, October). *Verpakkingen in de Circulaire Economie: Recycling verpakkingen Nederland 2017*. <https://www.nedvang.nl/wp-content/uploads/2019/02/Recycling-verpakkingen-Nederland-2017.pdf>

AGR International. (2020). *Vertical Load Tester* (3rd ed.). Agr International.

Aldinger, B. S., & de Haan, P. W. (2019). *Color Atlas of Glass Container Defects*. Blurb, Incorporated.

ASTM International. (2015). *Standard Terminology of Glass and Glass Products* (No. C162-05). <https://ipfs.io/ipfs/bafk2bzaced5e6n4p54c4pehgfoyh3b6lk5z2yq74gvwz7xuvvbwm3hldzok7c?filename=C%2520162%2520-%252005%2520%25282015%2529.pdf>

Batchelor, B. G. (2012). Inspecting Glass Bottles and Jars. In *Machine Vision Handbook* (1st ed., Vol. 2, pp. 1202–1220). Springer-Verlag London Limited.

Berlin Packaging. (2019, October 20). *Anatomy of a Bottle*. <https://www.berlinpackaging.com/anatomy-of-a-bottle/>

Bhargava, A., Wang, F., Wood, B., Higginbotham, G., & Gentle, I. (2000). Studies of polyethylene-coated tin oxide films on glass bottles. *Surface and Interface Analysis*, 29(2000), 663–670.

Boyer, M. (2014, August 21). *Petit Romain's Square Heineken Bottles Save Space in Your Six-Pack*. Inhabitat. Retrieved October 17, 2022, from <https://inhabitat.com/petit-romains-square-heineken-bottles-save-space-in-your-six-pack/>

CEN/TC 250. (2011). NEN-EN 1992-1-1+C2 - Eurocode 2: Design of concrete structures – Part 1-1: General rules and rules for buildings. In *NEN Connect*. NEN. <https://connect.nen.nl/Standard/Detail/159356?compId=10037&collectionId=0>

CEN/TC 250. (2005). NEN-EN 1995-1-1 (en) - Eurocode 5 - Design of timber structures - Part 1-1: General - Common rules and rules for buildings. In *NEN Connect*. NEN. <https://connect.nen.nl/Standard/Detail/38046>

CETIE. (2004, May). *Glass Container Nomenclature* (DT 23.01).

CETIE. (2020, May). DT 13.00 - Glass Containers - Surface Treatment (Revision 1).

CETIE. (2020, December). *Glass Finish Glossary and Nomenclature* (DT23.02).

Datsiou, K. C., & Overend, M. (2018). Weibull parameter estimation and goodness-of-fit for glass strength data. *Structural Safety*, 73, 29–41. <https://doi.org/10.1016/j.strusafe.2018.02.002>

Davis, M. W. (1994). Bottle Strength Analysis. *Glass*, 71(6), 225-227

Davis, M. W. (2009). *The Wiley Encyclopedia of Packaging Technology* (K. L. Yam, Ed.; 3rd ed.). Wiley.

Dyer, T. D. (2014). Glass Recycling. *Handbook of Recycling*, 191–209. <https://doi.org/10.1016/b978-0-12-396459-5.00014-3>

Fatima, S. (2017). SUSTAINABLE CONSTRUCTION OF BOTTLE WALL AND BINDING MATERIAL. In *International Research Journal of Engineering and Technology* (1st ed., Vol. 4). IRJET. <https://www.irjet.net/archives/V4/i4/IRJET-V4I4433.pdf>

- Feldmann, M., Kasper, R., Bucak, Ö., Illguth, M., & Bues, M. (2010). Curved Glass – Quality and Application. *Challenging Glass 2*, 2, 543–552. <https://journals.open.tudelft.nl/cgc/article/view/2353>
- FEVE. (2015). Glass recycling hits 73% in the EU. *Glass Worldwide*, 62, 139. <https://www.glassworldwide.co.uk/Digital-Issues/glass-worldwide-issue-62>
- FEVE. (2018). Food and beverage market growth for glass packaging. *Glass Worldwide*, 80, 114. <https://www.glassworldwide.co.uk/Digital-Issues/glass-worldwide-issue-80>
- Gauthier, M. M. (1995). Applications for Glasses. In *Engineered Materials Handbook Desk Edition* (1st ed., pp. 1188–1230). ASM International.
- Girling, P. J. (2003). Packaging of food in glass containers. In R. Coles, D. McDowell, & M. J. Kirwan (Eds.), *Food Packaging Technology* (1st ed., pp. 152–173). Blackwell Publishing Ltd.
- Glass Alliance Europe. (2013, October). EU glass industry performance, 2012. *Glass Worldwide*, 49, 116. <https://www.glassworldwide.co.uk/Digital-Issues/glass-worldwide-issue-49>
- Glass Alliance Group. (2019, October). EU glass industry performance in 2018-2019. *Glass Worldwide*, 85, 148. <https://www.glassworldwide.co.uk/Digital-Issues/glass-worldwide-issue-85>
- Graham, R. L., Lubachevsky, B. D., Nurmela, K. K., & Östergård, P. R. J. (1998, February). Dense packings of congruent circles in a circle. *Discrete Mathematics*, 181(1–3), 139–154. [https://doi.org/10.1016/s0012-365x\(97\)00050-2](https://doi.org/10.1016/s0012-365x(97)00050-2)
- Grayhurst, P. (2012). Glass Packaging. In *Packaging Technology - Fundamentals, Materials and Processes* (1st ed., pp. 109–121). Woodhead Publishing.
- Guin, J. P., & Gueguen, Y. (2019). 7. Mechanical Properties of Glass. In J. D. Musgraves, J. Hu, & L. Calvez (Eds.), *Springer Handbook of Glass* (pp. 227–272). Springer Nature Switzerland AG.
- Hann, J. (2013). Annealing of glass containers and hollowware. *Glass International*, 22–28.
- Hansen, E., & Tuazon, O. (2014). *COMPLETED BEER BOTTLE COLUMN, 2014*. Artsy. Retrieved October 17, 2022, from <https://www.artsy.net/artwork/eli-hansen-and-oscar-tuazon-completed-beer-bottle-column>
- Harder, J. (2018). Glass recycling - Current market trends. *Recovery*, 5. https://www.recovery-worldwide.com/en/artikel/glass-recycling-current-market-trends_3248774.html
- Heineken. (n.d.). *Volte Sempre*. Programavoltresempre. Retrieved October 21, 2022, from <http://www.programavoltresempre.com.br/#por-que>
- Heineken Collection Foundation. (n.d.). *The story behind the WOBO*. Retrieved October 17, 2022, from <https://www.heinekencollection.com/en/stories/the-story-behind-the-wobo>
- Hoekman, L. C. (2019). *COATING COMPOSITION FOR GLASS CONTAINERS* (EP 3 502 077 A1). European Patent Office. <https://data.epo.org/publication-server/document?iDocId=5963236&iFormat=0>
- Hu, W., W.G.S., & Smay, G. (2016). FEA performance comparisons of NNPB and BB refillable bottles. *Glass Worldwide*, 68, 114–117.
- ISO. (1992). *ISO 7348:1992(en) Glass containers — Manufacture — Vocabulary*. <https://www.iso.org/obp/ui/#iso:std:iso:7348:ed-1:v1:en>
- Jackson, N., & Ford, J. (1981b). Experience in the control and evaluation of coatings on glass containers. *Thin Solid Films*, 77(1–3), 23–40. [https://doi.org/10.1016/0040-6090\(81\)90357-6](https://doi.org/10.1016/0040-6090(81)90357-6)

- Jones, O. (1971). Glass bottle push-ups and pontil marks. *Historical Archaeology*, 5(1), 62–73. <https://doi.org/10.1007/bf03374455>
- Jones, O. R., & Sullivan, C. (1989). Part II: Glass Containers. In *The Parks Canada Glass Glossary* (2nd ed., pp. 71–124). Archaeological Research Division Parks Canada.
- Kepple, J. B., & Wasylyk, J. S. (1994). Fracture of Glass Containers. In R. C. Bradt & R. E. Tressler (Eds.), *Fractography of Glass* (1st ed., Vol. 1, pp. 207–252). Springer Science & Business Media. https://doi.org/10.1007/978-1-4899-1325-8_7
- Kinsella, D. T., & Persson, K. (2016). On the Applicability of the Weibull Distribution to Model Annealed Glass Strength and Future Research Needs. *Challenging Glass 5 – Conference on Architectural and Structural Applications of Glass*, 5, 593–608.
- Kothe, C., & Weller, B. (2014). Effect of surface pretreatments on adhesive properties of glass and metals [E-book]. In C. Louter, F. Bos, J. Belis, & J. Lebet (Eds.), *Challenging Glass 4 & COST Action TU0905 Final Conference* (1st ed., pp. 353–359). Taylor & Francis.
- Lecacheur, J. (2020, July 12). Les maisons de bouteilles, à Cap-Egmont, fascinent toujours, 40 ans plus tard. *Radio-Canada.Ca*. Retrieved October 17, 2022, from <https://ici.radio-canada.ca/nouvelle/1719102/maison-bouteilles-cap-egmont-ile-prince-edouard-visite>
- Levene, L. (1989). How Container Coatings Affect Label Adhesion. *Glass Industry*, 70(1), 17–20.
- Liebenberg, C. J. (2007, October 1). Waste Recycling in Developing Countries in Africa: Barriers to Improving Reclamation Rates [Paper]. In *Eleventh International Waste Management and Landfill Symposium*. CISA. <http://www.resol.com.br/textos/136.pdf>
- Loadhog. (2017). *Smartpad*. <https://loadhog.com/wp-content/uploads/2017/11/Smartpad-UKEU.pdf>
- Lockhart, B., & Hoenig, R. (2016). The Bewildering Array of Ownes-Illinois Co. Logos and Codes. In P. D. Schulz, R. Allen, B. Lindsey, & J. K. Schulz (Eds.), *Baffle marks and pontil scars: A reader on historical bottle identification* (12th edition, pp. 481–506). The Society of Historical Archaeology.
- Machalická, K., & Eliášová, M. (2012). Influence of Various Factors on Mechanical Properties of Adhesive Joint in Glass Structures. *Challenging Glass 3*, 267–279. <https://doi.org/10.3233/978-1-61499-061-1-267>
- McFall, D. [David Mcfall]. (2015, November 17). *building beer bottle bricks, using adobe mud stabilized earth home technique to go green* [Video]. YouTube. https://www.youtube.com/watch?v=o3_0T4rGSM8
- Meyland, M. J., Nielsen, J. H., & Kocer, C. (2021). Tensile behaviour of soda-lime-silica glass and the significance of load duration – A literature review. *Journal of Building Engineering*, 44. <https://doi.org/10.1016/j.jobe.2021.102966>
- Müller-Simon, H., Jorg, W., & Armin, L. (1994). Practical strength of glass containers Part 1. Influence of the type of defect. *Glastechnische Berichte*, 67(5), 134–142.
- Mossert, P. N. (2015, June). *A filament wound pillar for a pedestrian bridge* [MSc Thesis]. Technische Universiteit Delft. <https://repository.tudelft.nl/islandora/object/uuid%3A3A3849ed5f-0d56-4769-9bd4-580808f8495a>
- Natarajan, S., Govindarajan, M., & Kumar, B. (2014). *FUNDAMENTALS OF PACKAGING TECHNOLOGY* (2nd edition). PHI Learning.
- Nakawaga, M., Amano, T., & Yokokura, S. (1997). Development of lightweight returnable bottles. *Journal of Non-Crystalline Solids*, 218(1997), 100–104.
- Normcommissie 353005 “Vlakglas.” (2014). *NEN2608 - Vlakglas voor gebouwen - Eisen en bepalingmethode* (ICS 81.040.20). Nederlands Normalisatie-instituut. <https://www.nen.nl/nen-2608-2014-nl-199169>

Normcommissie TGB Staalconstructies. (2016). NEN-EN 1993-1-1+C2+A1:2016 - Eurocode 3: Design of steel structures - Part 1-1: General rules and rules for buildings. In *NEN Connect*. NEN. <https://www.nen.nl/nen-en-1993-1-1-c2-a1-2016-nl-225000>

Oikonomopoulou, F., & Bristogianni, T. (2022). Adhesive solutions for cast glass assemblies: ground rules emerging from built case studies on adhesive selection and experimental validation. *Glass Structures & Engineering*, 7(2), 293–317. <https://doi.org/10.1007/s40940-022-00178-w>

Oikonomopoulou, F., van den Broek, E. A. M., Bristogianni, T., Veer, F. A., & Nijssen, R. (2017b, June 2). Design and experimental testing of the bundled glass column. *Glass Structures Engineering*, 2(2), 183–200. <https://doi.org/10.1007/s40940-017-0041-x>

Patano, C. G. (2016, June). *The Role of Coatings and Other Surface Treatments in the Strength of Glass* [Slides]. GMIC. <https://gmic.org/wp-content/uploads/2016/06/The-Role-of-Coating-and-Other-Surface-Treatments-in-the-Strength-of-Glass-Carlo-Pantano.pdf>

Penlington, R. (2000). Surface engineering in the glass container industry. *Vacuum*, 56(2000), 179–183.

Prakash, N. S. (2013). Neck finish in glass hollowware. *Glass International*, 2013(July/August). https://www.glass-international.com/content-images/news/prakash_for_web.qxp_00_GI_0909.pdf

Preston, F. W. (1933). GLASS AS A STRUCTURAL AND STRESS-RESISTING MATERIAL*. *Journal of the American Ceramic Society*, 16(4), 163–186. <https://doi.org/10.1111/j.1151-2916.1933.tb16965.x>

Robertson, G. L. (2012). *Food Packaging: Principles and Practice*, Third Edition (3rd ed.). CRC Press. <https://doi.org/10.1201/b21347>

Rom, J. (2015, May 22). *Bottle Houses of PEI*. Upcycle That. Retrieved October 17, 2022, from <https://www.upcyclethat.com/bottle-houses-of-pei/>

Roos, C., Rosin, A., Negahdari, Z., & Struppert, T. (2014). Hot-end coating: Strengths, risks and alternatives. *Glass International*, 37(5), 13–15.

Slusser, W. G., Salitrik, B. J., & Hu, W. (2018). Effects of distinctive recessed label panels. *Glass Worldwide*, 2018(July/August), 84–87. https://americanglassresearch.com/sites/default/files/gw78_jul-aug_2018_label_panel.pdf

Smay, G. L. (2017). Effect of coatings on adhesion of labels of glass containers. *Glass Worldwide*, 69, 68–70. https://americanglassresearch.com/sites/default/files/effect_of_coatings_white_paper_jan_2017_gw.pdf

Smith, D. A., & Gifford, J. (2007, January). *Selection of Food Containers: Glass Jars* (Nr. G1686). University of Nebraska. <https://foodbusiness.ces.ncsu.edu/wp-content/uploads/2019/02/Selection-of-Food-Containers-Glass-Jars.pdf?fwd=no>

Southwick, R. D. (1965, May). Pressure and Vertical Load Stress Indices in the Handy Beer Bottle (No. 65–027). AGR.

Southwick, R., Wasyluk, J., Smay, G., Kepple, J., Smith, E., & Augustsson, B. (1981). The mechanical properties of films for the protection of glass surfaces. *Thin Solid Films*, 77(1–3), 41–50. [https://doi.org/10.1016/0040-6090\(81\)90358-8](https://doi.org/10.1016/0040-6090(81)90358-8)

Spasojevic-Santic, T., & Stanojlovic, D. (2016, June). EARTHSHIP – A NEW HABITAT ON EARTH FOR QUALITY LIFE. In *1st International Conference on Quality of Life*. Center for Quality, Faculty of Engineering, University of Kragujevac.

Sunkara, L. (2018, October 9). This Thai Temple Was Built Using 1.5 Million Beer Bottles. *Architectural Digest*. Retrieved on October 17, 2022, from <https://www.architecturaldigest.com/story/this-thai-temple-built-using-millions-beer-bottles>

Syrett, D. (2006). Bottle design and manufacture and related packaging. In D. P. Steen & P. A. Ashurst (Eds.), *Carbonated Soft Drinks - Formulation and Manufacture* (1st edition, pp. 181–217). Blackwell Publishing.

The Bottle Houses. (n.d.). *Our story 40 years*. The Bottle Houses * Les Maisons De Bouteilles. Retrieved October 17, 2022, from <https://bottlehouses.com/our-story>

The Re:Generation Project [The Re:Generation Project]. (2014, February 18). *Bottle Brick Wall Workshop (Self-Building an Earthship)* [Video]. YouTube. <https://www.youtube.com/watch?v=nbAsz0OLaik>

UNIDO. (1982, March). *Technical Report: Glass Containers* (DP/JAM/77/008). United Nations Industrial Development Organization Vienna. <https://open.unido.org/api/documents/4792339/download/JAMAICA.%20TECHNICAL%20REPORT%20-%20GLASS%20CONTAINERS%20%2811525.en%29>

Veenstra, R. (2015, August 27). *Tubular Glass Columns* [MSc Thesis]. Technische Universiteit Delft. <https://repository.tudelft.nl/islandora/object/uuid%3A47667345-0cfa-4057-8c14-842d11df7d24>

Verleg, K. (n.d.). *The Structural Behaviour of Bundled Glass Columns* [MSc Thesis]. Technische Universiteit Delft. <https://repository.tudelft.nl/islandora/object/uuid%3A7737869c-21ad-4257-a12d-6ef43066ecb4>

Wagemans, L. A. G. (2014). *Quick Reference* (F. A. M. Soons, B. P. M. van Raaij, S. Pasterkamp, & S. H. J. van Es, Eds.; 2014 ed.) [Book]. Technische Universiteit Delft.

White, J. R. (1978). Bottle Nomenclature: A Glossary of Landmark Terminology for the Archaeologist. *Historical Archaeology*, 12, 58–67. <https://www.jstor.org/stable/25615337>

Yoneda, Y. (2012, November 5). *HEINEKEN WOBO: A Beer Bottle That Doubles as a Brick*. Inhabitat - Green Design, Innovation, Architecture, Green Building | Green Design & Innovation for a Better World. <https://inhabitat.com/heineken-wobo-the-brick-that-holds-beer/>

Figures

Figure 4: Fisher, M. (2011). [Image]. Million Bottle Temple. Flickr. <https://www.flickr.com/photos/fischerfotos/7447377506/in/photostream/>

Figure 5: Rom, J. (2015, May 22). [Image]. *Column design in The Bottle Houses*. Upcycle That. <https://www.upcyclethat.com/bottle-houses-of-peij/>

Figure 6: Byers, J. (2018, May 30). [Image]. *Circular column Design in The Bottle Houses*. TravelZoo. <https://www.travelzoo.com/ca/blog/bottle-houses-of-peij/>

Figure 8: Hansen, E., & Tuazon, O. (2014b). [Image]. *Completed Beer Bottle Column*. Artsy. <https://www.artsy.net/artwork/eli-hansen-and-oscar-tuazon-completed-beer-bottle-column>

Figure 9: Stark, G. (2009). [Image]. *Heineken WOBO Wall*. Flickr. <https://www.flickr.com/photos/greeezer/3300645265/>

Figure 10: Heineken International. (n.d.). [Image]. *WOBO House*. Cabinet. <https://www.cabinetmagazine.org/issues/13/collins.php>

Figure 11: Petit, R. (2008). [Image]. *Heineken Cube*. Intelligent Living. <https://www.intelligentliving.co/heineken-cube-concept-sustainable-beer-packaging/>

Figure 18: Smay, G. L. (2017). [Graph] Effect of coatings on adhesion of labels of glass containers. *Glass Worldwide*, 69, 68–70. https://americanglassresearch.com/sites/default/files/effect_of_coatings_white_paper_jan_2017_gw.pdf

Figure 19: Müller-Simon, H., Jorg, W., & Armin, L. (1994). [Graph]. Practical strength of glass containers Part 1. Influence of the type of defect. *Glastechnische Berichte*, 67(5), 134–142.

Figure 20: Müller-Simon, H., Jorg, W., & Armin, L. (1994). [Graph]. Practical strength of glass containers Part 1. Influence of the type of defect. *Glastechnische Berichte*, 67(5), 134–142.

Figure 25: Southwick, R. D. (1965, May 28). [Graph]. Longitudinal and circumferential vertical load distributions for the 12. oz capacity Handy Beer Bottle with spherical shoulder and heel with a wall thickness of 0.070 inches.

Figure 78: Livingston, L. (n.d.). [Image] *Wine Bottle Wall*. Pinterest.
<https://nl.pinterest.com/pin/512636370081470963/>

Tables

Table 1: (In order from left to right)

Allison, J. (n.d.). [Image]. *George's Glass Castle*. Spaces. <http://spacesarchives.org/explore/search-the-online-collection/george-plumb-bottle-castle/>

Maboulette. (n.d.). [Image]. *A house made of empty Champagne bottles*.

<https://maboulette.wordpress.com/2011/11/28/five-more-of-the-strangest-buildings-in-the-world/>

Schaller, B. W. (2011, July 28). [Image]. *Tom Kelly's bottle house*. Wikimedias Commons.
https://commons.wikimedia.org/wiki/File:A654_Tom_Kelly%27s_bottle_house_Rhyolite_Nevada_United_States_2011.jpg

Dias, D. (2022, April 14). [Image]. *Glass Bottle House*. Melhorcomsaude. <https://melhorcomsaude.com.br/casal-constroi-casa-propria-usando-dez-mil-garrafas-vidro/>

Vaca, L. (2022). [Image]. *El mirador hexagonal que corona la construcción*. Clarin.
https://www.clarin.com/zonales/fabulosa-casa-botellas-construyo-argentino-atrae-turistas-mundo_0_AC2WXc3AX.html#

Zvonarev, V. (n.d.). [Image]. *Palace of Oz*. The Drinks Business.
<https://www.thedrinksbusiness.com/2015/03/man-builds-house-with-12000-champagne-bottles/>

Gaudi, C. (2017). [Image]. *Glass Bottle House*. Estadão. https://fotos.estadao.com.br/fotos/casa_cabana-gaudi-florianopolis.700393

Daily Mail. (2014). [Image]. *Blotto Grotto*. <https://www.dailymail.co.uk/news/article-2692921/Blotto-grotto-5-000-wine-bottles-shortlisted-alongside-Dads-Army-museum-I-Shed-Year-competition.html>

Watamu Marine Association. (n.d.). [Image]. *Glass Bottle Constructions*. <https://www.watamumarine.co.ke/glass-bottle-constructions/>

Bott, M. (2018, July 5). [Image]. *Bottle House*. Flickr.
<https://www.flickr.com/photos/malcolmbott/43485213902/in/photostream/>

Shikharapur CLC. (n.d.). [Image]. *Glass Bottle School*. <https://shikharapurclc.org/environment-friendly-activities>

NPO. (2022, March 17). [Image]. *Glass Bottle House in Belize*. RTL Boulevard.
<https://www.rtlboulevard.nl/entertainment/tv/artikel/5295631/floortje-dessing-naar-het-einde-van-de-wereld-npo>

Table 2: Southwick, R., Wasylyk, J., Smay, G., Kepple, J., Smith, E., & Augustsson, B. (1981). The mechanical properties of films for the protection of glass surfaces. *Thin Solid Films*, 77(1–3), 41–50.
[https://doi.org/10.1016/0040-6090\(81\)90358-8](https://doi.org/10.1016/0040-6090(81)90358-8)

Table 9: Hu, W., W.G.S., & Smay, G. (2016). FEA performance comparisons of NNPB and BB refillable bottles. *Glass Worldwide*, 68, 114–117.

Table 10: Müller-Simon, H., Jorg, W., & Armin, L. (1994). Practical strength of glass containers Part 1. Influence of the type of defect. *Glastechnische Berichte*, 67(5), 134–142.

Table 11: Davis, M. W. (1994). Bottle Strength Analysis. *Glass*, 71(6). 225-227

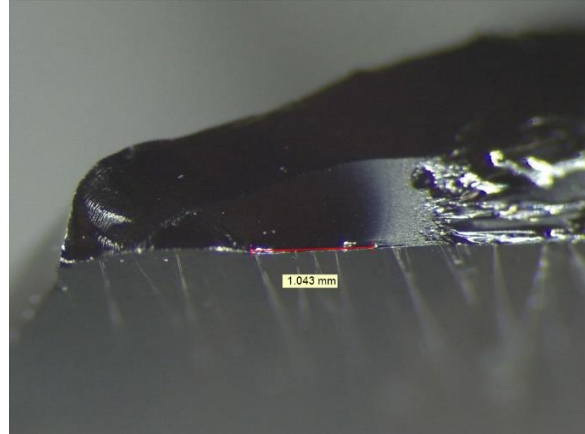
A₁

A1 Fracture Mirror Pictures

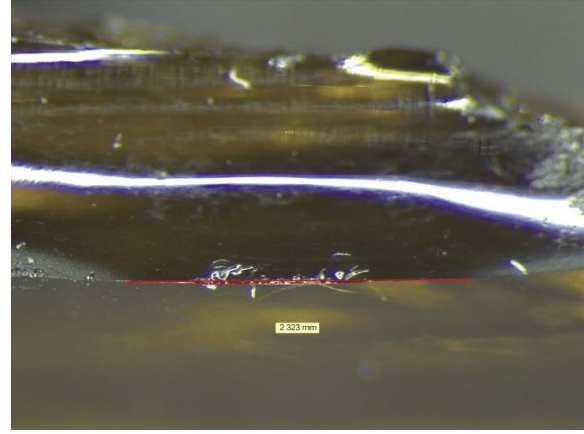
A1 Fracture Mirror Pictures

Manually Abraded

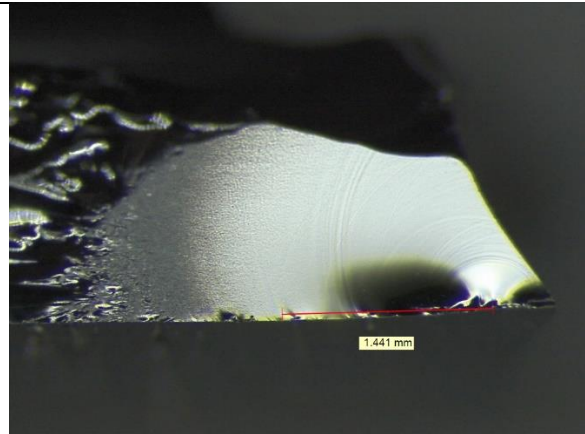
In all four samples, the fractures originated at a cleavage scratch, which is a mechanically created flaw.



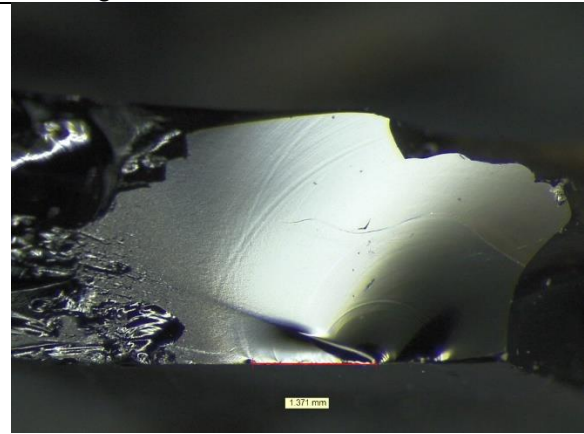
Sample B2 – Mirror radius measuring 1.04 mm. The fracture originated at a cleavage scratch



Sample B5 – Mirror diameter measuring 2.32 mm. The fracture originated at a cleavage scratch



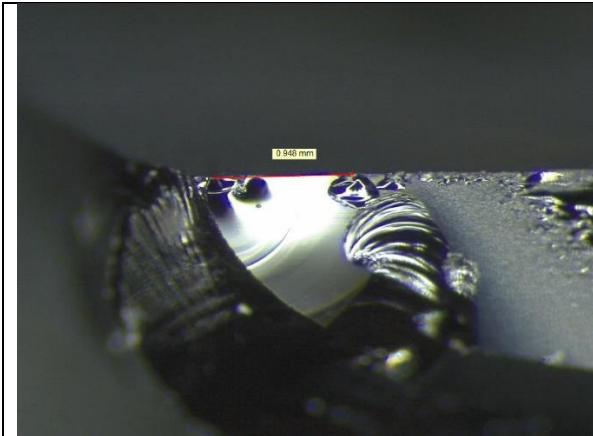
Sample B11 – Mirror radius measuring 1.44 mm. The fracture originated at a cleavage scratch.



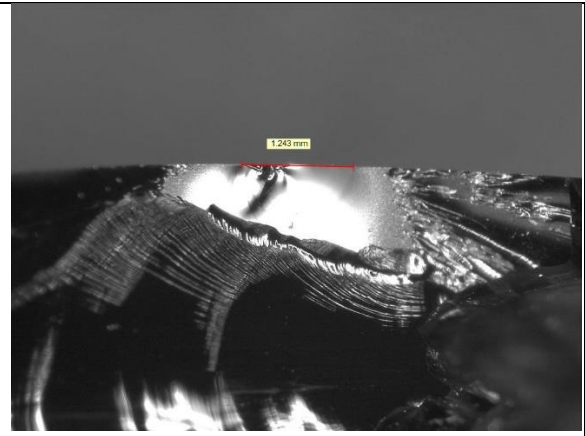
Sample B24 – Mirror radius measuring 1.37 mm. The fracture originated at a cleavage scratch.

Line Simulated

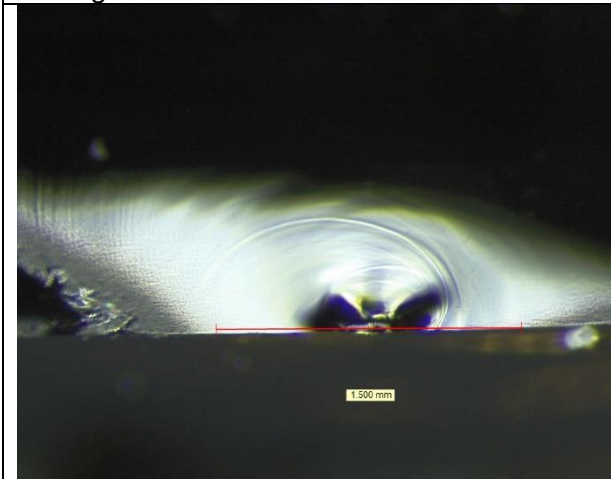
Two out of the three samples had fractures that originated at frictive damage, which is a mechanically created flaw. The remaining sample has a fracture that originated at a check, which is a manufacturing defect that is created during the forming of the bottle.



Sample A10 – Mirror radius measuring 0.95 mm. The fracture originated at frictive damage.



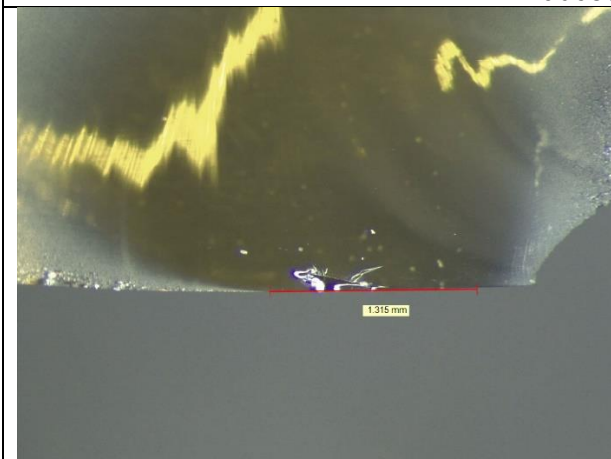
Sample A11 – Mirror diameter measuring 1.24 mm. The fracture originated at frictive damage.



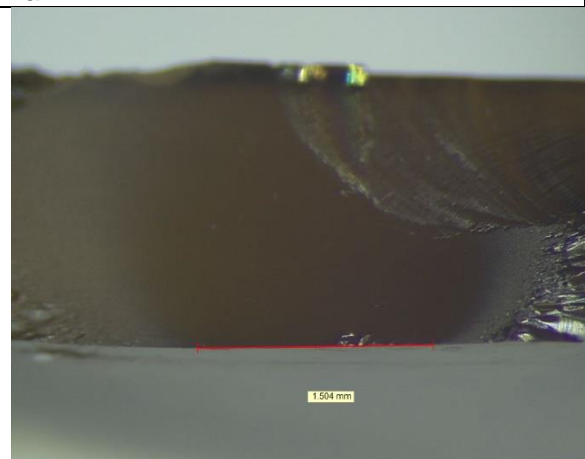
Sample A26 – Mirror diameter measuring 1.50 mm. The fracture originated at a check.

As Received

Both samples had fractures that originated at frictive damage, which is a mechanically induced flaw.



Sample C1 – Mirror diameter measuring 1.32 mm. The fracture originated at frictive damage.



Sample C12 – Mirror diameter measuring 1.50 mm. The fracture originated at frictive damage.

A₂

A2 Configuration models

To create an optimal design for a column consisting of glass bottles, which have complex geometry themselves, it is important to start a simple model and keep adding a higher degree of complexity. The goal of the column is not only to take up axial compressive forces, but also axial forces with an eccentricity that can create an additional bending moment in the column. Therefore, two different problems are analyzed and their effect on the bottles are investigated.

Firstly, a simple 2D model is created in MatrixFrame. It consists of two plates and two bottles and they are represented with line elements.

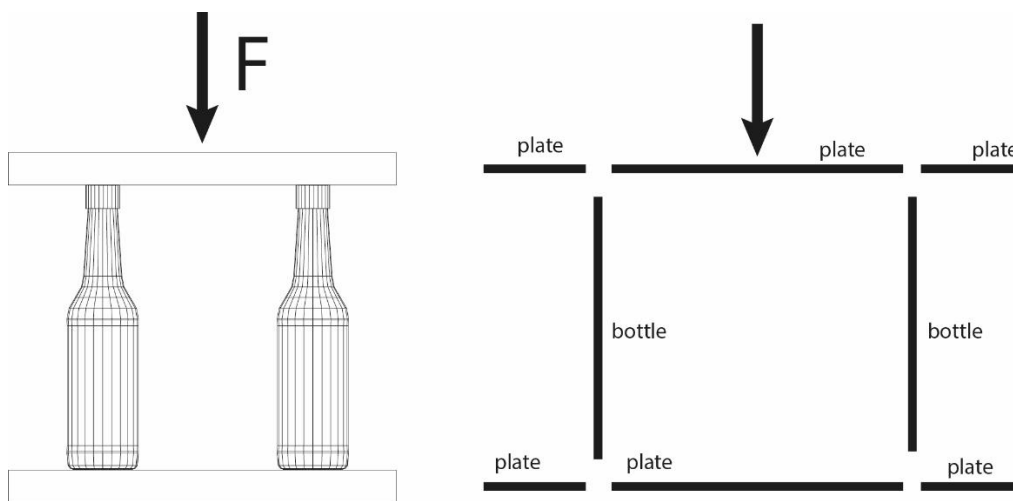


Figure A.2.1. – Discretization of the stacked option

Situation 1: An axial compressive force without eccentricity

There are several options that can be applied to alter the moments and axial forces in the bottles. The goals that need to be reached:

- Glass is generally weak in tension, but strong in compression. However, it has been shown that axial compressive forces on the bottle will create principle tensile stresses in the shoulder and heel region of the bottle. Therefore, a higher compressive force would increase these tensile stresses.
- Bending moment on the bottle can cause additional tensile stresses in the cross-section of the bottle. This could add up to the already tensile stresses present due to axial compressive loading. This means that the goal is to avoid these additional bending moments, or if not possible, reduce these moments as much as possible.

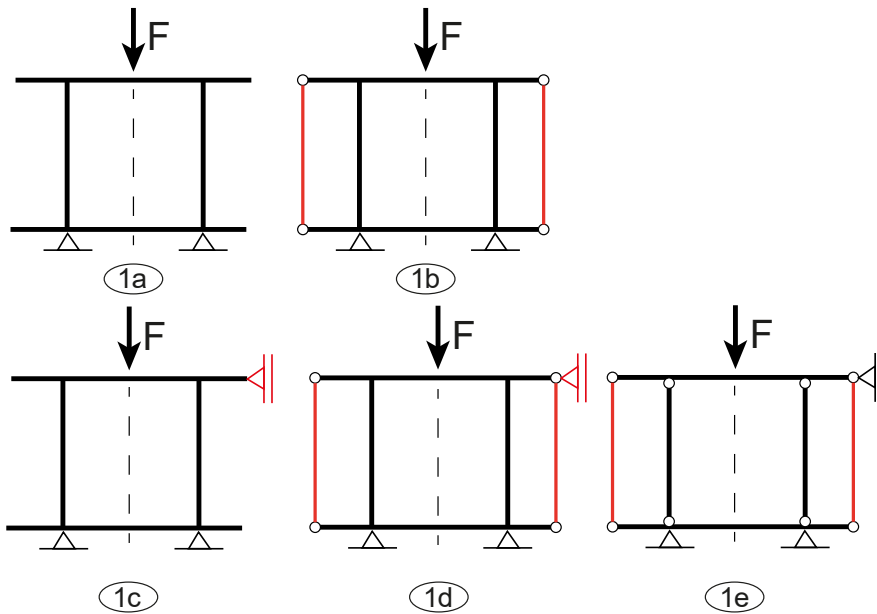


Figure A.2.2 – Structural models for centric loading

For situation one, five separate models are created with different design solutions to alter the cross-sectional forces in the bottles. Case 1a represents two plates with bottles in between, where the bottles are clamped or glued to the plate. Case 1b represents the same as case 1a, but cables or tension rods are added on the sides of the plates. Case 1c adds a support on the top plate. Case 1d combines the cables with this lateral support. Finally, case 1e combines the cables with the lateral supports, but the bottles are now connected with hinged connections to the plates.

Case 1a and 1b with hinged connections with the bottles is avoided, because those are unstable design solutions. The models are created in MatrixFrame and the difference between the cross-sectional forces between the cases is compared. A unit force of 1 kN is introduced on the top of the plate. In this instance, the following cross-sectional properties are introduced for the different line elements:

- Plate: C30 (wood), $h = 0.03$ m, $b = 0.9$ m
- Bottles: $E = 70$ GPA, Cylindrical cross-section with $D = 61$ mm and $t = 2.5$ mm
- Rods: $d = 10$ mm, S235

Case	Left Bottle	Right Bottle	Cable/Rods
Case 1a	<p>N_x S2: -0.50 to -0.50</p> <p>V_z S2: -0.20 to -0.20</p> <p>M_y S2: 0.01 to -0.04</p>	<p>N_x S3: -0.50 to -0.50</p> <p>V_z S3: 0.20 to 0.20</p> <p>M_y S3: -0.01 to 0.04</p>	x

Case 1b			<p>Left:</p> <p>Right:</p>
Case 1c			x
Case 1d			<p>Left:</p> <p>Right:</p>
Case 1e			<p>Left:</p> <p>Right:</p>

Table A.2.1 – Results from Matrix Frame

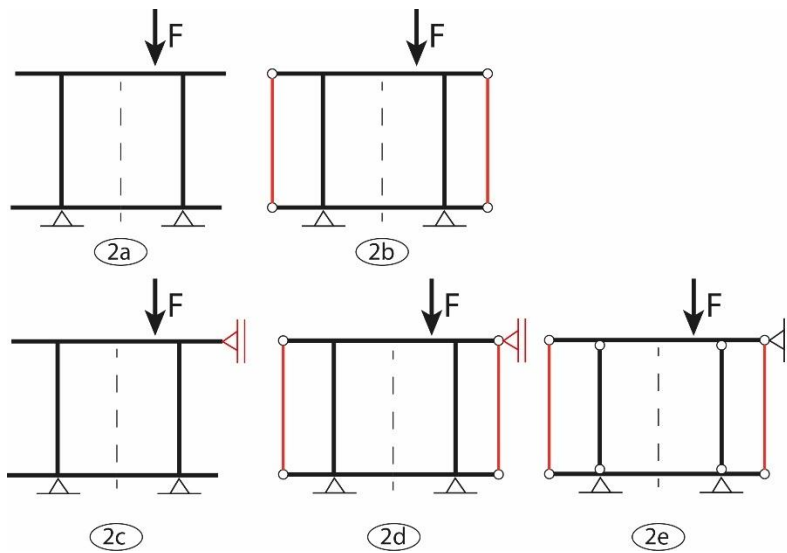
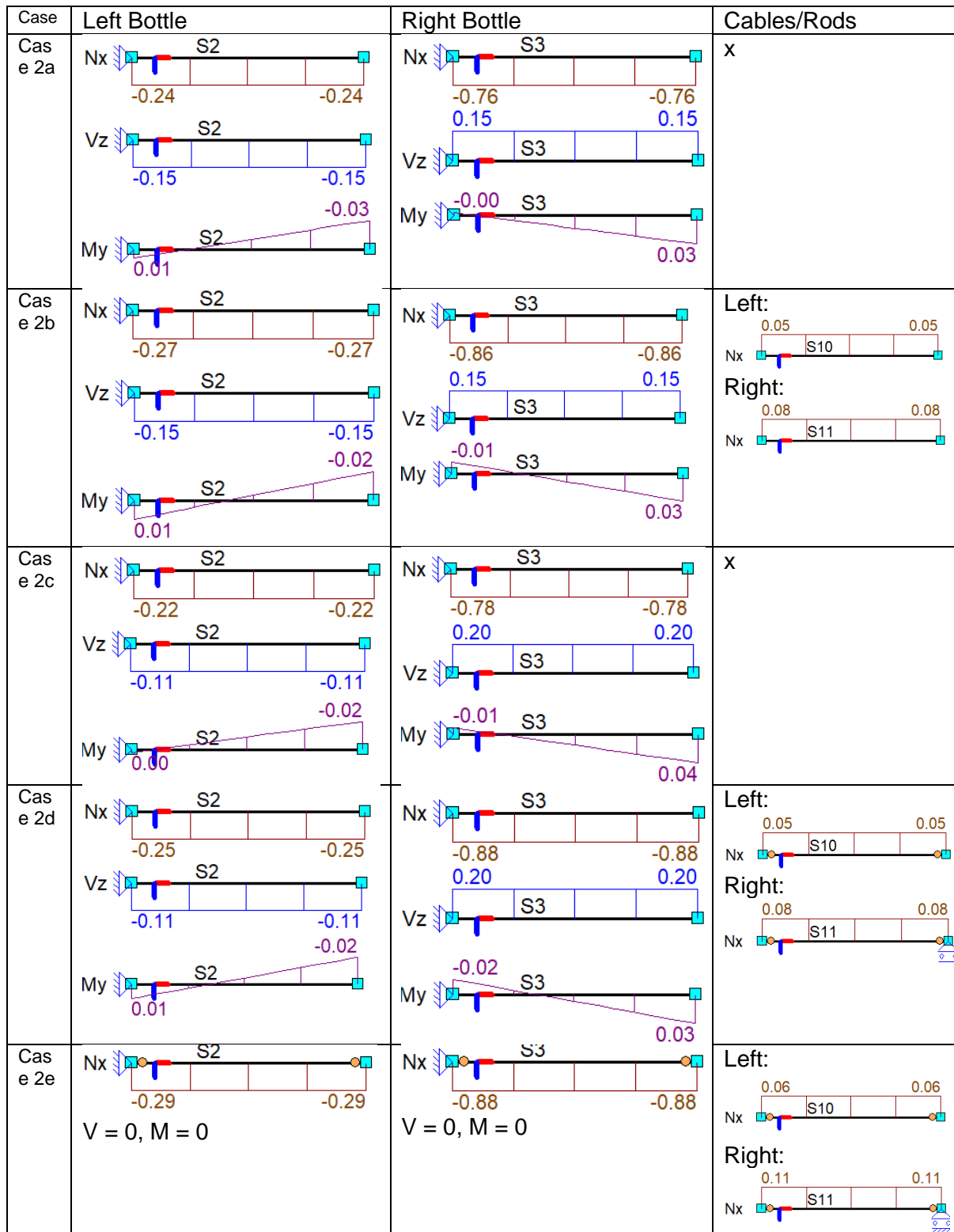


Figure XX – Structural models for eccentric loading



For all the cases, above the maximum cross-section forces for a unit force of 1 kN can be compared:

Case	Position of F	Cross-sec force	Bottle	Cable
A	Centric	N (kN)	-0.50 kN	x
		V (kN)	+/-0.20 kN	x
		M (kNm)	-0.04 kNm	x
	Eccentric	N (kN)	-0.76 kN	x
		V (kN)	+/-0.15 kN	x
		M (kNm)	+/-0.03 kNm	x
B	Centric	N (kN)	-0.59 kN	+0.09 kN
		V (kN)	+/-0.20 kN	x
		M (kNm)	+/-0.03 kNm	x
	Eccentric	N (kN)	-0.86 kN	+0.08 kN
		V (kN)	+/-0.15 kN	x
		M (kNm)	0.03 kNm	x
C	Centric	N (kN)	-0.50 kN	x
		V (kN)	0.21 kN	x
		M (kNm)	+/-0.04 kNm	x
	Eccentric	N (kN)	-0.78 kN	x
		V (kN)	0.20 kN	x
		M (kNm)	0.04 kNm	x
D	Centric	N (kN)	-0.59 kN	+0.12 kN
		V (kN)	+0.21 kN	x
		M (kNm)	+/-0.03 kNm	x
	Eccentric	N (kN)	-0.88 kN	+0.08 kN
		V (kN)	+0.20 kN	x
		M (kNm)	0.03 kNm	x
E	Centric	N (kN)	-0.62 kN	+0.12 kN
		V (kN)	x	x
		M (kNm)	x	x
	Eccentric	N (kN)	-0.88 kN	0.11 kN
		V (kN)	x	x
		M (kNm)	x	x

Table A.2.2. – Summary of maximum of cross-sectional forces for different cases

The following observations can be made:

- Case E allows for no shear force and bending moment in the glass bottle, only axial compression. In this case, the cables help with taking up the other forces. However, this case has the largest axial compression in the bottle for both centric and eccentric loading. However, a lateral support has to be provided for the top plate.
- Cases that involve cables show that the cables take up tension forces even when centric loading is applied. This results in a lower maximum bending moment in the glass bottles. This means that cables or rods are indeed beneficial for the load-carrying capacity. By including cables or tension rods, the axial compressive force in the bottles does increase.

Another difference between case D and E is the bending moment line in the plates, because of the different kind of connections between the plate and bottles. Case E has a larger sagging moment in the middle of the plate, which is larger than the largest hogging moment in case 1D. This means that case E can be more unfavourable for the plates.

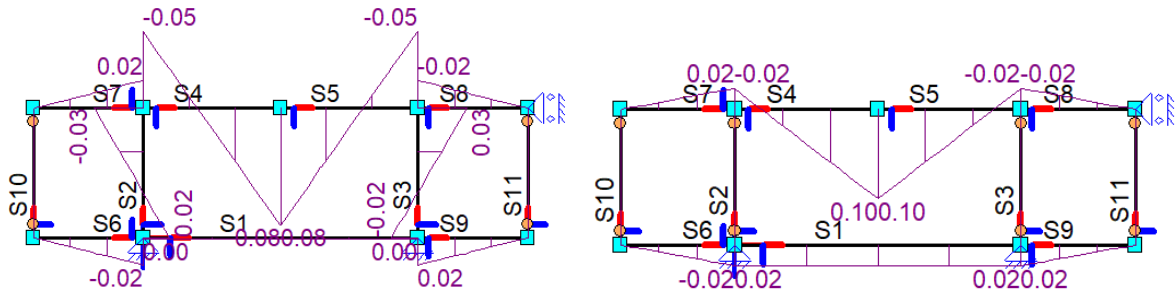


Figure A.2.3. – Comparison M-line clamped and hinged connections for bottles

Now that the different design possibilities for taking up compressive loads with and without eccentricities have been shown, the next step is to render solutions for three design aspects:

- Using whole or cut glass bottles
- Orientation of the bottles (finish facing up or down)
- Using multiple bottles together for a single element

These three design aspects are used to create the following solutions for the **compressive elements**.

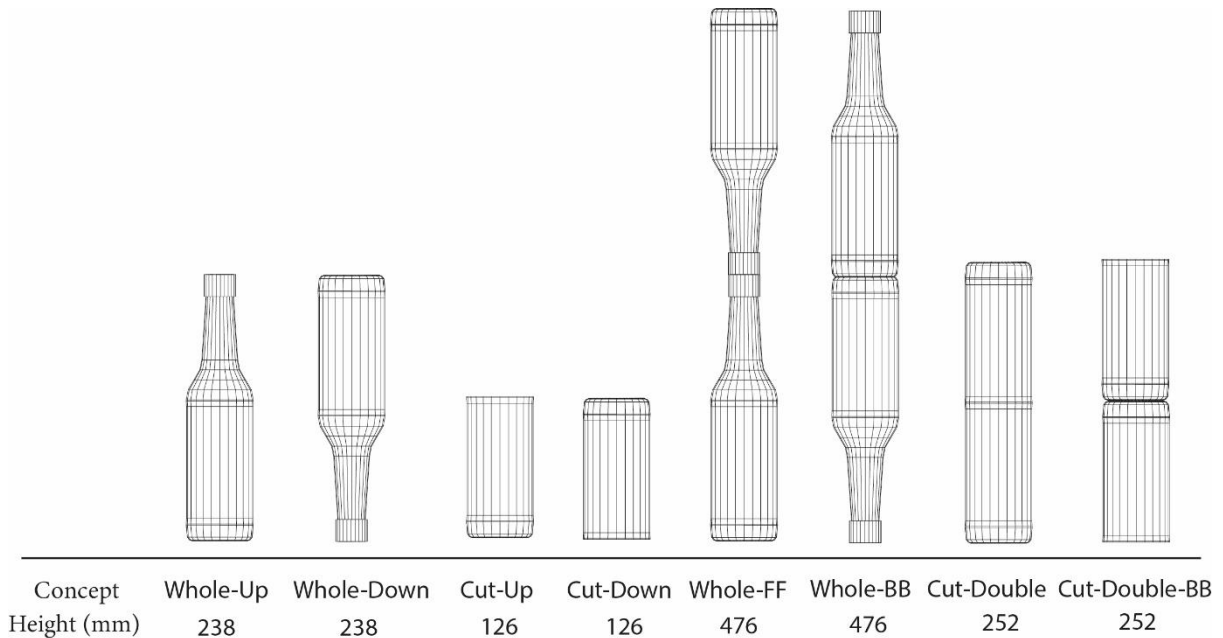


Figure A.2.4. – Design options for glass bottles between the plates

Figure XX shows the design options for glass bottles between the plates that will be investigated further in this thesis. It is important to also include cut glass bottles, because they will show a different stress-distribution due to applied compressive loading and bending moment.

DIANA FEA is used to create models of these bottles. Afterwards, material properties are assigned to the bottles similar to that of soda-lime glass ($E = 70 \text{ GPa}$, $\nu = 0.22$) and a thickness of 2.5 mm (0.0025 m) is applied to the bottle. The loads are then attached to the bottles with the corresponding boundary conditions from the cases formulated early on.

The bottles in MatrixFrame were represented as linear cylindrical elements, but as was shown earlier in this thesis project, the complex geometry of the bottle influences the stress

distribution. After the concepts are investigated in DIANA FEA, the maximum principle tensile stress is retrieved in the bottle and its location. The numerical values from MatrixFrame are used as input for the applied loads and bending moments. The goal of this is not necessarily to retrieve design values for these options, but it is to compare the different options together to synthesize and evaluate them based upon their load carrying capabilities. Moreover, it will show which boundary conditions are the most optimal for these options in terms of load carrying capabilities. The result of this comparison will thus show which type of connections (hinged or clamped) should be applied.

For now, the design options whole-FF, whole-BB, Cut-Double and Cut-Double-BB are designed as a monolithic element for simplicity, which means that a connection element is not included in this stage.

DIANA Models

Because DIANA FEA works with distributed forces and moments, the output from MatrixFrame has to be distributed on the relevant edges and faces. To do this, the circumference of the finish and the area of the bottom has to be calculated. Only the right bottle is evaluated in this analysis.

$$c_{finish} = d_{finish} \times \pi = 25\pi = 78.5398 \text{ mm} = 0.07854 \text{ m}$$

$$A_{bottom} = \frac{\pi}{4} \times d_{bottom}^2 = 867.3025\pi = 2724.7112 \text{ mm}^2 = 0.00272 \text{ m}^2$$

To check the results from the finite element program, a few simple hand calculations can be made. For instance, certain parts of the bottle are modelled as a cylinder. The normal and bending stress can be calculated for points of interest, for example at the supports where the maximum bending moment is.

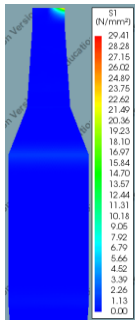
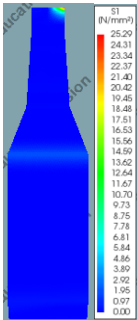
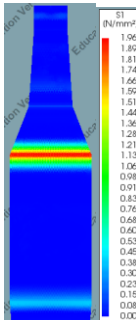
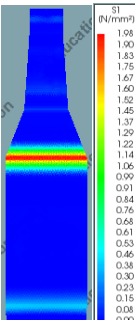
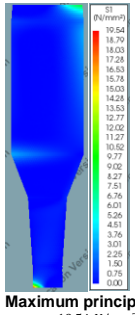
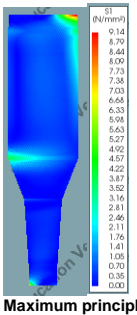
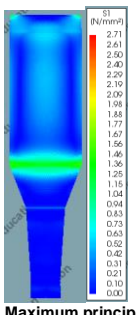
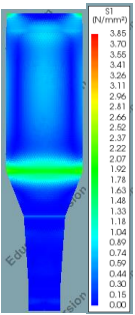
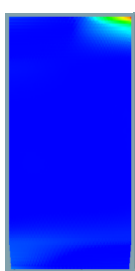
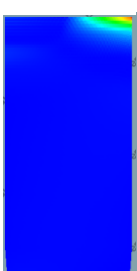


$$\sigma_N = \frac{-F_z}{A}$$

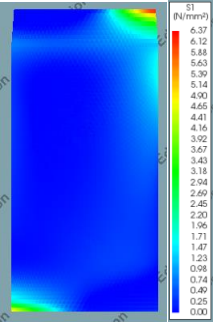
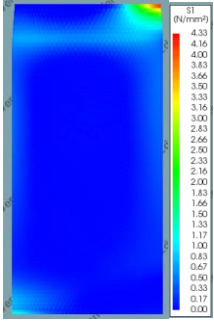
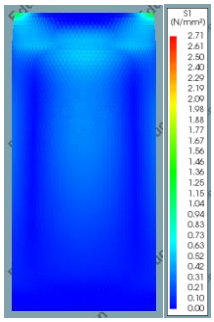
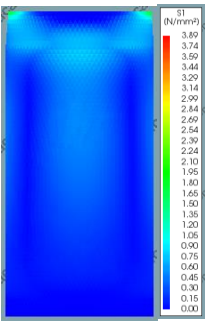
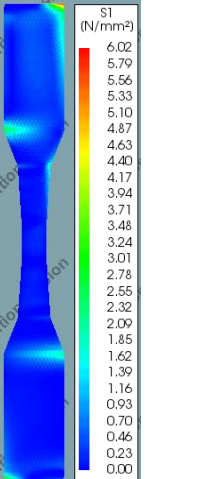
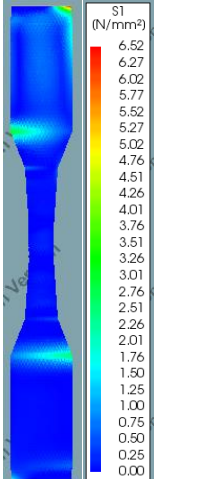
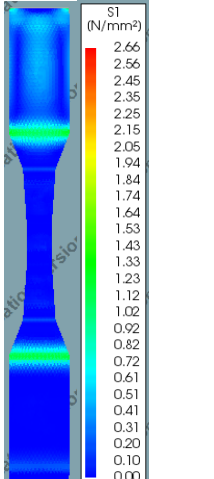
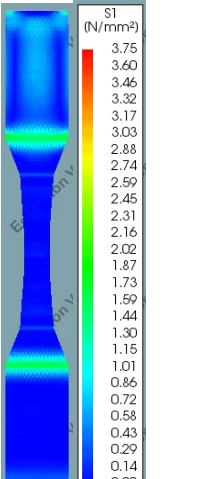
$$|\sigma_M| = \frac{M_y}{W}$$

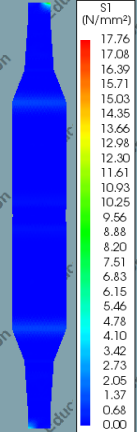
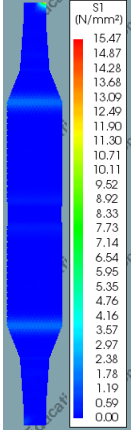
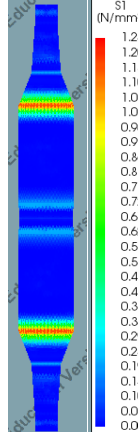
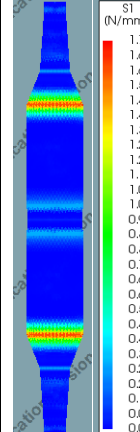
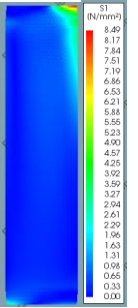
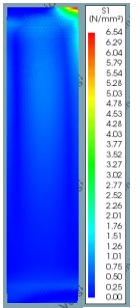
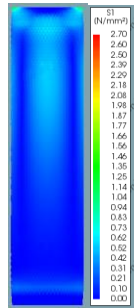
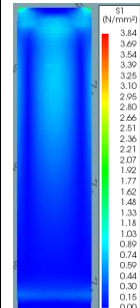
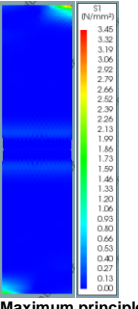
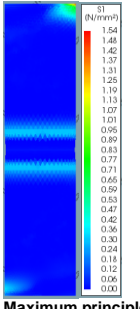
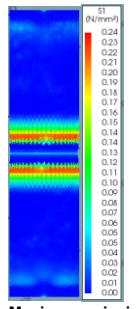
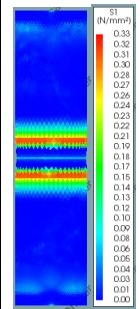
$$A_{finish} = \frac{\pi}{4} \times 27.5^2 - \frac{\pi}{4} \times 22.5^2 = 196.35 \text{ mm}^2$$

$$W_{finish} = \frac{\pi}{32} \times \left(\frac{27.5^4 - 22.5^4}{27.5} \right) = 1126.78 \text{ mm}^3$$

For every case and concept, the accuracy in percentage can be calculated to showcase the difference between the hand calculations and the finite element analysis calculations. These accuracy percentages are placed in the table with the corresponding concept and case.

	Case 1b	Case 2b	Case 1e	Case 2e
Whole-Up	<p> $F_{v,top,Matrix} = -0.59 \text{ kN}$ $M_{v,top,Matrix} = +0.03 \text{ kNm}$ $M_{v,bottom,Matrix} = -0.02 \text{ kNm}$ Input values for DIANA: $q_{v,top} = -7512.10 \text{ N/m}$ $m_{v,top,Matrix} = +30 \text{ N}$ $m_{v,bottom,Matrix} = -7352.94 \text{ N/m}$ </p>  <p> Maximum principle stress σ_1 $\sigma_{1,max} = 29.41 \text{ N/mm}^2$ Hand-calculations at top support: $\sigma_N = -0.59 \times 10^3 = -3.005 \text{ N/mm}^2$ $\sigma_M = \frac{0.03 \times 10^6}{1126.78} = \pm 26.62 \text{ N/mm}^2$ Numerical values from Diana: $\sigma_N = -2.85 \text{ N/mm}^2$ $\sigma_M = \pm 28.48 \text{ N/mm}^2$ </p>	<p> $F_{v,top,Matrix} = -0.86 \text{ kN}$ $M_{v,top,Matrix} = +0.03 \text{ kNm}$ $M_{v,bottom,Matrix} = -0.01 \text{ kNm}$ Input values for DIANA: $q_{v,top} = -10949.83 \text{ N/m}$ $m_{v,top,Matrix} = +30 \text{ N}$ $m_{v,bottom,Matrix} = -3676.47 \text{ N/m}$ </p>  <p> Maximum principle stress σ_1 $\sigma_{1,max} = 25.29 \text{ N/mm}^2$ Hand-calculations at top support: $\sigma_N = -0.86 \times 10^3 = -4.38 \text{ N/mm}^2$ $\sigma_M = \frac{0.03 \times 10^6}{1126.78} = \pm 26.62 \text{ N/mm}^2$ Numerical values from Diana: $\sigma_N = -4.29 \text{ N/mm}^2$ $\sigma_M = \pm 28.48 \text{ N/mm}^2$ </p>	<p> $F_{v,top,Matrix} = -0.62 \text{ kN}$ $M_{v,top,Matrix} = 0 \text{ kNm}$ $M_{v,bottom,Matrix} = 0$ Input values for DIANA: $q_{v,top} = -7894.07 \text{ N/m}$ $m_{v,top,Matrix} = 0 \text{ N}$ $m_{v,bottom,Matrix} = 0 \text{ N/m}$ </p>  <p> Maximum principle stress σ_1 $\sigma_{1,max} = 1.96 \text{ N/mm}^2$ Hand-calculations at top support: $\sigma_N = -0.62 \times 10^3 = -4.29 \text{ N/mm}^2$ $\sigma_M = \frac{196.35}{1126.78} = -4.29 \text{ N/mm}^2$ Numerical values from Diana: $\sigma_N = -4.29 \text{ N/mm}^2$ </p>	<p> $F_{v,top,Matrix} = -0.88 \text{ kN}$ $M_{v,top,Matrix} = 0 \text{ kNm}$ $M_{v,bottom,Matrix} = 0$ Input values for DIANA: $q_{v,top} = -11204.48 \text{ N/m}$ $m_{v,top,Matrix} = 0 \text{ N}$ $m_{v,bottom,Matrix} = 0 \text{ N/m}$ </p>  <p> Maximum principle stress σ_1 $\sigma_{1,max} = 1.98 \text{ N/mm}^2$ Hand-calculations at top support: $\sigma_N = -0.88 \times 10^3 = -4.48 \text{ N/mm}^2$ $\sigma_M = \frac{196.35}{1126.78} = -4.48 \text{ N/mm}^2$ Numerical values from Diana: $\sigma_N = -4.32 \text{ N/mm}^2$ </p>
Whole-Down	<p> $F_{v,top,Matrix} = -0.59 \text{ kN}$ $M_{v,top,Matrix} = +0.03 \text{ kNm}$ $M_{v,bottom,Matrix} = -0.02 \text{ kNm}$ Input values for DIANA: $q_{v,top} = -216911.76 \text{ N/m}^2$ $m_{v,top,Matrix} = +11029.41 \text{ N}$ $m_{v,bottom,Matrix} = -20 \text{ N}$ </p>  <p> Maximum principle stress σ_1 $\sigma_{1,max} = 19.54 \text{ N/mm}^2$ Hand-calculations at bottom support: $\sigma_N = -0.59 \times 10^3 = -3.005 \text{ N/mm}^2$ $\sigma_M = \frac{196.35}{0.02 \times 10^6} = \pm 17.75 \text{ N/mm}^2$ Numerical values from Diana: $\sigma_N = -2.92 \text{ N/mm}^2$ $\sigma_M = \pm 17.32 \text{ N/mm}^2$ </p>	<p> $F_{v,top,Matrix} = -0.86 \text{ kN}$ $M_{v,top,Matrix} = +0.03 \text{ kNm}$ $M_{v,bottom,Matrix} = -0.01 \text{ kNm}$ Input values for DIANA: $q_{v,top} = -316176.46 \text{ N/m}^2$ $m_{v,top,Matrix} = +11029.41 \text{ N}$ $m_{v,bottom,Matrix} = -10 \text{ N}$ </p>  <p> Maximum principle stress σ_1 $\sigma_{1,max} = 9.14 \text{ N/mm}^2$ Hand-calculations at bottom support: $\sigma_N = -0.86 \times 10^3 = -4.38 \text{ N/mm}^2$ $\sigma_M = \frac{0.01 \times 10^6}{1126.78} = \pm 8.87 \text{ N/mm}^2$ Numerical values from Diana: $\sigma_N = -4.25 \text{ N/mm}^2$ $\sigma_M = \pm 8.66 \text{ N/mm}^2$ </p>	<p> $F_{v,top,Matrix} = -0.62 \text{ kN}$ $M_{v,top,Matrix} = 0 \text{ kNm}$ $M_{v,bottom,Matrix} = 0$ Input values for DIANA: $q_{v,top} = -227941.18 \text{ N/m}^2$ $m_{v,top,Matrix} = 0 \text{ N/m}$ $m_{v,bottom,Matrix} = 0 \text{ N}$ </p>  <p> Maximum principle stress σ_1 $\sigma_{1,max} = 2.71 \text{ N/mm}^2$ Hand-calculations at bottom support: $\sigma_N = -0.62 \times 10^3 = -3.06 \text{ N/mm}^2$ $\sigma_M = \frac{196.35}{1126.78} = -3.07 \text{ N/mm}^2$ Numerical values from Diana: $\sigma_N = -3.07 \text{ N/mm}^2$ </p>	<p> $F_{v,top,Matrix} = -0.88 \text{ kN}$ $M_{v,top,Matrix} = 0 \text{ kNm}$ $M_{v,bottom,Matrix} = 0$ Input values for DIANA: $q_{v,top} = -323529.42 \text{ N/m}^2$ $m_{v,top,Matrix} = 0 \text{ N/m}$ $m_{v,bottom,Matrix} = 0 \text{ N}$ </p>  <p> Maximum principle stress σ_1 $\sigma_{1,max} = 3.85 \text{ N/mm}^2$ Hand-calculations at bottom support: $\sigma_N = -0.88 \times 10^3 = -4.48 \text{ N/mm}^2$ $\sigma_M = \frac{196.35}{1126.78} = -4.48 \text{ N/mm}^2$ Numerical values from Diana: $\sigma_N = -4.35 \text{ N/mm}^2$ </p>
Cut-up	<p> $F_{v,top,Matrix} = -0.59 \text{ kN}$ $M_{v,top,Matrix} = +0.04 \text{ kNm}$ $M_{v,bottom,Matrix} = -0.02 \text{ kNm}$ Input values for DIANA: $q_{v,top} = -216911.76 \text{ N/m}$ $m_{v,top,Matrix} = +14705.88 \text{ N/m}$ $m_{v,bottom,Matrix} = -3.83 \text{ N}$ </p> 	<p> $F_{v,top,Matrix} = -0.85 \text{ kN}$ $M_{v,top,Matrix} = +0.03 \text{ kNm}$ $M_{v,bottom,Matrix} = -0.01 \text{ kNm}$ Input values for DIANA: $q_{v,top} = -312500 \text{ N/m}$ $m_{v,top,Matrix} = +11029.41 \text{ N/m}$ $m_{v,bottom,Matrix} = -1.92 \text{ N}$ </p>  <p> Maximum principle stress σ_1 </p>	<p> $F_{v,top,Matrix} = -0.62 \text{ kN}$ $M_{v,top,Matrix} = 0 \text{ kNm}$ $M_{v,bottom,Matrix} = 0 \text{ kNm}$ Input values for DIANA: $q_{v,top} = -227941.18 \text{ N/m}$ $m_{v,top,Matrix} = 0 \text{ N/m}$ $m_{v,bottom,Matrix} = 0 \text{ N}$ </p> 	<p> $F_{v,top,Matrix} = -0.89 \text{ kN}$ $M_{v,top,Matrix} = 0 \text{ kNm}$ $M_{v,bottom,Matrix} = 0 \text{ kNm}$ Input values for DIANA: $q_{v,top} = -327205.88 \text{ N/m}$ $m_{v,top,Matrix} = 0 \text{ N/m}$ $m_{v,bottom,Matrix} = 0 \text{ N}$ </p> 

	<p>Maximum principle stress σ_1 $\sigma_{1,max} = 6.70 \text{ N/mm}^2$ Hand-calculations at top support: $\sigma_N = \frac{-0.59 \times 10^3}{479.09} = -1.23 \text{ N/mm}^2$ $\sigma_M = \frac{0.04 \times 10^6}{7030.31} = \pm 5.69 \text{ N/mm}^2$ Numerical values from Diana: $\sigma_N = -1.18 \text{ N/mm}^2$ $\sigma_M = \pm 6.37 \text{ N/mm}^2$</p>	<p>$\sigma_{1,max} = 5.03 \text{ N/mm}^2$ Hand-calculations at top support: $\sigma_N = \frac{-0.85 \times 10^3}{479.09} = -1.77 \text{ N/mm}^2$ $\sigma_M = \frac{0.03 \times 10^6}{7030.31} = \pm 4.27 \text{ N/mm}^2$ Numerical values from Diana: $\sigma_N = -1.73 \text{ N/mm}^2$ $\sigma_M = \pm 4.32 \text{ N/mm}^2$</p>	<p>Maximum principle stress σ_1 $\sigma_{1,max} = 0.39 \text{ N/mm}^2$ Hand-calculations at top support: $\sigma_N = \frac{-0.62 \times 10^3}{479.09} = -1.29 \text{ N/mm}^2$ Numerical values from Diana: $\sigma_N = -1.26 \text{ N/mm}^2$</p>	<p>Maximum principle stress σ_1 $\sigma_{1,max} = 0.56 \text{ N/mm}^2$ Hand-calculations at top support: $\sigma_N = \frac{-0.89 \times 10^3}{479.09} = -1.86 \text{ N/mm}^2$ Numerical values from Diana: $\sigma_N = -1.81 \text{ N/mm}^2$</p>
<p>Cut-down</p>	<p>$F_{v,top,Matrix} = -0.59 \text{ kN}$ $M_{y,top,Matrix} = +0.04 \text{ kNm}$ $M_{y,bottom,Matrix} = -0.02 \text{ kNm}$ Input values for DIANA: $q_{v,top} = -216911.76 \text{ N/m}^2$ $m_{v,top,Matrix} = +7352.94 \text{ N/m}$ $m_{v,bottom,Matrix} = -7.67 \text{ N}$</p>  <p>Maximum principle stress σ_1 $\sigma_{1,max} = 6.37 \text{ N/mm}^2$ Hand-calculations at bottom support: $\sigma_N = \frac{-0.59 \times 10^3}{479.09} = -1.23 \text{ N/mm}^2$ Numerical values from Diana: $\sigma_N = -1.33 \text{ N/mm}^2$</p>	<p>$F_{v,top,Matrix} = -0.85 \text{ kN}$ $M_{y,top,Matrix} = +0.03 \text{ kNm}$ $M_{y,bottom,Matrix} = -0.01 \text{ kNm}$ Input values for DIANA: $q_{v,top} = -312500 \text{ N/m}^2$ $m_{v,top,Matrix} = +3676.47 \text{ N/m}$ $m_{v,bottom,Matrix} = -3.83 \text{ N}$</p>  <p>Maximum principle stress σ_1 $\sigma_{1,max} = 4.33 \text{ N/mm}^2$ Hand-calculations at bottom support: $\sigma_N = \frac{-0.85 \times 10^3}{479.09} = -1.77 \text{ N/mm}^2$ Numerical values from Diana: $\sigma_N = -1.79 \text{ N/mm}^2$</p>	<p>$F_{v,top,Matrix} = -0.62 \text{ kN}$ $M_{y,top,Matrix} = 0 \text{ kNm}$ $M_{y,bottom,Matrix} = 0 \text{ kNm}$ Input values for DIANA: $q_{v,top} = -227941.18 \text{ N/m}^2$ $m_{v,top,Matrix} = 0 \text{ N/m}$ $m_{v,bottom,Matrix} = 0 \text{ N}$</p>  <p>Maximum principle stress σ_1 $\sigma_{1,max} = 2.71 \text{ N/mm}^2$ Hand-calculations at bottom support: $\sigma_N = \frac{-0.62 \times 10^3}{479.09} = -1.29 \text{ N/mm}^2$ Numerical values from Diana: $\sigma_N = -1.31 \text{ N/mm}^2$</p>	<p>$F_{v,top,Matrix} = -0.89 \text{ kN}$ $M_{y,top,Matrix} = 0 \text{ kNm}$ $M_{y,bottom,Matrix} = 0 \text{ kNm}$ Input values for DIANA: $q_{v,top} = -327205.88 \text{ N/m}^2$ $m_{v,top,Matrix} = 0 \text{ N/m}$ $m_{v,bottom,Matrix} = 0 \text{ N}$</p>  <p>Maximum principle stress σ_1 $\sigma_{1,max} = 3.89 \text{ N/mm}^2$ Hand-calculations at bottom support: $\sigma_N = \frac{-0.89 \times 10^3}{479.09} = -1.86 \text{ N/mm}^2$ Numerical values from Diana: $\sigma_N = -1.89 \text{ N/mm}^2$</p>
<p>Whole-FF</p>	<p>$F_{z,top,Matrix} = -0.59 \text{ kN}$ $M_{y,top,Matrix} = +0.02 \text{ kNm}$ $M_{y,bottom,Matrix} = -0.02 \text{ kNm}$ Input values for DIANA: $q_{v,top} = -216912 \text{ N/m}^2$ $m_{v,top,Matrix} = +7352.94 \text{ N/m}^2$ $m_{v,bottom,Matrix} = -7352.94 \text{ N/m}^2$</p>  <p>Maximum principle stress σ_1 $\sigma_{1,max} = 6.02 \text{ N/mm}^2$ Hand-calculation in middle: $\sigma_N = \frac{-0.59 \times 10^3}{196.35} = -3.005 \text{ N/mm}^2$ Numerical values from Diana: $\sigma_N = -3.01 \text{ N/mm}^2$</p>	<p>$F_{z,top,Matrix} = -0.85 \text{ kN}$ $M_{y,top,Matrix} = +0.02 \text{ kNm}$ $M_{y,bottom,Matrix} = -0.01 \text{ kNm}$ Input values for DIANA: $q_{v,top} = -312500 \text{ N/m}^2$ $m_{v,top,Matrix} = +7352.94 \text{ N/m}^2$ $m_{v,bottom,Matrix} = -3676.47 \text{ N/m}^2$</p>  <p>Maximum principle stress σ_1 $\sigma_{1,max} = 6.52 \text{ N/mm}^2$ Hand-calculation in middle: $\sigma_N = \frac{-0.85 \times 10^3}{196.35} = -4.33 \text{ N/mm}^2$ Numerical values from Diana: $\sigma_N = -4.33 \text{ N/mm}^2$</p>	<p>$F_{z,top,Matrix} = -0.61 \text{ kN}$ $M_{y,top,Matrix} = 0 \text{ kNm}$ $M_{y,bottom,Matrix} = 0 \text{ kNm}$ Input values for DIANA: $q_{v,top} = -224264.71 \text{ N/m}^2$ $m_{v,top,Matrix} = 0 \text{ N/m}^2$ $m_{v,bottom,Matrix} = 0 \text{ N/m}^2$</p>  <p>Maximum principle stress σ_1 $\sigma_{1,max} = 2.66 \text{ N/mm}^2$ Hand-calculation in middle: $\sigma_N = \frac{-0.61 \times 10^3}{196.35} = -3.11 \text{ N/mm}^2$ Numerical values from Diana: $\sigma_N = -3.11 \text{ N/mm}^2$</p>	<p>$F_{z,top,Matrix} = -0.86 \text{ kN}$ $M_{y,top,Matrix} = 0 \text{ kNm}$ $M_{y,bottom,Matrix} = 0 \text{ kNm}$ Input values for DIANA: $q_{v,top} = -316176.47 \text{ N/m}^2$ $m_{v,top,Matrix} = +0 \text{ N/m}^2$ $m_{v,bottom,Matrix} = -0 \text{ N/m}^2$</p>  <p>Maximum principle stress σ_1 $\sigma_{1,max} = 3.75 \text{ N/mm}^2$ Hand-calculation in middle: $\sigma_N = \frac{-0.86 \times 10^3}{196.35} = -4.38 \text{ N/mm}^2$ Numerical values from Diana: $\sigma_N = -4.40 \text{ N/mm}^2$</p>
<p>Whole-BB</p>	<p>$F_{z,top,Matrix} = -0.59 \text{ kN}$ $M_{y,top,Matrix} = +0.02 \text{ kNm}$ $M_{y,bottom,Matrix} = -0.02 \text{ kNm}$ Input values for DIANA: $q_{v,top} = -7512.10 \text{ N/m}$ $m_{v,top,Matrix} = +20 \text{ N}$ $m_{v,bottom,Matrix} = -20 \text{ N}$</p>	<p>$F_{z,top,Matrix} = -0.85 \text{ kN}$ $M_{y,top,Matrix} = +0.02 \text{ kNm}$ $M_{y,bottom,Matrix} = -0.01 \text{ kNm}$ Input values for DIANA: $q_{v,top} = -10822.51 \text{ N/m}$ $m_{v,top,Matrix} = +20 \text{ N}$ $m_{v,bottom,Matrix} = -10 \text{ N}$</p>	<p>$F_{z,top,Matrix} = -0.61 \text{ kN}$ $M_{y,top,Matrix} = 0 \text{ kNm}$ $M_{y,bottom,Matrix} = 0 \text{ kNm}$ Input values for DIANA: $q_{v,top} = -7766.74 \text{ N/m}$ $m_{v,top,Matrix} = 0 \text{ N}$ $m_{v,bottom,Matrix} = 0 \text{ N}$</p>	<p>$F_{z,top,Matrix} = -0.86 \text{ kN}$ $M_{y,top,Matrix} = 0 \text{ kNm}$ $M_{y,bottom,Matrix} = 0 \text{ kNm}$ Input values for DIANA: $q_{v,top} = -316176.47 \text{ N/m}$ $m_{v,top,Matrix} = +0 \text{ N}$ $m_{v,bottom,Matrix} = -0 \text{ N}$</p>

	 <p>Maximum principle stress σ_1 $\sigma_{1,max} = 17.76 \text{ N/mm}^2$ Hand-calculation at top support: $\sigma_N = -0.59 \times 10^3 = -3.005 \text{ N/mm}^2$ $\sigma_M = \frac{196.35}{1126.78} = \pm 17.75 \text{ N/mm}^2$ Numerical values from Diana: $\sigma_N = -2.90 \text{ N/mm}^2$ $\sigma_M = \pm 17.38 \text{ N/mm}^2$</p>	 <p>Maximum principle stress σ_1 $\sigma_{1,max} = 15.47 \text{ N/mm}^2$ Hand-calculation at top support: $\sigma_N = -0.85 \times 10^3 = -4.33 \text{ N/mm}^2$ $\sigma_M = \frac{196.35}{1126.78} = \pm 17.75 \text{ N/mm}^2$ Numerical values from Diana: $\sigma_N = -4.21 \text{ N/mm}^2$ $\sigma_M = \pm 17.40 \text{ N/mm}^2$</p>	 <p>Maximum principle stress σ_1 $\sigma_{1,max} = 1.24 \text{ N/mm}^2$ Hand-calculation at top support: $\sigma_N = -0.61 \times 10^3 = -3.11 \text{ N/mm}^2$ $\sigma_M = \frac{196.35}{1126.78} = \pm 17.75 \text{ N/mm}^2$ Numerical values from Diana: $\sigma_N = -3.01 \text{ N/mm}^2$</p>	 <p>Maximum principle stress σ_1 $\sigma_{1,max} = 1.76 \text{ N/mm}^2$ Hand-calculation at top support: $\sigma_N = -0.62 \times 10^3 = -4.38 \text{ N/mm}^2$ $\sigma_M = \frac{196.35}{479.09} = \pm 17.75 \text{ N/mm}^2$ Numerical values from Diana: $\sigma_N = -4.25 \text{ N/mm}^2$</p>
Cut-Double	<p>$F_{z,top,Matrix} = -0.59 \text{ kN}$ $M_{y,top,Matrix} = +0.03 \text{ kNm}$ $M_{y,bottom,Matrix} = -0.02 \text{ kNm}$ Input values for DIANA: $q_{v,top} = -216911.76 \text{ N/m}^2$ $m_{v,top,Matrix} = +11029.41 \text{ N/m}$ $m_{v,bottom,Matrix} = -7352.94 \text{ N/m}$</p>  <p>Maximum principle stress σ_1 $\sigma_{1,max} = 8.49 \text{ N/mm}^2$ Hand-calculation in middle: $\sigma_N = -0.59 \times 10^3 = -1.23 \text{ N/mm}^2$ $\sigma_M = \frac{479.09}{1126.78} = \pm 1.77 \text{ N/mm}^2$ Numerical values from Diana: $\sigma_N = -1.17 \text{ N/mm}^2$</p>	<p>$F_{z,top,Matrix} = -0.86 \text{ kN}$ $M_{y,top,Matrix} = +0.02 \text{ kNm}$ $M_{y,bottom,Matrix} = -0.01 \text{ kNm}$ Input values for DIANA: $q_{v,top} = -316176.47 \text{ N/m}^2$ $m_{v,top,Matrix} = +7352.94 \text{ N/m}$ $m_{v,bottom,Matrix} = -7367.47 \text{ N/m}$</p>  <p>Maximum principle stress σ_1 $\sigma_{1,max} = 6.54 \text{ N/mm}^2$ Hand-calculation in middle: $\sigma_N = -0.86 \times 10^3 = -1.80 \text{ N/mm}^2$ $\sigma_M = \frac{479.09}{1126.78} = \pm 1.77 \text{ N/mm}^2$ Numerical values from Diana: $\sigma_N = -1.79 \text{ N/mm}^2$</p>	<p>$F_{z,top,Matrix} = -0.62 \text{ kN}$ $M_{y,top,Matrix} = 0 \text{ kNm}$ $M_{y,bottom,Matrix} = 0 \text{ kNm}$ Input values for DIANA: $q_{v,top} = -227941.18 \text{ N/m}^2$ $m_{v,top,Matrix} = 0 \text{ N/m}$ $m_{v,bottom,Matrix} = 0 \text{ N/m}$</p>  <p>Maximum principle stress σ_1 $\sigma_{1,max} = 2.70 \text{ N/mm}^2$ Hand-calculation in middle: $\sigma_N = -0.62 \times 10^3 = -1.29 \text{ N/mm}^2$ $\sigma_M = \frac{479.09}{1126.78} = \pm 1.77 \text{ N/mm}^2$ Numerical values from Diana: $\sigma_N = -1.30 \text{ N/mm}^2$</p>	<p>$F_{z,top,Matrix} = -0.88 \text{ kN}$ $M_{y,top,Matrix} = 0 \text{ kNm}$ $M_{y,bottom,Matrix} = 0 \text{ kNm}$ Input values for DIANA: $q_{v,top} = -323529.41 \text{ N/m}^2$ $m_{v,top,Matrix} = 0 \text{ N/m}$ $m_{v,bottom,Matrix} = 0 \text{ N/m}$</p>  <p>Maximum principle stress σ_1 $\sigma_{1,max} = 3.84 \text{ N/mm}^2$ Hand-calculation in middle: $\sigma_N = -0.88 \times 10^3 = -1.84 \text{ N/mm}^2$ $\sigma_M = \frac{479.09}{1126.78} = \pm 1.77 \text{ N/mm}^2$ Numerical values from Diana: $\sigma_N = -1.84 \text{ N/mm}^2$</p>
Cut-Double-BB	<p>$F_{z,top,Matrix} = -0.59 \text{ kN}$ $M_{y,top,Matrix} = +0.03 \text{ kNm}$ $M_{y,bottom,Matrix} = -0.02 \text{ kNm}$ Input values for DIANA: $q_{v,top} = -3078.73 \text{ N/m}$ $m_{v,top,Matrix} = +5.75 \text{ N}$ $m_{v,bottom,Matrix} = -3.83 \text{ N}$</p>  <p>Maximum principle stress σ_1 $\sigma_{1,max} = 3.45 \text{ N/mm}^2$ Hand-calculation at top: $\sigma_N = -0.59 \times 10^3 = -1.23 \text{ N/mm}^2$ $\sigma_M = \frac{479.09}{7030.31} = \pm 4.27 \text{ N/mm}^2$ Numerical values from Diana:</p>	<p>$F_{z,top,Matrix} = -0.86 \text{ kN}$ $M_{y,top,Matrix} = +0.02 \text{ kNm}$ $M_{y,bottom,Matrix} = -0.01 \text{ kNm}$ Input values for DIANA: $q_{v,top} = -4487.65 \text{ N/m}$ $m_{v,top,Matrix} = +3.83 \text{ N}$ $m_{v,bottom,Matrix} = -1.92 \text{ N}$</p>  <p>Maximum principle stress σ_1 $\sigma_{1,max} = 1.54 \text{ N/mm}^2$ Hand-calculation at top: $\sigma_N = -0.86 \times 10^3 = -1.80 \text{ N/mm}^2$ $\sigma_M = \frac{479.09}{7030.31} = \pm 2.84 \text{ N/mm}^2$ Numerical values from Diana:</p>	<p>$F_{z,top,Matrix} = -0.62 \text{ kN}$ $M_{y,top,Matrix} = 0 \text{ kNm}$ $M_{y,bottom,Matrix} = 0 \text{ kNm}$ Input values for DIANA: $q_{v,top} = -3235.28 \text{ N/m}$ $m_{v,top,Matrix} = 0 \text{ N}$ $m_{v,bottom,Matrix} = 0 \text{ N}$</p>  <p>Maximum principle stress σ_1 $\sigma_{1,max} = 0.24 \text{ N/mm}^2$ Hand-calculation at top: $\sigma_N = -0.62 \times 10^3 = -1.29 \text{ N/mm}^2$ $\sigma_M = \frac{479.09}{7030.31} = \pm 1.77 \text{ N/mm}^2$ Numerical values from Diana: $\sigma_N = -1.25 \text{ N/mm}^2$</p>	<p>$F_{z,top,Matrix} = -0.88 \text{ kN}$ $M_{y,top,Matrix} = 0 \text{ kNm}$ $M_{y,bottom,Matrix} = 0 \text{ kNm}$ Input values for DIANA: $q_{v,top} = -4592.01 \text{ N/m}$ $m_{v,top,Matrix} = 0 \text{ N}$ $m_{v,bottom,Matrix} = 0 \text{ N}$</p>  <p>Maximum principle stress σ_1 $\sigma_{1,max} = 0.33 \text{ N/mm}^2$ Hand-calculation at top: $\sigma_N = -0.88 \times 10^3 = -1.84 \text{ N/mm}^2$ $\sigma_M = \frac{479.09}{7030.31} = \pm 1.77 \text{ N/mm}^2$ Numerical values from Diana: $\sigma_N = -1.77 \text{ N/mm}^2$</p>

	$\sigma_N = -1.19 \text{ N/mm}^2$ $\sigma_M = \pm 4.33 \text{ N/mm}^2$	$\sigma_N = -1.74 \text{ N/mm}^2$ $\sigma_M = \pm 2.88 \text{ N/mm}^2$		
--	---	---	--	--

Table XX – Stress distributions and maximum principle stress results from different configurations and cases.

The results from table XX can now be summarized in a bar chart for every case. This is shown in figure XX.

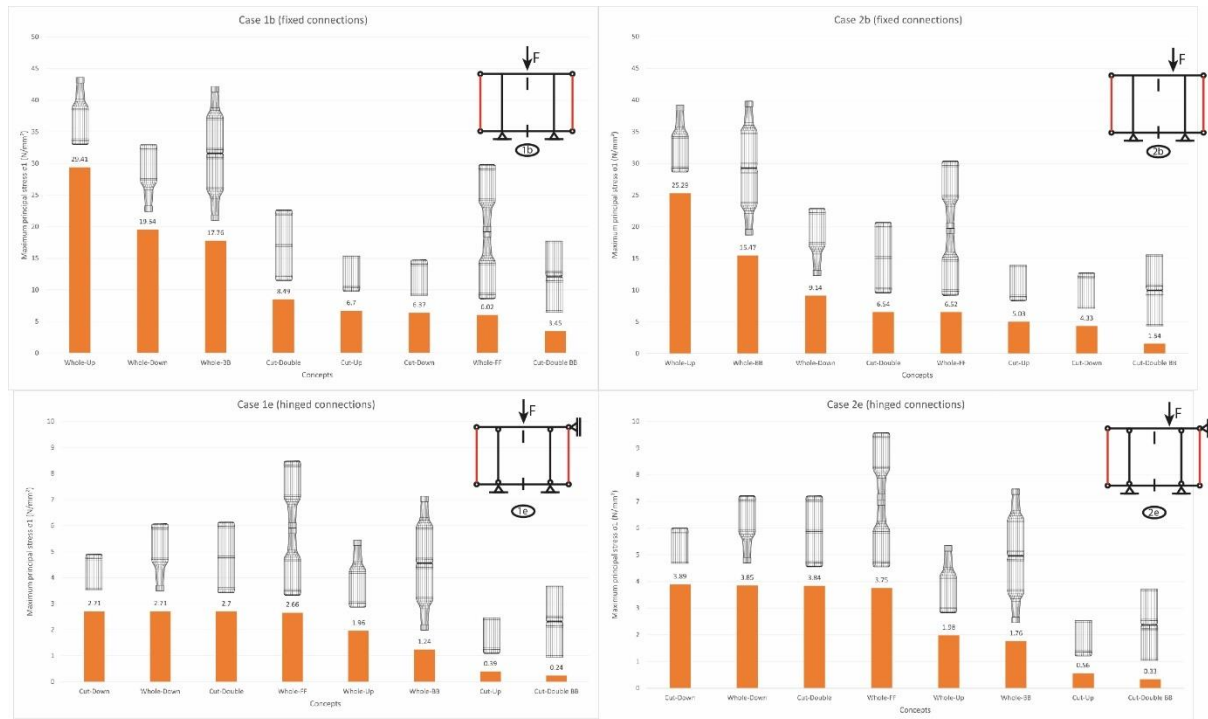


Figure XX – Summary of maximum principle stresses for every concept and case

The following conclusions can be made from this chart on the choice of concept:

- Concepts that have the finish of the bottle on the boundaries of the element (i.e. Whole-Up, Whole-Down, Whole-BB) have relatively higher principal stresses than elements without the finish or the finish on the inside of the element for case b. In case b, a bending moment is introduced at the boundaries of the element. Because the finish has the smallest cross-section of the whole bottle, the section modulus W will therefore be small, which means that the bending stresses will be high.
- The difference between orientations of the concepts (i.e. between Whole-Up or Whole-Down) arise due to the following two reasons:
 - 1. The cross-section of the bottom of the bottle is bigger than in the body of the bottle, which means that the bending stresses will be lower. Therefore, the down configuration tends to score better in case b, where relatively larger bending moments are introduced at the top of the element than on the bottom of the element.
 - 2. In case e, the up-configuration seems to behave better than the down-configuration. This seems to be because the vertical load is applied on the bottom of the bottle rather than on the wall of the element itself. This can lead to bending of the bottom of the bottle, which would create additional bending stresses.

- For the combined concepts Whole-FF and Whole-BB, the whole-BB concept seems to behave better with hinged connections than the whole-FF concept. For the case with hinged connections, this is the other way around.
- For all cases, the concept Cut-Double BB seems to behave the best mechanically. This is because for the fixed connections problem, the bending moments are taken up by relatively large cross-sections (i.e. the cross-section of the body of the bottle). Moreover, the vertical load is taken up fully by the walls of the bottle at the supports. Lastly, the tensile principle stresses due to vertical load at the heel are already much lower than those at the shoulder. Removing the shoulder would thus be better for the vertical load carrying capability of the element.
- Generally, whole bottles tend to behave poorly with the introduction of bending moments with fixed connection in comparison to cut bottles.

A₃

A3 Hand Calculation Axial Stiffness Whole-Up

A3 Hand-calculation Axial Stiffness Whole-Up

This document contains a hand-calculation of the axial stiffness of the whole-Up concept. This will be compared with the slope found in the dataset, i.e. the axial stiffness of the unit. A few considerations are made at first:

- The hinges on the outside and steel elements on the boundaries of the unit are neglected in this hand-calculation. These elements are relatively much stiffer than the timber and plastic in between.
- Results from a FEM-model are used to determine the axial stiffness of the bottle. This is done by putting a unit load of 1 kN on top of the bottom and the vertical displacement of the top of the bottle is retrieved.
- Because the steel in the unit is much stiffer than the other elements, it can be estimated that a uniform stress distribution is introduced from the steel elements. For the less stiffer elements, i.e. the timber, it is estimated that the load is introduced with an angle of 45 degrees. Moreover, the load distribution in the timber plate is considered as a collection of springs to determine the total axial stiffness of the plates.
- The unit is modelled as a collection of springs in series and parallel. This is used for the hand-calculation.
- The effective area of the plastic elements (i.e. POM and Nylon) is hard to determine. Two considerations are made. Firstly, it is considered that all of the area of the plastic is used. This is an overestimation. Secondly, only a small contact area on the plastic is considered as the effective area. Then, the two results are compared to evaluate the contribution of the plastic elements.

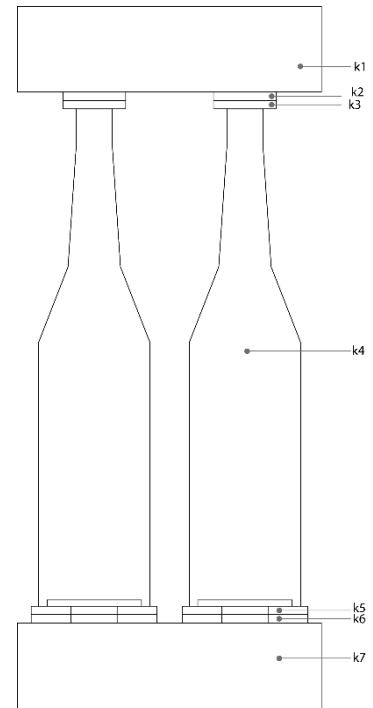
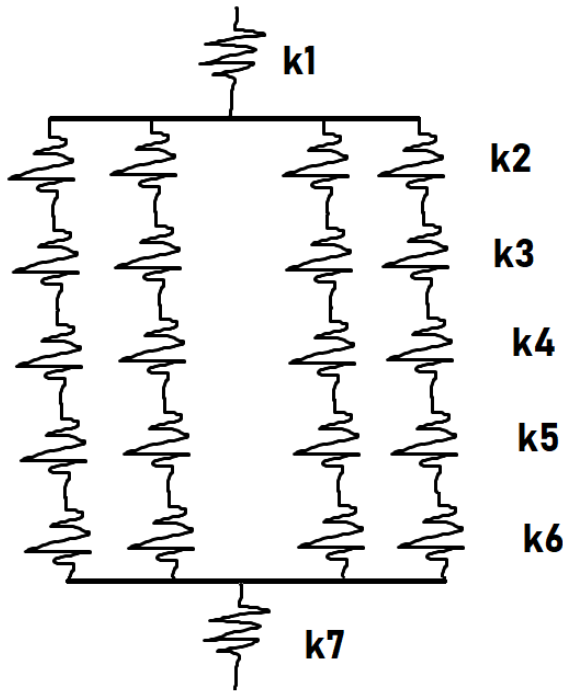
The axial stiffness can be retrieved from the following formula:

$$u = \frac{NL}{EA}$$
$$\frac{u}{N} = \frac{L}{EA} \text{ or } \frac{N}{u} = \frac{EA}{L} = k$$

The term EA/L is equal to an equivalent spring stiffness. The term L in this case is the thickness of the respective elements. E is the Young's Modulus of the material and A is the effective area that is loaded and not the total area of the element.

Spring model:

A spring model can be developed to model the axial stiffness of the unit:

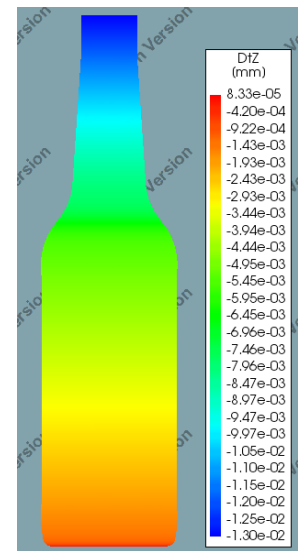


It is important to know the difference between springs in parallel and springs in series:

- Same load, different displacement: Spring in series
- Different load, same displacement: Springs in parallel

Between the timber plates, the load is **spread** over four elements. This means that this part can be modelled with parallel springs.

Springs	Element
k_1	Upper timber plate
k_2	Steel Disk
k_3	POM Disk
k_4	Glass Bottle
k_5	Nylon Ring
k_6	Steel Ring
k_7	Lower timber plate



Axial Stiffness Steel Disk k_2 :

$$k_2 = \frac{E_{steel} A_{steel,disk}}{t_{disk}} = \frac{200000 \times \pi \times 15^2}{4} = 3534291.74 \text{ N/mm}$$

Axial Stiffness Glass Bottle k_4 :

A shell thickness of 2.5 mm is chosen for the bottle. A unit force of 1 kN is applied on the top of the bottle. The displacement at the top is equal to 0.013 mm. See picture for contour plot above.

$$k_4 = \frac{F_z}{u_z} = \frac{1000}{0.013} = 76923.08 \text{ N/mm}$$

This value is checked with the help of a hand-calculation. The problem is simplified to a glass cylinder with an average diameter. For simplicity, one third of the bottle has a diameter of the neck ($d_{neck} = 25$ mm) and two thirds of the bottle has a diameter of the body ($d_{neck} = 61$ mm). It is assumed that the cylinder has an average thickness of 2.5 mm

The average diameter is then equal to:

$$d_{avg} = \frac{1}{3} \times 25 + \frac{2}{3} \times 61 = 49 \text{ mm}$$

$$A_{avg} = \frac{1}{4} \times \pi \times 49^2 - \frac{1}{4} \times \pi \times (49 - 2.5 \times 2)^2 = 365.21 \text{ mm}^2$$

$$u_z = \frac{NL}{EA} = \frac{1000 \times 238}{70000 \times 365.21} = 0.0093 \text{ mm}$$

The relative difference between the value from DIANA and the hand-calculation is thus:

$$\frac{0.013 - 0.0093}{0.013} * 100 = 29\%$$

The absolute difference is equal to 0.0037 mm.

Axial Stiffness Steel Ring k6:

The outer diameter of the steel ring is equal to 60 mm. The inner diameter is equal to 22 mm.

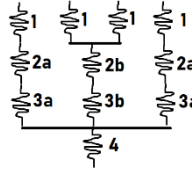
$$k_6 = \frac{E_{steel} A_{steel,ring}}{t_{ring}} = \frac{200000 \times (\pi \times (30^2 - 11^2))}{4} = 122365033.9 \text{ N/mm}$$

Axial Stiffness Lower Timber plate k7:

As mentioned before, the load is uniformly distributed and introduced into the timber from the steel. Because the large steel elements below the lower timber plate had equal width and length, the full bottom area of the timber plate was used. As can be seen in the schematic pictures, the first drawing looks at the bottom timber plate. The load is introduced via the steel rings. The load is introduced with an angle of 45 degrees. The holes of the steel rings have to be taken into account. An estimation of E_{90} of about 700 MPa is assumed for the lower timber plate.

Green zone:

$$k_{7_zone1} = \frac{E_{90} A_{zone1,avg}}{t_{zone1}} = \frac{700 \times \left(\frac{19+31}{2} \right)^2}{6} = \frac{700 \times 625}{6} = 72916.67 \text{ N/mm}$$



Blue zones:

$$k_{7_zone2a} = \frac{E_{90} A_{zone2a,avg}}{t_{zone2a}} = \frac{700 \times \left(\frac{31+32}{2} \right)^2}{0.5} = \frac{700 \times 992.25}{0.5} = 1389150 \text{ N/mm}$$

$$k_{7_zone2b} = \frac{E_{90} A_{zone2b,avg}}{t_{zone2b}} = \frac{700 \times \left(\frac{62+64}{2} \right)^2}{0.5} = \frac{700 \times 3969}{0.5} = 5556600 \text{ N/mm}$$

Red zones:

$$k_{7_zone3a} = \frac{E_{90} A_{zone3a,avg}}{t_{zone3a}} = \frac{700 \times \left(\frac{32+36.5}{2} \right)^2}{4.5} = \frac{700 \times 1173.06}{4.5} = 182476.39 \text{ N/mm}$$

$$k_{7_zone3b} = \frac{E_{90} A_{zone3b,avg}}{t_{zone3b}} = \frac{700 \times \left(\frac{64+72}{2} \right)^2}{4.5} = \frac{700 \times 4624}{4.5} = 719288.89 \text{ N/mm}$$

Yellow zone:

$$k_{7_zone4} = \frac{E_{90} A_{zone4,avg}}{t_{zone4}} = \frac{700 \times ((145)^2)}{30} = \frac{700 \times 21025}{30} = 490583.33 \text{ N/mm}$$

Combining zones:

Edge springs:

$$k_{7,1,2a,3a} = \frac{1}{\frac{1}{k_{7_zone1}} + \frac{1}{k_{7_zone2a}} + \frac{1}{k_{7_zone3a}}} = \frac{1}{\frac{1}{72916.67} + \frac{1}{1389150} + \frac{1}{182476.39}} = 50215.14 \text{ N/mm}$$

Middle spring:

$$k_{7,1,2b,3b} = \frac{1}{\frac{1}{4 \times k_{7_zone1}} + \frac{1}{k_{7_zone2b}} + \frac{1}{k_{7_zone3b}}} = \frac{1}{\frac{1}{4 \times 72916.67} + \frac{1}{5556600} + \frac{1}{719288.89}} = 200048.03 \text{ N/mm}$$

Total axial stiffness of the lower plate k_7 :

$$k_7 = \frac{1}{\frac{1}{4 \times k_{7,1,2a,3a}} + \frac{1}{k_{7_zone4}}} = \frac{1}{\frac{1}{4 \times 50215.14} + \frac{1}{490583.33}} = 220618.21 \text{ N/mm}$$

Axial Stiffness Upper Timber plate k_1 :

For the upper timber plate, the same calculation can be made. However, a steel plate was put on top of the timber that did not have the same width and length as the plate. This needs to be taken into account. Therefore, two different sides have to be considered. See the bottom two images above. Moreover, the timber being used for the upper plate was a stiffer wood than the bottom, so therefore a $E_{90} = 900 \text{ MPa}$ is chosen.

Green zones

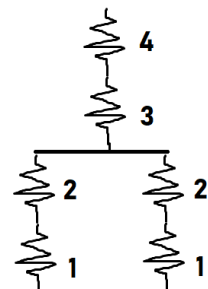
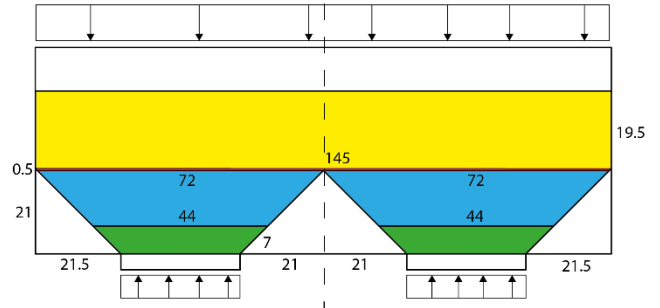
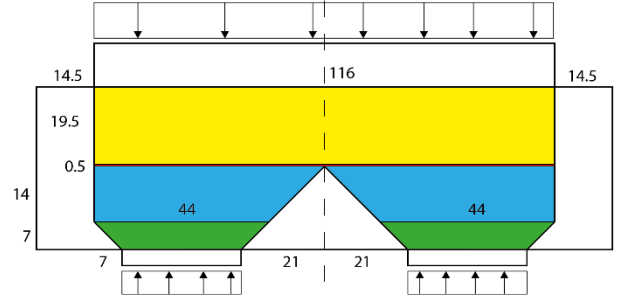
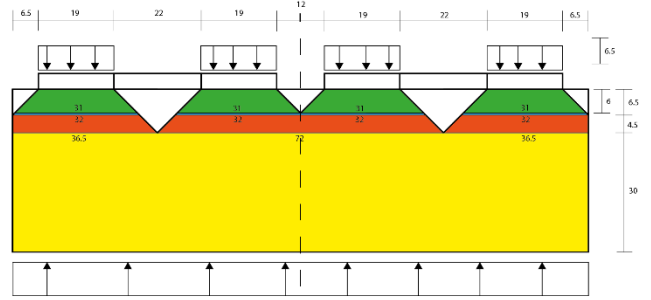
$$k_{1_zone1} = \frac{E_{90} A_{zone1,avg}}{t_{zone1}} = \frac{900 \times \left(\frac{30+44}{2} \right)^2}{7} = 176014.29 \text{ N/mm}$$

Red zones

$$k_{1_zone2} = \frac{E_{90} A_{zone2,avg}}{t_{zone2}} = \frac{900 \times \left(\frac{44+72}{2} \right) \times \left(\frac{44+116}{2} \right)}{14} = 298285.71 \text{ N/mm}$$

Blue zone

$$k_{1_zone3} = \frac{E_{90} A_{zone3,avg}}{t_{zone3}} = \frac{900 \times 116 \times \left(\frac{144+145}{2} \right)}{0.5} = 30171600 \text{ N/mm}$$



Yellow zone

$$k_{1_zone4} = \frac{E_{90} A_{zone4,avg}}{t_{zone4}} = \frac{900 \times 116 \times 145}{19.5} = 776307.69 \text{ N/mm}$$

Combining zones:

$$k_{1:1,2} = \frac{1}{\frac{1}{k_{1_zone1}} + \frac{1}{k_{1_zone2}}} \times 4 = \frac{1}{\frac{1}{176014.29} + \frac{1}{298285.71}} \times 4 = 442779.23 \text{ N/mm}$$

Total axial stiffness of upper lower plate k1:

$$k_1 = \frac{1}{\frac{1}{k_{1:1,2}} + \frac{1}{k_{1_zone3}} + \frac{1}{k_{1_zone4}}} = \frac{1}{\frac{1}{442779.23} + \frac{1}{30171600} + \frac{1}{776307.69}} = 279348.75 \text{ N/mm}$$

Axial Stiffness POM Disk k3 and Nylon Ring k5

It is assumed that not the full width of the POM is being used during the loading. After the testing of samples with the highest failure loads (i.e. above 100), plastic deformation was seen on the POM rings. The method that is being used here is applicable for elastic deformation with a linear slope in the F-u curve. However, this hand calculation can give an indication of the order of magnitude of the stiffness.

The top of the bottle is a ring of glass that is being pushed into the POM. On the bottom, the knurling of the bottle is pushed into the nylon. It is assumed that the nylon rings are type PA6. The Young's Modulus for PA6 is between 800 MPa and 2000 MPa. For this hand calculation, an average is taken of 1400 MPa. For POM, a Young's Modulus of about 3000 MPa is taken.

Next, the contact area of both plastic's has to be measured. Plastically deformed POM and Nylon were analysed after loading and the deformed surface was measured. Marks of the knurling is clearly visible on the nylon, but for this hand calculation, a ring is assumed for the contact area with the width of the knurling.



Figure XX - Pictures of the deformed plastic elements (left: M20 Nylon ring, right: POM disk)

$$A_{POM;Contact} = \pi \times (19^2 - (19 - 4)^2) = 427.26 \text{ mm}^2$$

$$A_{Nylon;Contact} = \pi \times (48^2 - (48 - 6)^2) = 1696.46 \text{ mm}^2$$

$$k_3 = \frac{E_{POM} A_{POM;Contact}}{t_{POM}} = \frac{3000 \times 427.26}{4} = 320445 \text{ N/mm}$$

$$k_5 = \frac{E_{Nylon} A_{Nylon;Contact}}{t_{POM}} = \frac{1400 \times 1696.46}{4} = 593761 \text{ N/mm}$$

Result:

$$k_{unit} = \frac{1}{\frac{1}{k_1} + \frac{1}{k_7} + \frac{4}{\frac{1}{k_2} + \frac{1}{k_3} + \frac{1}{k_4} + \frac{1}{k_5} + \frac{1}{k_6}}} = 79136.1 \frac{N}{mm} \text{ or } 7.9 \times 10^4 N/mm$$

The slope of the Whole-Up concept is about 40000 N/mm or $4.0 \times 10^4 N/mm$.

A₄

A4 AGR Experiments Tables

A4 AGR Experiments

Tables

Sample set description		Heel height: 13.8 mm; Body height: 67.7 mm; Shoulder height: 127.5 mm; BS: 2.13 mm; Neck height: 176.8 mm; Diameter upper neck (height: 198.5 mm): 27.87 mm; Diameter lower neck (height: 163 mm): 31.04 mm											
Sample nr.	Cavity nr.	Height in mm		Diameter shoulder in mm		Diameter heel in mm		Diameter body in mm		Finish A/E diameter in mm		Finish B/T diameter in mm	
		Min.	Max.	Min.	Max.	Min.	Max.	Min.	Max.	Min.	Max.	Min.	Max.
1	40	238.09	238.05	60.17	60.84	60.37	60.54						
2	17	238.03	238.19	60.09	60.37	60.30	60.77						
3	24	238.00	238.16	60.14	60.54	60.38	60.55						
4	50	238.05	238.32	60.25	60.76	60.41	60.62						
5	53	237.97	238.12	60.12	60.71	60.24	60.92						
6	5	238.10	238.22	60.29	60.45	60.38	60.59						
7	47	237.97	238.14	60.14	60.73	60.35	60.81						
8	47	237.87	238.14	60.13	60.64	60.32	60.90						
9	2	237.94	238.15	60.35	60.57	60.43	60.60						
10	14	237.80	237.94	60.16	60.56	60.26	60.68	59.08	59.92	26.38	26.46	28.33	28.72
Average		237.98	238.14	60.18	60.62	60.34	60.70	59.08	59.92	26.38	26.46	28.33	28.72

Table A.4.1. – Dimensional measurements of glass bottles. Data by Clarissa Justino de Lima on 01/03/2022

Sample nr.	Cavity nr.	Neck thickness in mm		Shoulder thickness in mm		Shoulder contact thickness in mm		Mid-sidewall thickness in mm		Heel contact thickness in mm		Lower most heel thickness in mm		Bearing surface thickness in mm		Bottom thickness in mm
		Min.	Max.	Min.	Max.	Min.	Max.	Min.	Max.	Min.	Max.	Min.	Max.	Min.	Max.	Value
1	2	3.09	3.74	2.46	3.07	2.24	2.70	2.75	3.42	2.76	3.38	2.68	3.29	4.58	6.06	5.94
2	47	3.15	4.45	2.36	3.13	2.20	3.12	2.68	3.40	2.55	2.97	2.50	2.90	4.56	5.51	5.56
3	14	3.02	3.49	2.18	2.76	2.14	2.73	3.38	3.71	2.75	3.58	2.68	3.77	4.74	6.38	6.00
Min. of samples		3.02		2.18		2.14		2.68		2.55		2.50		4.56		5.56
Max. of samples		4.45		3.13		3.12		3.71		3.58		3.77		6.38		6.00
Average		3.49		2.66		2.52		3.22		3.00		2.97		5.31		5.83

Table A.4.2. – Thickness measurements of glass bottles. Data by Clarissa Justino de Lima on 25/02/2022

Sample set	Sample nrs.	Cavity nrs.	Sample Arrangement		Test Condition	Tilt Angle in degrees θ	Coefficient of Friction $\tan(\theta)$
			Bottom	Top			
1	1-2-3	Sample 1: 40 Sample 2: 17 Sample 3: 24	2-3	1	DRY	10	0.176
			3-1	2	DRY	10.5	0.185
			1-2	3	DRY	9.5	0.167
Average					10	0.176	

Table A.4.3. – Tilt table measurements of glass bottles. Data by Clarissa Justino de Lima on 01/03/2022

Bottle conditioning		5 min line simulation, line-sim (tape marked with pink ink)			
Sample set description		33 cl amber bottles, line-simulated by Laura and Clarissa on 23/02/2022			
Sample nr.	Cavity nr.	Vertical load at fracture		Origin Location	
		kg_f	kN		
1	21	1825	17.90	Shoulder Contact	
2	53	1790	17.56	Shoulder Contact	
3	41	1835	18.00	Shoulder Contact	
4	26	1865	18.30	Shoulder Contact	
5	17	1885	18.49	Heel Contact	
6	40	1460	14.32	Shoulder Contact	
7	25	1555	15.25	Shoulder Contact	
8	30	1450	14.22	Shoulder Contact	
9	32	1845	18.10	Heel Contact	
10	15	1360	13.34	Heel Contact	
11	52	1025	10.06	Shoulder Contact	
12	34	1495	14.67	Shoulder Contact	
13	5	Nb (> 2050)	20.11	No Break	
14	32	1545	15.16	Shoulder Contact	
15	12	1770	17.36	Shoulder Contact	
16	27	1815	17.80	Shoulder Contact	
17	16	1765	17.31	Shoulder Contact	
18	31	1795	17.61	Shoulder Contact	
19	16	1870	18.34	Shoulder Contact	
20	48	1015	9.96	Heel Contact	
21	23	1970	19.33	Shoulder Contact	
22	43	1970	19.33	Shoulder Contact	
23	9	1670	16.38	Shoulder Contact	
24	25	1560	15.30	Shoulder Contact	
25	43	1590	15.60	Shoulder Contact	
26	33	1155	11.33	Shoulder Contact	
27	33	1630	15.99	Shoulder Contact	
28	27	1430	14.03	Shoulder Contact	

Table A.4.4. – Vertical load fractures data of line-simulated glass bottles.

Bottle conditioning		Abraded with 150 grit emery paper, shoulder and heel contact regions (blue ink)			
Sample set description		33 cl amber bottles, abraded by Younes Maachi on 23/02/2022			
Sample nr.	Cavity nr.	Vertical load at fracture		Origin Location	
		kg_f	kN		
1	41	1820	17.85	Heel Contact	
2	32	1390	13.64	Shoulder Contact	
3	45	1410	13.83	Shoulder Contact	
4	26	1900	18.64	Shoulder Contact	
5	6	1355	13.29	Shoulder Contact	
6	5	2050	20.11	Heel Contact	
7	27	1725	16.92	Shoulder Contact	
8	9	2040	20.01	Shoulder Contact	
9	33	Nb (> 2050)	Nb (> 20.11)	No Break	
10	12	1515	14.86	Shoulder Contact	
11	37	1370	13.44	Shoulder Contact	
12	50	1950	19.13	Shoulder Contact	
13	52	1890	18.54	Shoulder Contact	
14	16	2050	20.11	Shoulder Contact	
15	37	1845	18.10	Heel Contact	
16	3	1835	18.00	Shoulder Contact	
17	5	1740	17.07	Shoulder Contact	
18	23	1595	15.65	Shoulder Contact	
19	17	2045	20.06	Heel Contact	
20	13	1855	18.20	Shoulder Contact	
21	23	1690	16.58	Shoulder Contact	
22	47	2045	20.06	Heel Contact	
23	21	1725	16.92	Shoulder Contact	
24	9	1140	11.18	Heel Contact	
25	24	1675	16.43	Shoulder Contact	
26	21	1630	15.99	Shoulder Contact	
27	32	Nb (> 2050)	Nb (> 20.11)	No Break	
28	45	2000	19.62	Shoulder Contact	

Table A.4.5. – Vertical load fractures data of manually glass bottles.

A5

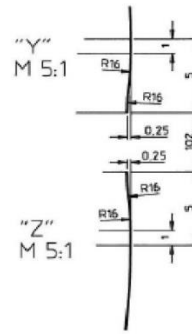
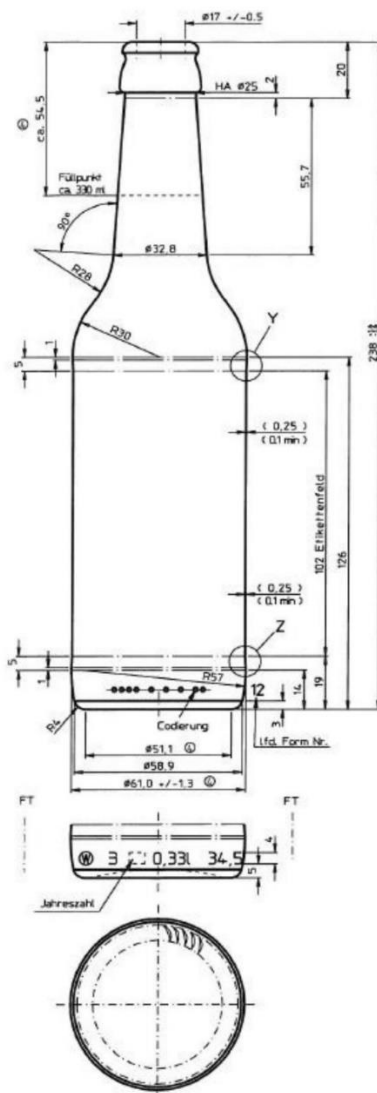
A5 Technical Drawing Brouwland Bottle

BROUWLAND



Specifications

017.525.7 Beer bottle Longneck 33 cl, brown, 26 mm



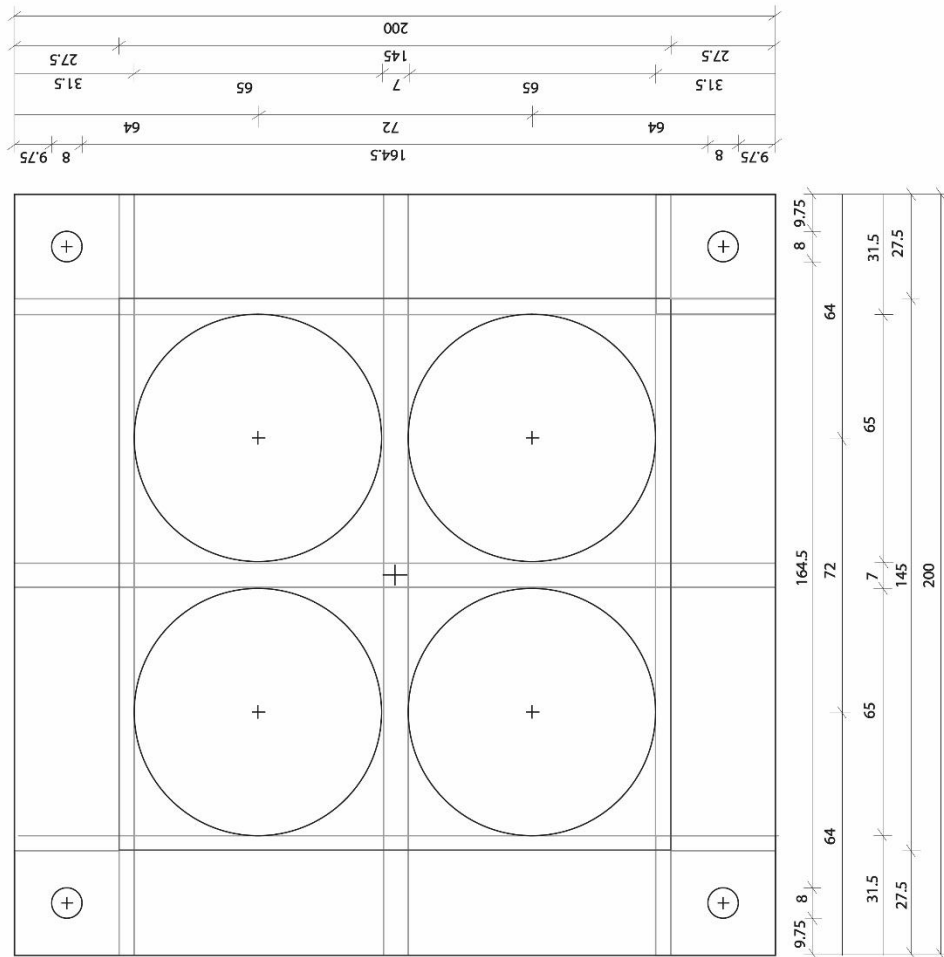
Weight	Ca. 300 gr
Refillable	Yes
CO2 content	4-6 g/L
Internal pressure T101	12 bar
Axial loading	5 kp
Temperature shock	42°C
Filling temperature	6-8°C

Brouwland
Korspelsesteenweg 86 • B-3581 Beverlo - Belgium
Tel. +32 11 40 14 08 • Fax. +32 11 89 03 09
info@brouwland.com • www.brouwland.com

A6

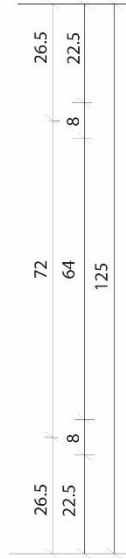
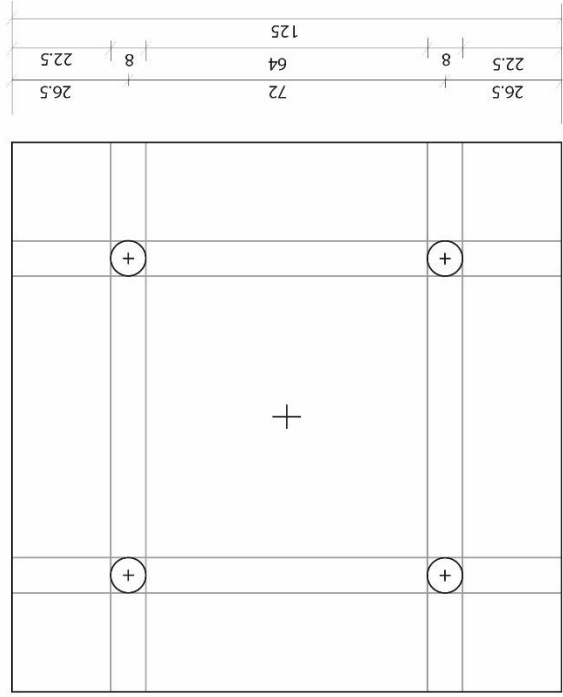
A6 MDF Plate Drawings

Stevinlab

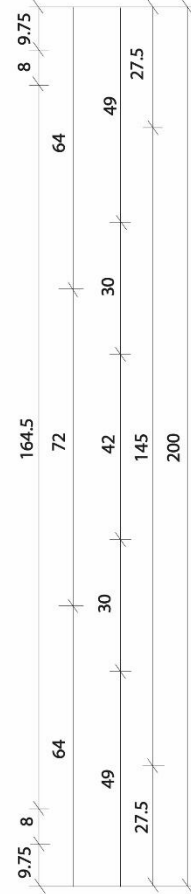
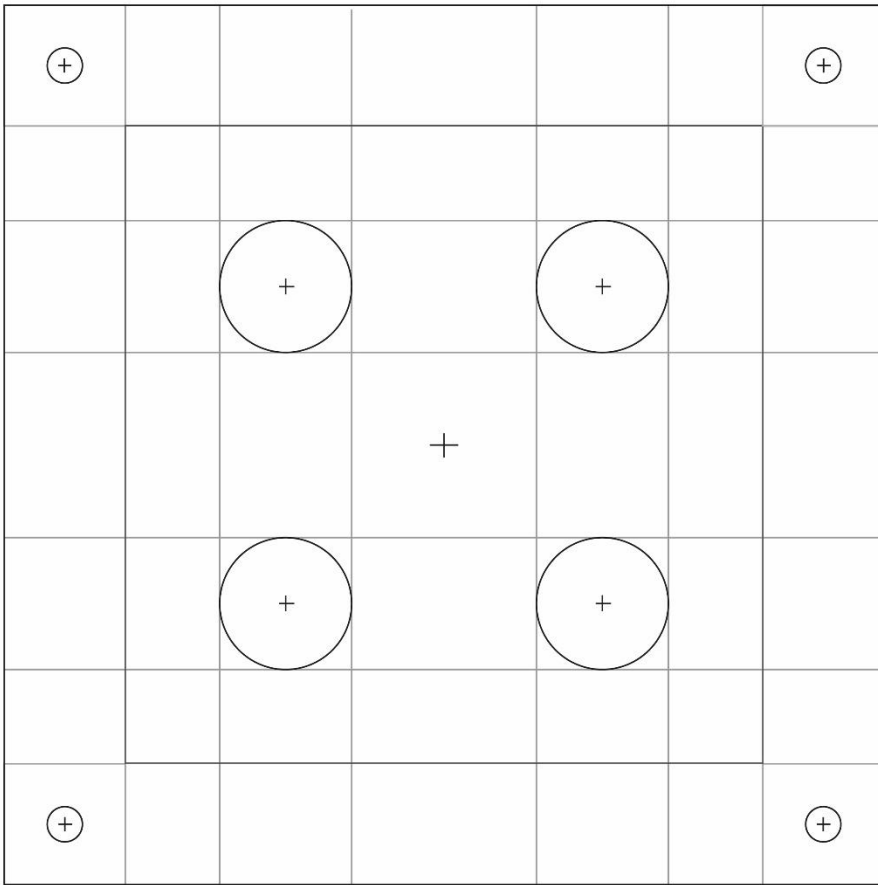
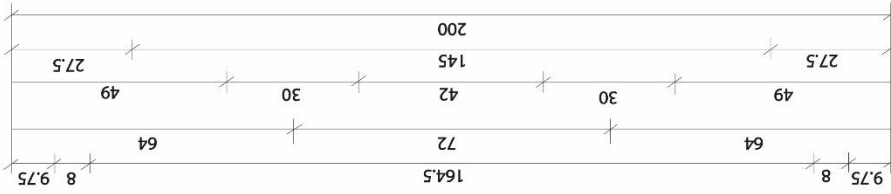


Top View Bottom Plate

Scale 1:1



Top View Steel Plate
Whole-FF



Top View Top Plate

Scale 1:1

A7

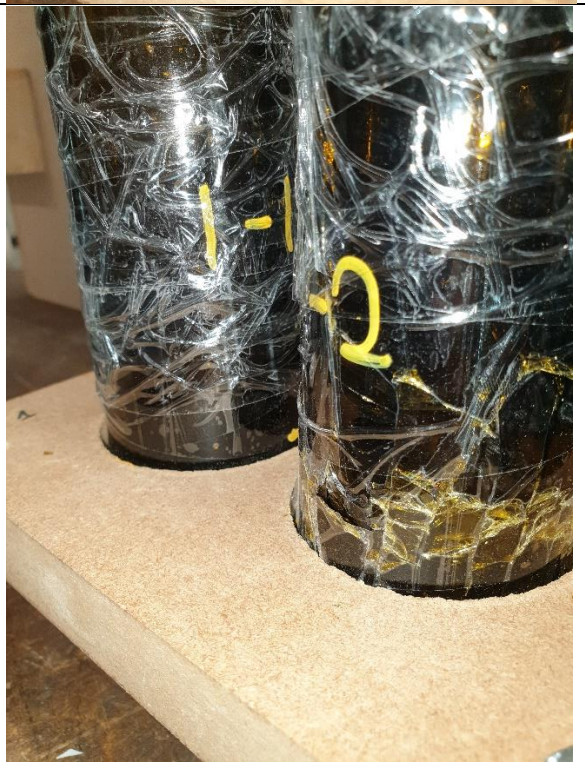
A7 Fractured Samples

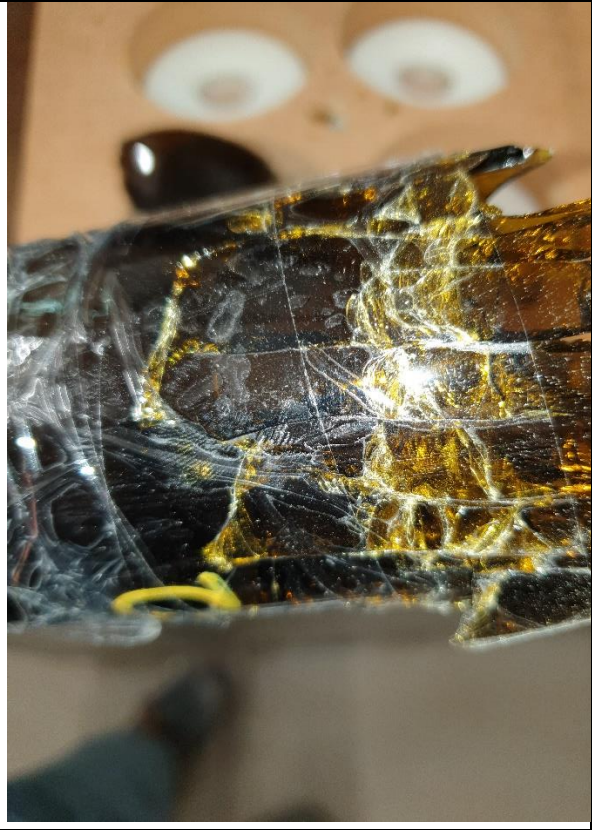
Stevinlab

A.7.1. Whole Samples

A.7.1.1. Fractured Whole-Up Samples

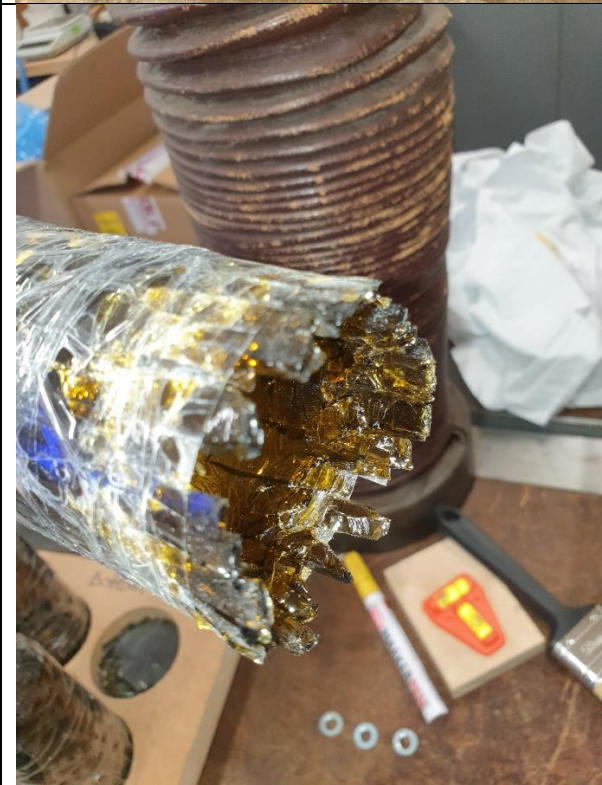






Sample 2 [Whole-Up]

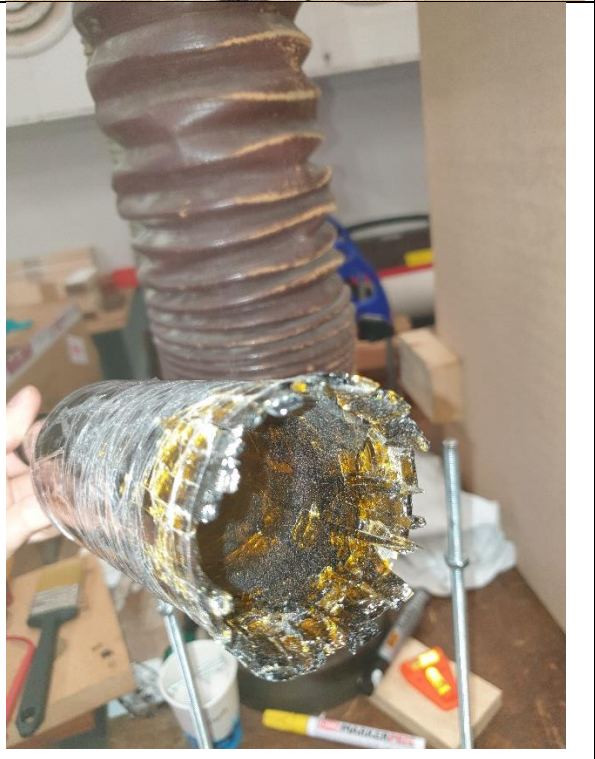






Sample 3 [Whole-Up]





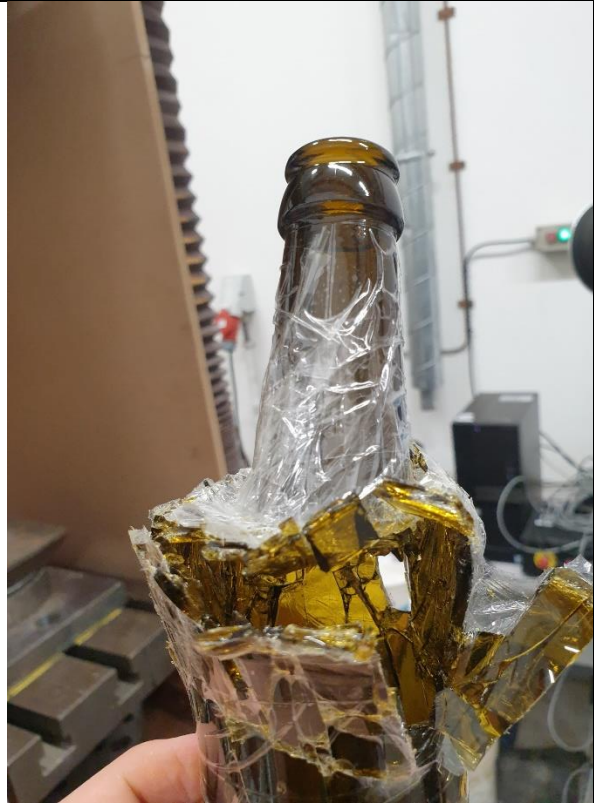
Sample 4 [Whole-Up]



A.7.1.2. Fractured Whole-FF Samples

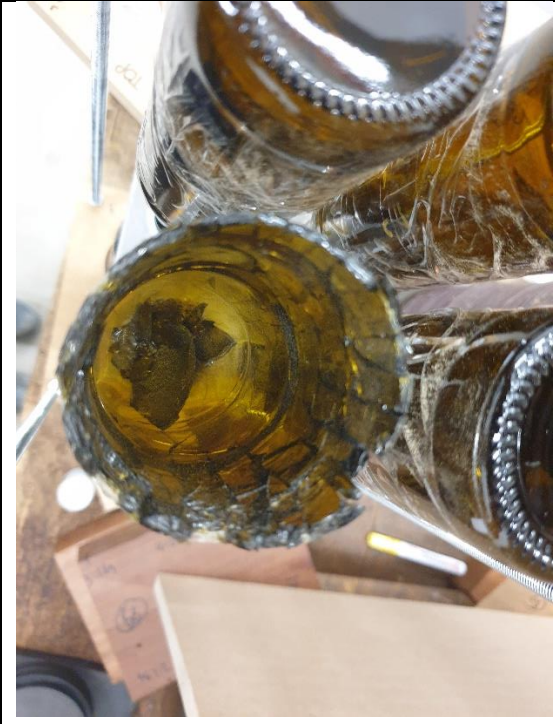
Sample 1 [Whole-FF]





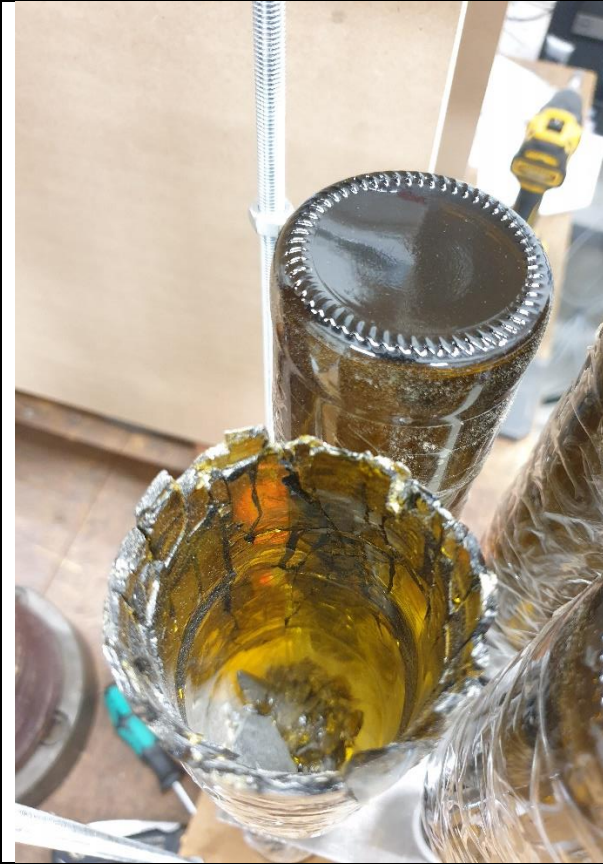
Sample 2 [Whole-FF]





Sample 3 [Whole-FF]



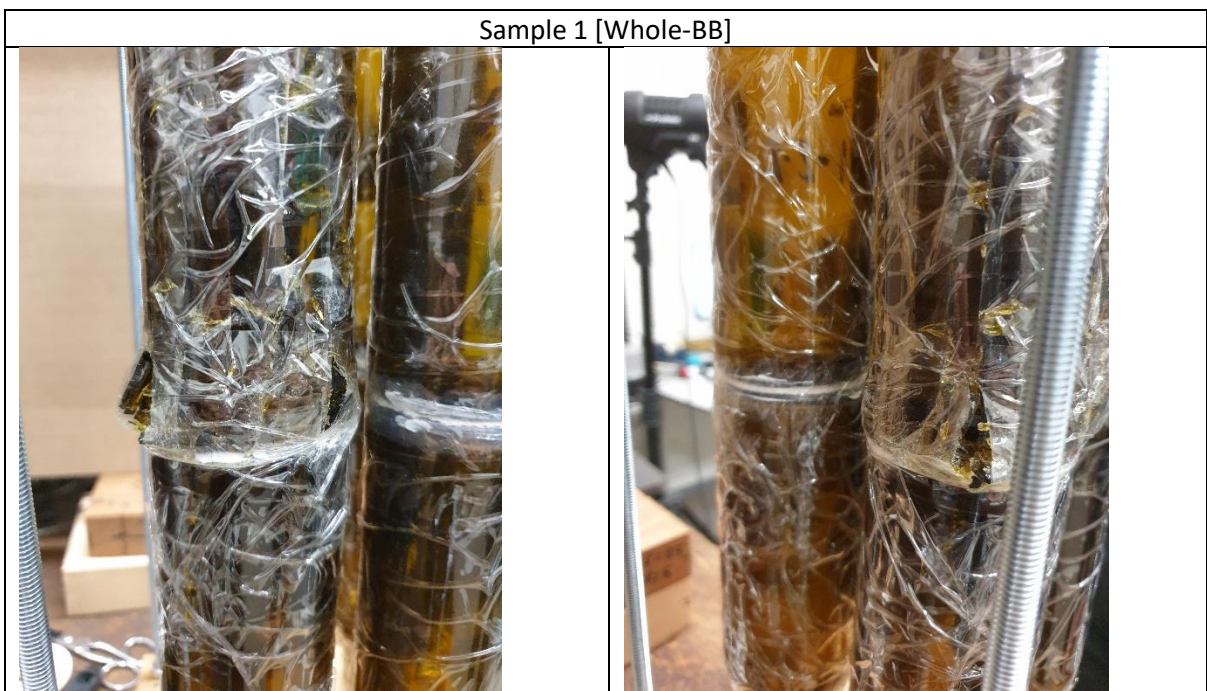


Sample 4 [Whole-FF]





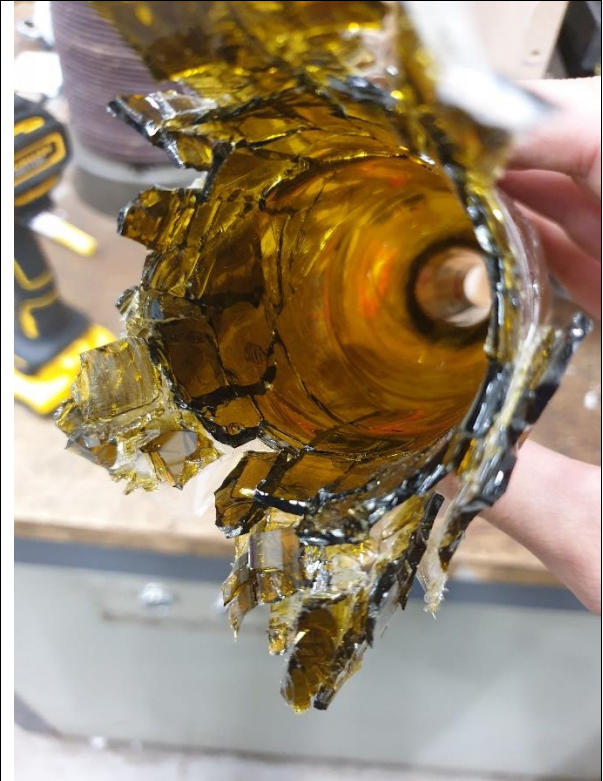
A.7.1.3. Fractured Whole-BB Samples



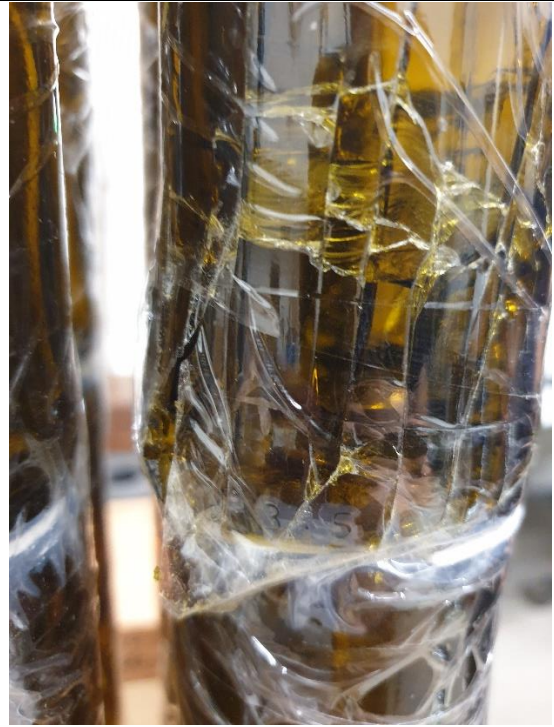
Sample 2 [Whole-BB]



Sample 3 [Whole-BB]



Sample 4 [Whole-BB]



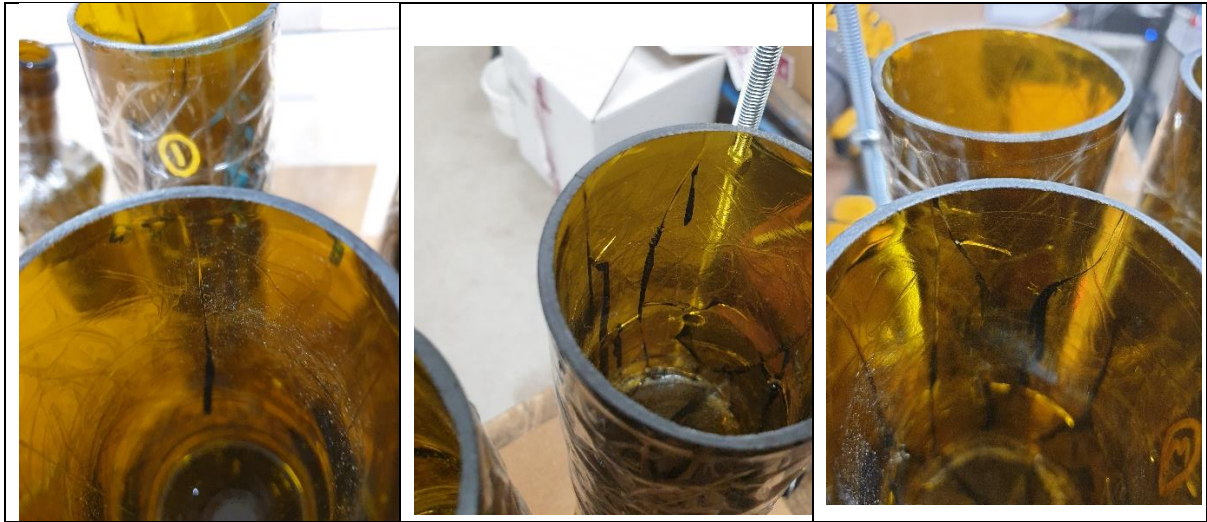
A.7.2. Cut Samples (Cut-Double-BB)

Before Testing: Notice the small cuts and the imperfections at the cut surfaces



After Testing: Notice the small cuts and the imperfections at the cut surfaces. Cracks at these imperfections



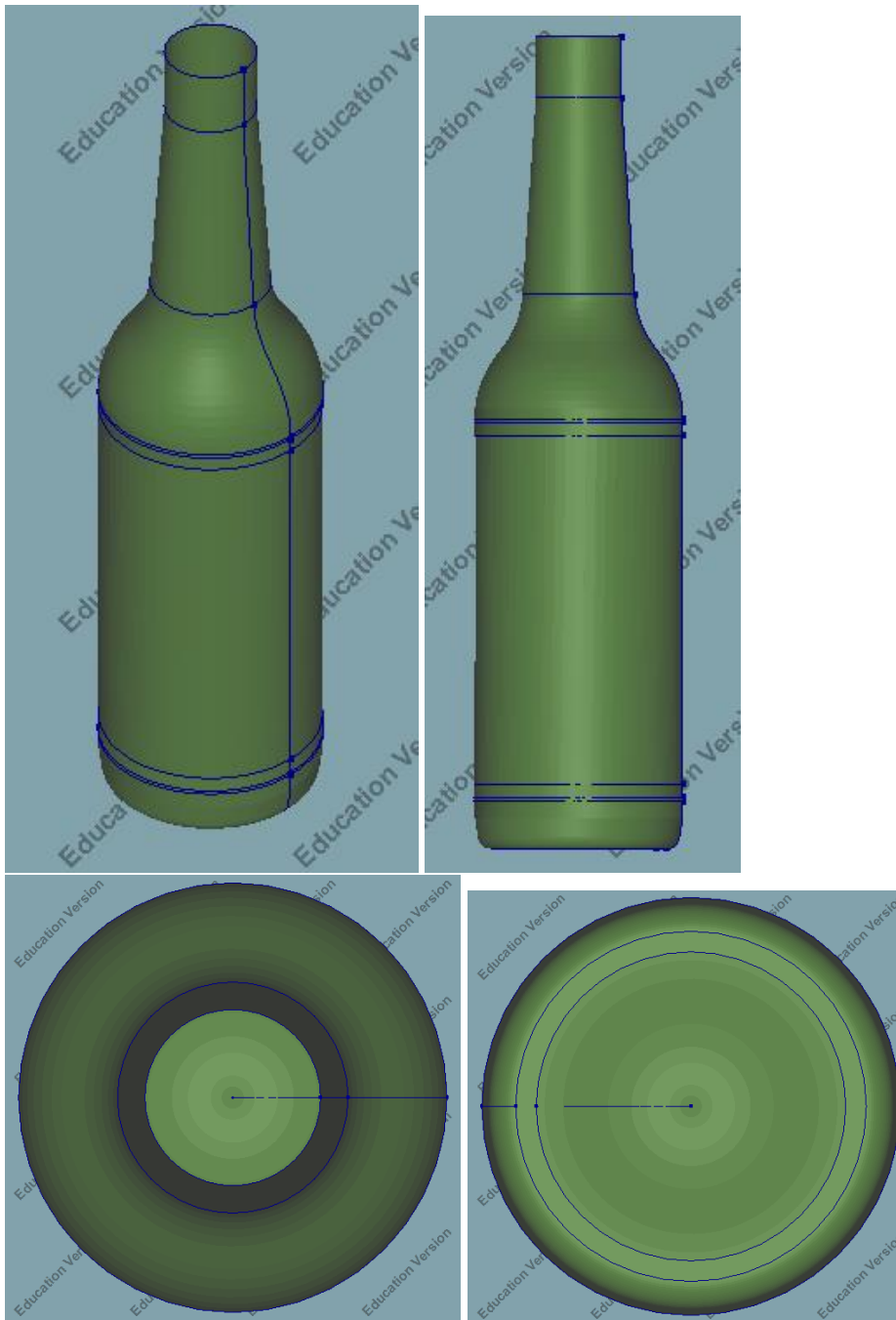


A₈

A8 Finite Element Model Bottle

A.8.1. DIANA Model

Geometry:



Top left: 3D, Top right: Front, Bottom left: Top view, Bottom Right: Bottom View

Material settings:

Properties		
Description		Value
Aspect		[]
Linear material properties		
Elasti		
Young's modulus		70000 N/mm ²
Poisson's ratio		0.22

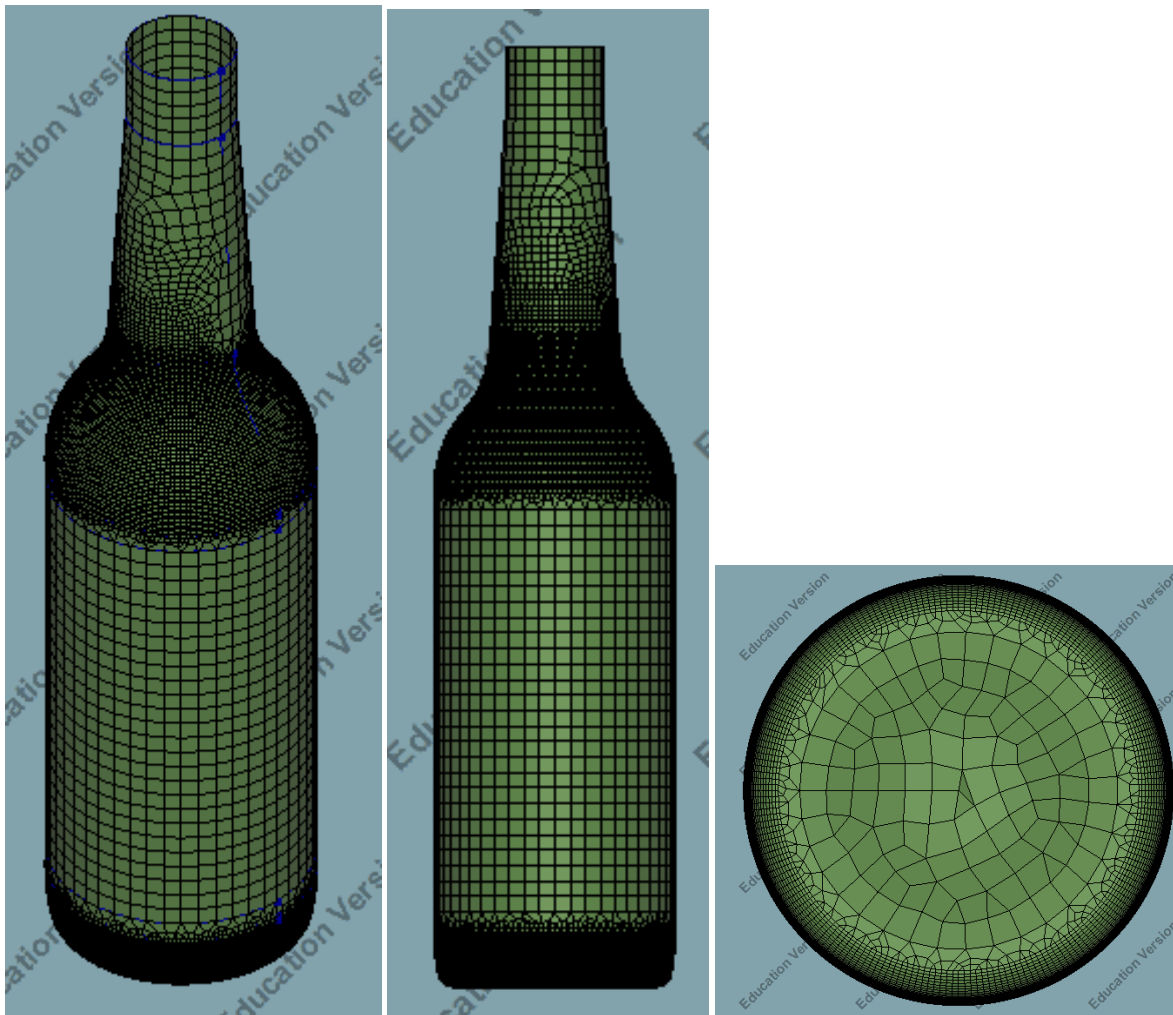
Loading and boundary conditions:



Element geometry:

Properties		
Description		Value
Thickness		2.5 mm
Local element axes		<input type="checkbox"/>
Underlying geometry		<input type="checkbox"/>
Eccentricities		<input type="checkbox"/>

Mesh:

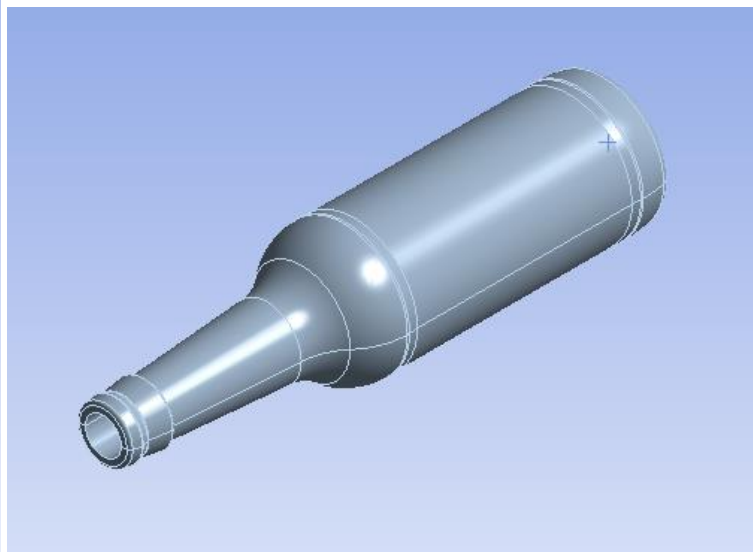
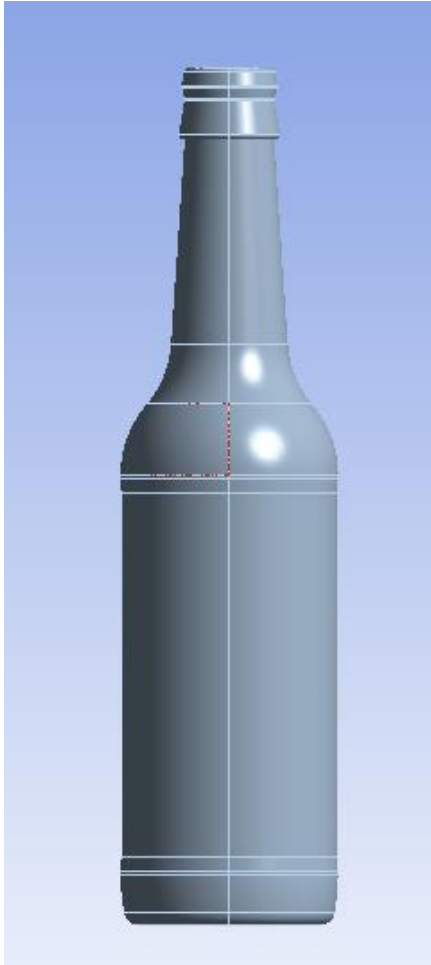


A maximum principle stress output:

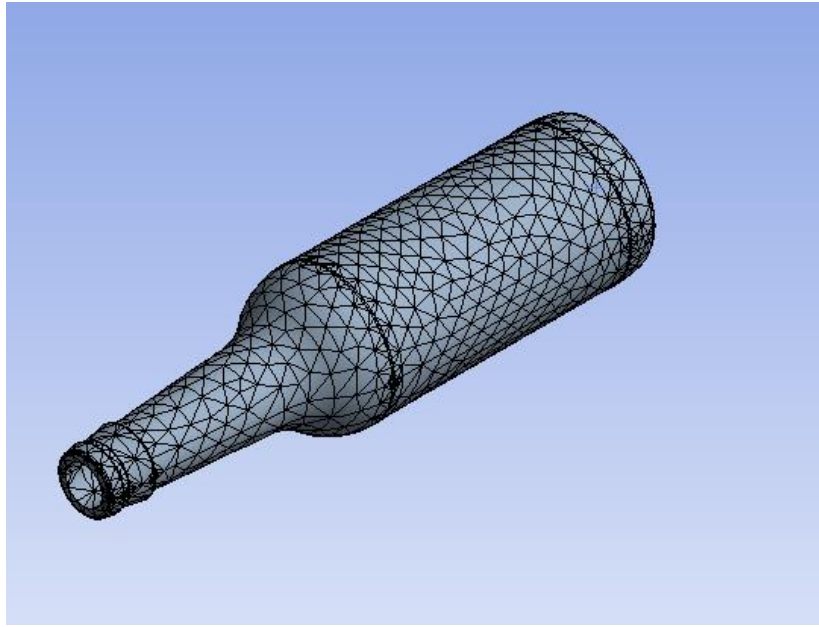


A.8.2. ANSYS Model

Geometry:



Mesh:



Materials:



Glass, soda lime (common glass)



Soda-lime glass (Corning 0080)

Data compiled by the [Granta Design](#) team at ANSYS, incorporating various sources including JAHM and MagWeb. ANSYS Inc. provides no warranty for this data.

Density	2,465e-06 kg/mm ³
---------	------------------------------

Structural

▼ Isotropic Elasticity	
Derive from	Young's Modulus and Poisson's Ratio
Young's Modulus	69930 MPa
Poisson's Ratio	0,21490
Bulk Modulus	40880 MPa
Shear Modulus	28780 MPa
Isotropic Secant Coefficient of Thermal Expansion	9,35e-06 1/°C
Tensile Ultimate Strength	32,560 MPa
Tensile Yield Strength	32,560 MPa

Thermal

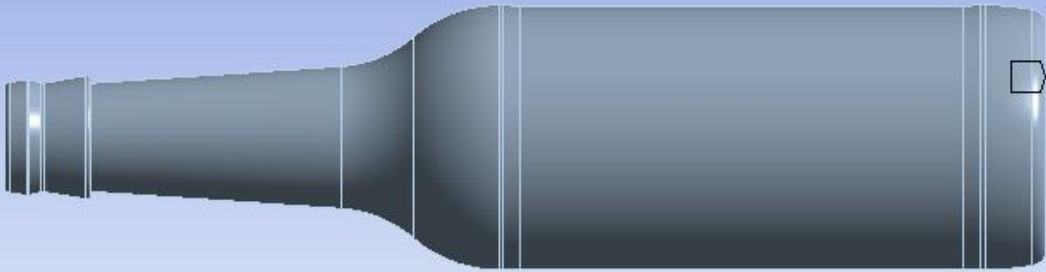
Isotropic Thermal Conductivity	0,0010780 W/mm·°C
Specific Heat Constant Pressure	8,986e+05 mJ/kg·°C

Boundary conditions:

A: Static Structural

Fixed Support
Time: 1, s
28-10-2022 15:03

Fixed Support

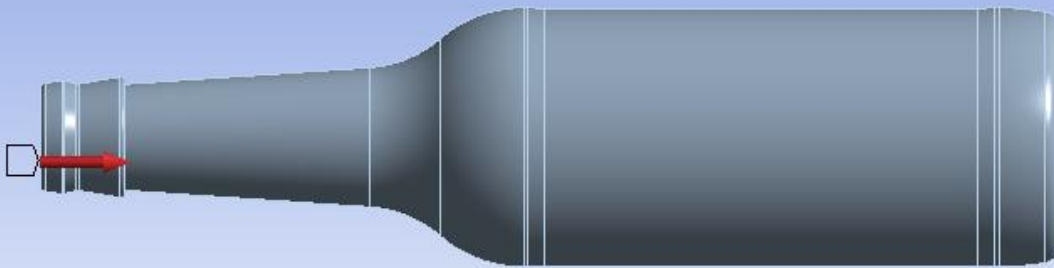


Loading:

A: Static Structural

Force
Time: 1, s
28-10-2022 15:04

Force: 19326 N
Components: 0,0,-19326 N



A maximum principle stress output:

